COPPE
Instituto Alberto Luiz Coimbra de Pós-Graduação e Pesquisa de Engenharia
UFRJ

OPTIMIZATION OF SUBSEA ARRANGEMENT FOR PRODUCTION SYSTEM

Cheng Hong

Tese de Doutorado apresentada ao Programa de Pós-graduação em Engenharia Oceânica, COPPE, da Universidade Federal do Rio de Janeiro, como parte dos requisitos necessários à obtenção do título de Doutor em Engenharia Oceânica.

Orientadores: Segen Farid Estefen
Marcelo Igor Lourenço de Souza

Rio de Janeiro
Novembro de 2019

OPTIMIZATION OF SUBSEA ARRANGEMENT FOR PRODUCTION SYSTEM

Cheng Hong

TESE SUBMETIDA AO CORPO DOCENTE DO INSTITUTO ALBERTO LUIZ COIMBRA DE PÓS-GRADUAÇÃO E PESQUISA DE ENGENHARIA (COPPE) DA UNIVERSIDADE FEDERAL DO RIO DE JANEIRO COMO PARTE DOS REQUISITOS NECESSÁRIOS PARA A OBTENÇÃO DO GRAU DE DOUTOR EM CIÊNCIAS EM ENGENHARIA OCEÂNICA.

Orientadores: Segen Farid Estefen
Marcelo Igor Lourenço de Souza

Aprovada por: Prof. Segen Farid Estefen
Prof. Breno Pinheiro Jacob
Prof. Celso Kazuyuki Morooka
Prof. Murilo Augusto Vaz
Prof. Virgílio José Martins Ferreira Filho

RIO DE JANEIRO, RJ – BRASIL
NOVEMBRO DE 2019

Hong, Cheng

Optimization of Subsea Arrangement for Production System/Cheng Hong. – Rio de Janeiro: UFRJ/COPPE, 2019.

XIII, 122 p.: il.; 29, 7cm.

Orientadores: Segen Farid Estefen

Marcelo Igor Lourenço de Souza

Tese (doutorado) – UFRJ/COPPE/Programa de Engenharia Oceânica, 2019.

Referncia Bibliogrfica: p. 114 – 122.

1. Subsea production system. 2. Layout optimization. 3. Cost optimization. 4. Operational research. 5. Mixed integer programming (MIP). 6. Gradient descent. I. Estefen, Segen Farid *et al.* II. Universidade Federal do Rio de Janeiro, COPPE, Programa de Engenharia Oceânica. III. Título.

Acknowledgement

First of all, I would like to extend my deepest gratitude to my supervisor, Professor Segen Farid Estefen, for his careful guidance and encouragement to me during the past four years. He guided me enter the new research area, providing me with many enlightening ideas that have inspired me to a great extent. He helped me revise the thesis and every publications very carefully and patiently, sentence by sentence, improving the outlines and argumentations and correcting the grammatical errors. His rigorous attitude towards academic research makes me sincerely admire from the bottom of my heart. I feel so lucky that I could work with this so kind man during the past four years, who helps me grow up not only about the academic research, but also the personality.

Secondly, I would like to express my heartfelt gratitude to Professor Marcelo Igor Lourenço de Souza, who is the co-advisor of my thesis. He provided me with lots of valuable suggestions for my thesis. He answered every questions of mine so patiently and helped me understand my research area deeper and deeper.

I also want to appreciate my colleague, Ms. Yuxi Wang, who helped me so much. She was always at my side when I was facing difficulties. Our friendship is my most precious wealth.

I would like to extend my deep gratefulness to my parents. They always encourage me to go out and see what the world is like, and they tried their best to support me and put all their love on me.

Thank all my Chinese and Brazilian friends here, who brought me a unforgettable experience in this enthusiastic country. The past four years was the most colorful period of my life.

Resumo da Tese apresentada à COPPE/UFRJ como parte dos requisitos necessários para a obtenção do grau de Doutor em Ciências (D.Sc.)

OTIMIZAÇÃO DE ARRANJO SUBMARINO DE SISTEMA DE PRODUÇÃO

Cheng Hong

Novembro/2019

Orientadores: Segen Farid Estefen
Marcelo Igor Lourenço de Souza

Programa: Engenharia Oceânica

Este tese apresenta a otimização do arranjo do sistema de produção submarina, com foco em dois conceitos básicos: o sistema de poço satélite com Unidade flutuante de produção, armazenamento e transferência (FPSO) e o sistema de manifold submarina com FPSO, respectivamente. Dois cenários típicos para cada conceito são considerados para estabelecer os modelos de otimização: sistema de poço satélite considerando poços verticais, sistema de poço satélite considerando poços horizontais, sistema de manifold submarino com poços verticais distribuídos por satélite e sistema de manifold submarino com poços horizontais agrupados. Os modelos são desenvolvidos através da programação inteira mista (PIM). Três objetivos principais são considerados: menor custo, menor período de retorno e perda mínima de pressão. Através dos modelos de otimização propostos, a rede e as rotas de dutos, capacidades de processamento do FPSOs, tamanhos e localizações dos manifolds (para o sistema de manifold submarina), localizações das cabeças de poço e poços trajetórias, e taxas de produção poderiam ser descobertas.

Os modelos de PIM propostos são com não linearidades. Com base no algoritmo de descida de gradiente, os modelos são decompostos em uma série de modelos lineares, resolvidos pelo otimizador GUROBI. As soluções ótimas finais são obtidas através do processo de iteração. O método da triangulação de Delaunay é aplicado para separar o espaço da solução, a fim de obter boas soluções iniciais em pouco tempo. Os estudos de caso dos modelos propostos são conduzidos no mesmo campo offshore e os resultados de diferentes cenários são comparados. Os estudos de caso indicam bom desempenho dos modelos propostos e estratégia de solução, fornecendo ferramentas convenientes e confiáveis para aplicações do mundo real.

Abstract of Thesis presented to COPPE/UFRJ as a partial fulfillment of the requirements for the degree of Doctor of Science (D.Sc.)

OPTIMIZATION OF SUBSEA ARRANGEMENT FOR PRODUCTION SYSTEM

Cheng Hong

November/2019

Advisors: Segen Farid Estefen
Marcelo Igor Lourenço de Souza

Department: Ocean Engineering

This thesis presents the optimization of subsea production system arrangement, focusing on two basic concepts: satellite well system with Floating Production Storage Offloading unit (FPSO), and manifold system with FPSO, respectively. Two typical scenarios for each concept are considered to establish the optimization models: satellite well system considering vertical wells, satellite well system considering horizontal wells, manifold system with satellite distributed vertical wells and manifold system with clustered horizontal wells. The models are developed through mixed-integer programming (MIP). Three major objectives are considered: lowest cost, shortest payback period, and minimum pressure loss. Through the proposed optimization models, the subsea flowline network, flowline route, FPSO processing capacities, manifold sizes and locations (for the manifold system), wellhead locations and well trajectories, and well production rates could be figured out.

The proposed MIP models are with nonlinearities. Based on the gradient descent algorithm, the MIP models are decomposed to a series of linear models, which are solved by optimizer GUROBI. The final optimal solutions are obtained through the iteration process. The Delaunay triangulation method is applied to discrete the solution space in order to obtain good initial solutions. The proposed models are applied to the arrangement optimization of the same offshore field, and the results of different scenarios are compared, as well as the results of different objective functions. The case studies indicate good performance of the proposed models and solution method, providing convenient and reliable tools for real-world applications.

Contents

List of Figures

List of Tables

Nomenclature

(x_k^m, y_k^m) Continuous variables, manifold positions on the $X - Y$ plane

α Step length factor

δx_i A small perturbation of element x_i

$\mathcal{I}_{\mathcal{F}}$ The node set of FPSO nodes

$\mathcal{I}_{\mathcal{M}}$ The node set of manifold nodes

$\mathcal{I}_{\mathcal{O}}$ The node set of obstacle areas vertices

$\mathcal{I}_{\mathcal{V}}$ Virtual node set for manifold system with satellite vertical wells

$\mathcal{I}_{\mathcal{W}}$ The node set of wellhead nodes

$\mathcal{I}$ The whole node set including all kinds of nodes

d_{ij} the distance between node i and node j

D_{mf} Internal diameter of the flowline between manifolds and riser bases

D_{mf} Price per length of the flowline between manifolds and riser bases

D_{wm} Internal diameter of the flowline between wellheads and manifolds

L_h Length of horizontal drilling

L_J Lenght of short jumper for cluster manifold system

L_v Length of vertical drilling

L_{riser} Riser length

N_M Number of manifolds

N_M^{ava} Number of avaible manifold sizes

N_W Number of wells

N_{fpso}^{ava} The number of available FPSO sizes

P_{mf}^{line} Price per length of the flowline between manifolds and riser bases

P^{riser} Price per length of riser

P_h Price per length for horizontal drilling

P_v Price per length for vertical drilling

$p_{k,tm}$ Binary variable, $p_{k,tm} = 1$ indicates that the kth manifold selects type tm from the avaible ones

P_{wm}^{line} Price per length of the flowline between wellheads and manifolds

Q_{ij} Continuous variable that indicates flow rate between node i and node j

x_{ij} Binary variale that indicates the connection relationship between the node i and node j

X_k The soltuon at kth iteration step

y_{ij} Binary variable indicates the connection relationship between manifold i and well j

z_{ts} Binary variable that indicates the selection of FPSO from the available options

L_{hl} Horizontal displacement of well l

$Q_{f_{ij}}$ Continuous variables, represent the total flow rates from node i to node j toward FPSO

$q_{f_{ij}}$ Non-negative integer variables, represent the number of flowlines between node i and node j toward FPSO

$Q_{m_{ij}}$ Continuous variables, represent the total flow rates from node i to node j toward manifold

$q_{m_{ij}}$ Non-negative integer variables, represent the number of flowlines between node i and node j toward manifold

Chapter 1

Introduction

1.1 Background

The development of a subsea field involves a complex design procedure with very high costs. Due to the low oil price, harsh environment, very deep water, high drilling costs and other complicated issues, the challenge of reducing both the CAPEX and OPEX while maintaining an effective development performance is a key consideration. Some research work have presented an integrated view of several cycles of field development design, to help find better solutions for the offshore project [1, 2]. The development of an offshore field must be based on a project's ability to deliver the maximum economic benefits to the project partners while maintaining safety and environmental goals [3].

In the whole production system of an offshore oil field, typically there are three key parts. The first part is the well system that penetrates into the reservoir to make the hydrocarbons flow out and move out of the surface through the wellbore. The second part is the subsea production system, including the flowlines, jumpers, umbilicals, wellheads, manifolds, compressors, pumps and other related equipment required for the field development, which are installed on the seabed, to transport the produced fluids toward the terminal system, which is the third part that receives and processes the produced fluid. For deepwater fields, floating platform is the most widely used, such as the Floating production storage and offloading unit (FPSO). Risers are installed as the flow path for the fluids to the floating platform, and they are also classified as a part of the terminal system.

Figure 1.1 presents a schematic overview of the whole system. The hydrocarbons start from the reservoir, flow through the above-defined three parts, and finally arrive at the topside of the floating platform for further processing and future offloading. It is easy to find that these three parts are located in three different spaces: under the seafloor (well system), on the seafloor (subsea production system), and

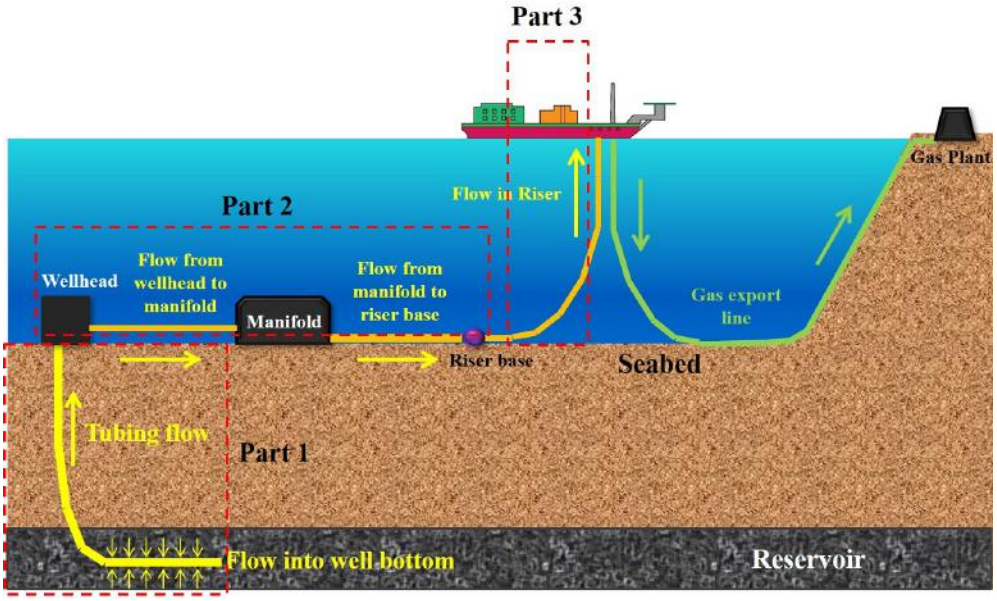

Figure 1.1: Flow process of hydrocarbons

above the seafloor (terminal system). Among these three parts, the subsea production system acts as the bridge for the first part (well system) and the third part (terminal system), and its arrangement should be determined at the early stage of FEED (Front to the end engineering design). Here the word "arrangement" includes two aspects of meaning, one is the subsea production system concept, such as the satellite well system, template or cluster manifold system and so on, and the other is the system layout under the chosen concept, which is about the location of the related subsea facilities, and the pipeline network that connects them. It is with the most influence since the project scheduling including the facility procurement, installations, operations and maintenance, and the production performance are all directly related to the system arrangement.

The arrangement of the subsea production system is affected by the well system and terminal system, as shown in Figure 1.2. For example, different well types (vertical well or directional well) lead to different locations of wellhead and different production rates, affecting the subsea flowline network, which further influences the processing capacities selection of the floating platform. In turn, the processing capacities and riser numbers limit the number of wells connected, which provides some constraints for the subsea production system arrangement design. When designing the subsea production system arrangement, these three parts should be integrally taken into consideration, in order to balance their interactions and achieve better development plan. For each part, we usually have series of options, we could choose vertical well or directional well, we could select manifolds to gather the production from different wells, there are different sizes of flowlines and risers, and different processing capacities of floating platforms. Different options also lead to different

cost and benefit. As a result, practically, the subsea production system arrangement design is to find the combinations of these various options, considering the interconnection among the defined three parts, with the relevant trade-offs between production, cost and schedule [4], to provide the potential of good return of investment, which becomes an optimization problem.

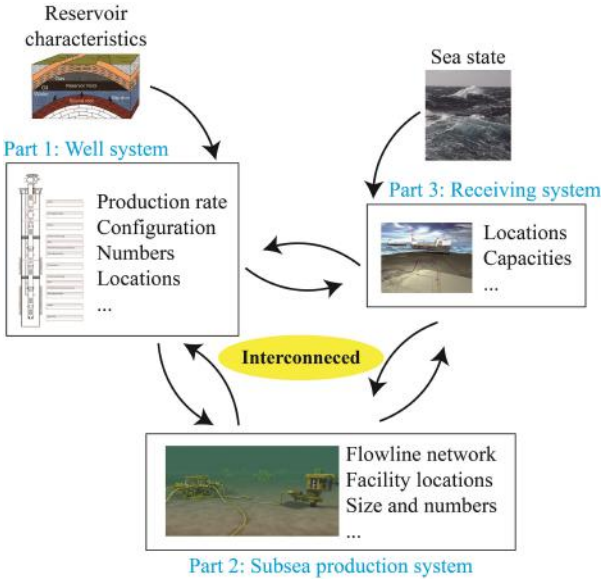

Figure 1.2: Relationship between different parts of the offshore field

1.2 Objective

The objective of the thesis is to establish a unified process for the arrangement optimization of the subsea production system, including the mathematical model, solution process and application suggestions, under the constraints from environment, techniques and production, aiming at minimizing the total cost of the system. Two major concepts are studied, including the satellite well system and the manifold system. This work expects to provide an effective tool to determine the subsea production system arrangement quickly with both economic and technical feasibilities.

The thesis is organized as follows. Chapter 2 is the literature review, including the development of a subsea production system concept and the related scientific research about this topic. Through the literature review, two typical subsea production system concepts are selected as the basic, which are the satellite well system and manifold system. The mathematical models, solution methods and case studies of these two concepts are presented in Chapter 4, Chapter 5, respectively. Before these mathematical models, in Chapter 3, the assumptions, related simplifications and some general considerations and treatment for the mathematical modelling are proposed. Chapter 6 summarizes the thesis and presents potential future works.

Chapter 2

Literature review

2.1 Typical concepts of Subsea production system

The offshore oil and gas industry started from the first successful completed offshore well in the Gulf of Mexico (GoM) off Louisiana in water depth about 4.6m [5]. In the 1970s, a concept of subsea field development was proposed, in which the individual wellheads and production equipment such as manifold, were encapsulated on the ocean floor within sealed pressure chambers, and the produced hydrocarbons would flow from the well to a nearby processing facility, either on land or on offshore platforms [6]. It was successfully applied in Garoupa field located 259km east-northeast of Rio de Janeiro, and 80km offshore, with water depth between 120-166m [7]. This concept was the start of subsea engineering, and the systems that consist of the wellheads, manifolds and other related equipment, as well as the flowlines and umbilicals that connect the facilities below the water surface is referred as "Subsea Production System" [8].

After decades of development, subsea production system becomes more sophisticated, advancing from shallow water manually operated systems to systems capable of operating through remote control in water depth up to 3000m. And different kinds of concept arose to accommodate the field environment, meet the requirement of production with both economic and technical feasibilities. Several typical subsea production system concepts are introduced here, as well as practical applications.

2.1.1 Satellite well system

A satellite well is an individual subsea well which is connected directly to the host through two dedicated flowlines/risers. Figure 2.1 presents a schematic view of a typical satellite well system. FPSO is the host. The production well has one production and one service flowline/riser, and the injection well has one water injection and one gas injection flowline/riser.

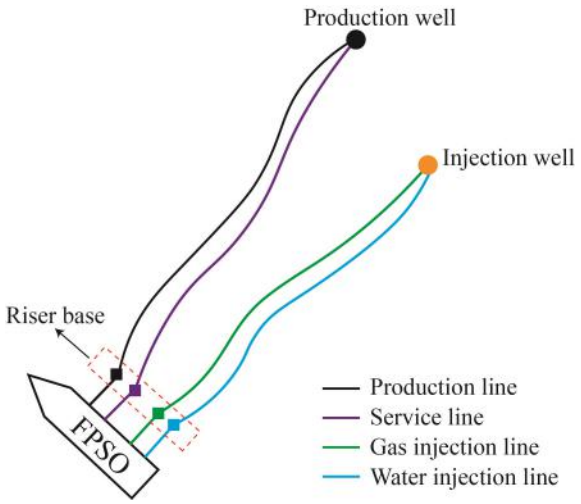

Figure 2.1: Schematic view of a typical satellite well system

These two dedicated flowlines/risers are connected by a pigging loop inside the Xmas tree, allowing for fluid displacement and round trip pigging operation of the flowlines. Besides, each well is connected with one unique umbilical which is also directed to the host, in order to remotely control the wellhead.

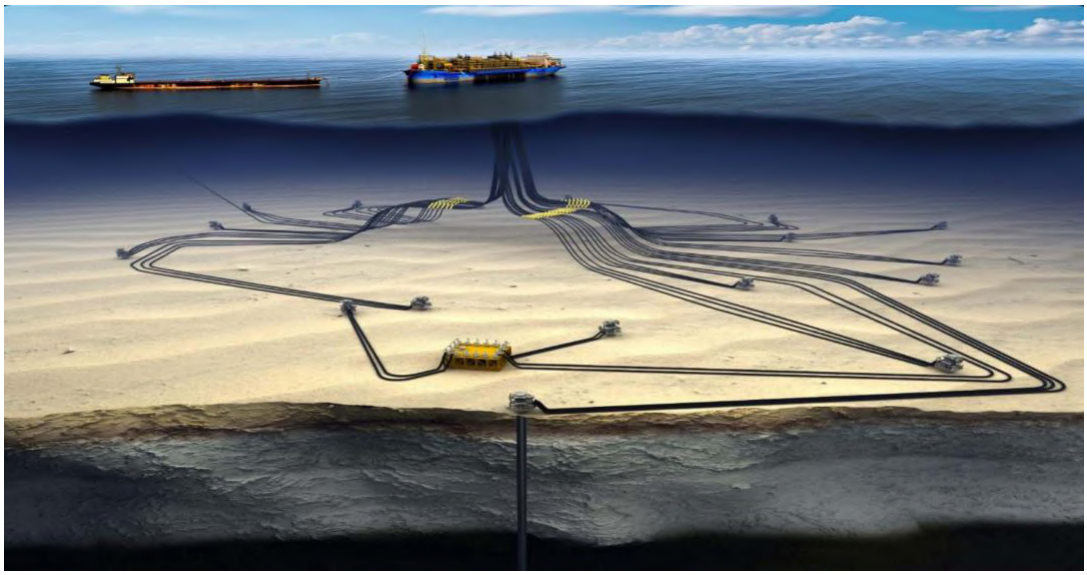

Figure 2.2: The layout of Sapinhoá field [9]

Satellite well system provides the flexibility of locating the wellhead on the seabed. Wells can be vertical which is less complicated and cheaper compared with directional wells and horizontal wells. Besides, the production or injection from one well does not affect another. And the independent control of the wellheads provides very good operability[4]. But this concept requires very long flowlines and risers (two lines for one well), making the cost for materials and installation of flowlines and risers huge.

In deep water Brazil, this concept is very popular. Albacora Leste Field and Marlim giant field in Campos Basin were all producing with tens of satellite wells connected directly to Floating Production Storage Offloading Unit (FPSO) [10, 11]. Several newly developed pre-salt fields in Brazil Santos Basin are also developed with lots of satellite wells as pilot system, due to the single well high production rate, and the need of acquiring reservoir information over the entire area, for example, the Sapinhoá field [9], Lula giant field [12, 13] and Libra field[14]. Figure 2.2 presents the layout of satellite wells in Sapinhoá pre-salt field in the Santos basin.

2.1.2 Manifold system

Instead of immediately connecting to the host facility, the production from wellheads could be commingled first and then transported to the host together. The facility for commingling the productions is manifold. Depending on the way of organizing the location of wellheads and their connection with manifolds, there are mainly three different kinds of manifold system: template system, cluster manifold system, and satellite well-manifold system.

Subsea wellheads can be grouped closely together, productions from the wellheads in one group will commingle at the manifold and then flow to the host facility such as FPSO. The template system and cluster manifold system are both based on this "well group idea".

The template is a subsea production facility where the wells, connections and manifolds are gathered on a common supporting structure called "Template". Wellheads usually distribute at the corners or the edges of the template, and manifold is installed on the central part. Two flowlines are needed to connect the host facility with the manifold to offer a loop for the need of pigging operation. The schematic view of the template system is shown in Figure 2.3 (a).

Cluster manifold system separates the wellheads and the manifold compared with the template system. The independent wells are drilled with relatively close spacing, presenting clustered distribution, and connected to the centrally located manifold through jumpers and short flowlines. Similarly, there are also two flowlines connect the manifold to the host facility, providing the flow loop for pigging operation, as shown in Figure 2.3 (b).

Template and cluster well system is the most widely used concept in offshore field development. In North Sea area, several oil and gas fields are developed with a template system, such as Frigg gas field [16], Tommeliten gas condensate field [17], Kristin gas condensate field [18] and Aasta Hansteen gas field [19]. In deepwater Brazil, template system also has been applied in Albacora giant oil field in Campos Basin, in order to reduce the cost of flowline [20]. Cluster manifold system is even

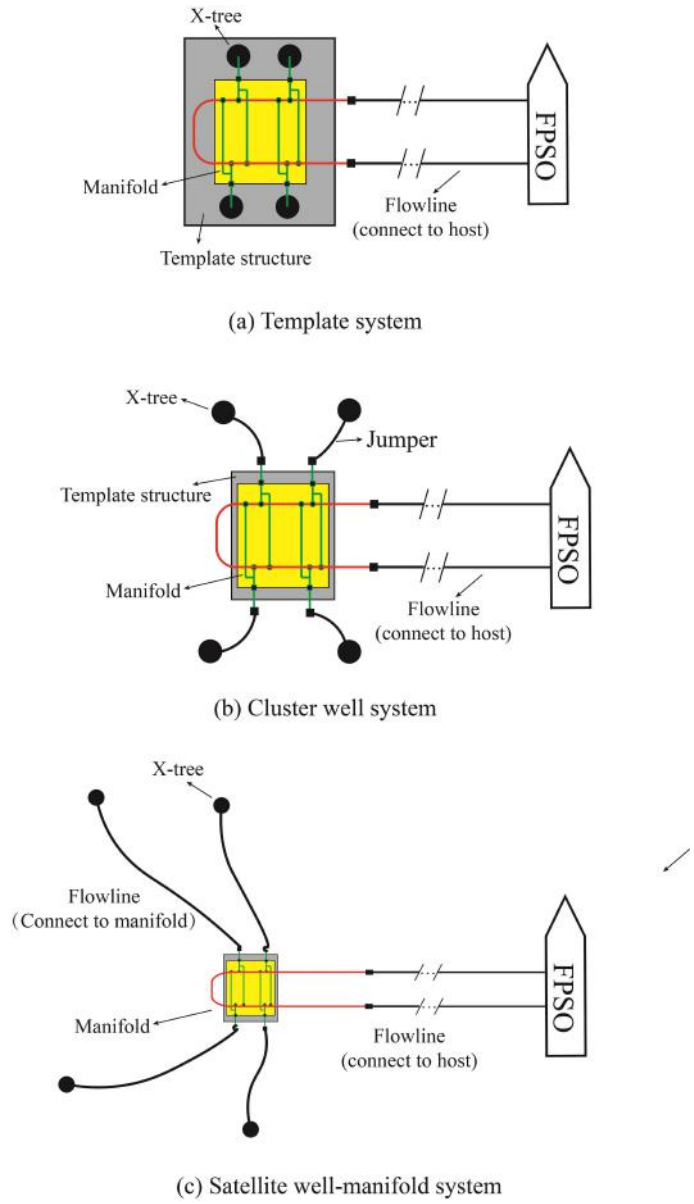

Figure 2.3: Schematic view of template system and cluster well system

more widely applied. For example, Troika oil field [21, 22], Gemini oil field [3] and Tahiti oil field [15] in deepwater Gulf of Mexico (GoM), and Kuito oil field [23], Ceiba oil field [24], Moho Bilondo field [25–27] in deepwater West Africa are all developed with cluster manifold system. These developments provide lots of experience for deepwater oil field development. Figure 2.4 presents the layout of the Tahiti field in the Gulf of Mexico, which is developed by cluster manifold system.

If the wellheads are satellite distributed, applying the manifold requires relatively longer flowlines to connect the wellheads due to the far distance, which is the satellite well-manifold system, as shown in Figure 2.3 (c). For example, in the Perdido field in the Gulf of Mexico, several faraway satellite wellheads were tied back to the manifold system [28]. This kind of concept makes the well drilling locations flexible and could

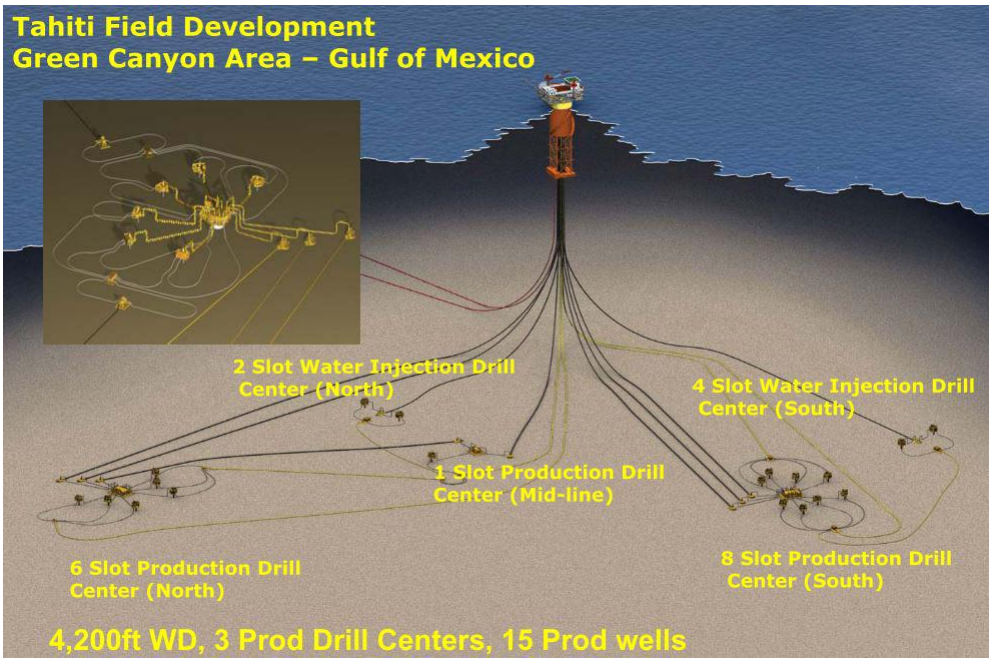

Figure 2.4: Layout of Tahiti field [15]

be changed for better ones if new subsurface data comes in later. But due to the long flowline length and the difficulty of building a flow loop for pigging operation between manifolds and wellheads, the flow assurance issues should be considered carefully.

2.1.3 Daisy chain system

Daisy chain system is another alternative for offshore field development. This configuration may also be called production ring, or loop. A daisy chain usually consists of at least two subsea satellite wells that link to a trunk line. The trunk line starts from the host with one riser, being laid on the seabed, reaching each well along the way and then returns to the host through another riser, thus forming a flow loop. The short jumper is used to connect the wellhead to the trunk line. Therefore, compared with the satellite well system, which requires two risers per well, riser number in daisy chain system is much fewer. But since the trunk line will gather the production from the included wellheads, the diameter should be relatively large, and the wellhead location could not change too much after determining the layout, because the trunk line is designed based on the wellhead locations.

Figure 2.5 (a) presents a schematic view of a daisy chain system that includes several wellheads. In Albacora giant field of Brail, daisy chain concept was applied to construct raw water injection system, in which the injection wells were connected by a trunk line [29]. Na Kita oil field in the Gulf of Mexico was also developed with daisy chain system, in which the production loop included five production wells [30].

Besides wellhead, cluster manifold could also be daisy-chained. There are two ways of organizing cluster manifolds. One is to connect both two flowline joint of the cluster manifold to the trunk line through the jumper, as shown in Figure 2.5 (b), the manifolds present a "parallel distribution". The Usan field in Nigeria was developed through this way [31]. The other one is to organize the manifolds in a "series distribution" shape, as shown in Figure 2.5 (c). The last manifold is equipped with a pigging loop, thus permitting round trip pigging. This way is also applied in many offshore oil fields, for example, the Girassol oil field [32], Dalia oil field [33], AKPO field [34], and Bonga field [35] in West Africa. Figure 2.6 presents the layouts of the daisy-chained manifold system under the two different ways of organizing manifolds.

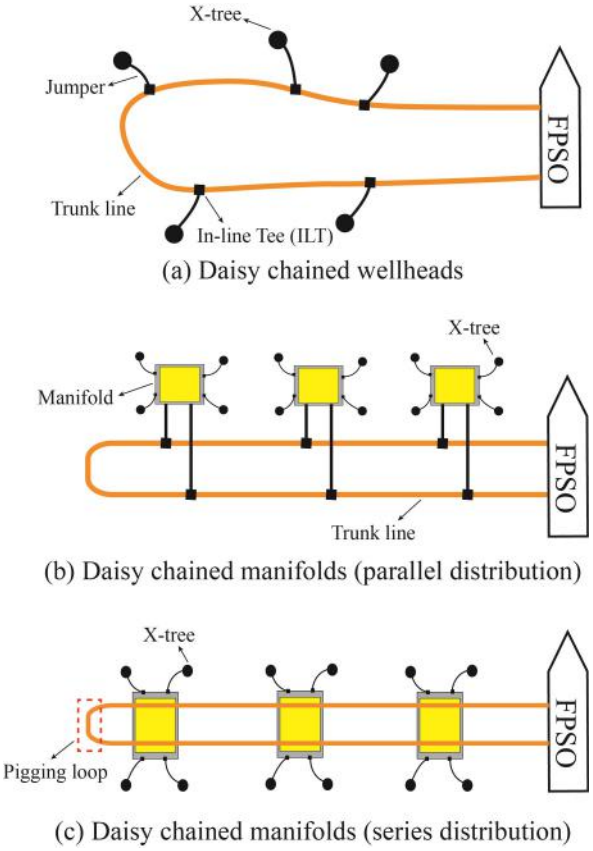

Figure 2.5: Schematic view of daisy chain system

There are also some fields developed by a mixture of the above concepts. For example, the BC-10 project (Parque das Conchas) in Campos basin of Brazil was developed by cluster manifolds with several satellite wellheads directly connected to the FPSO [36, 37].

Each kind of concept has strengths and weaknesses simultaneously. For the satellite well system, the well locations are flexible and could be changed if new subsurface data comes in later, and wells could be vertical, which is much cheaper. The operations and installations are easy and could be standardized. However, it

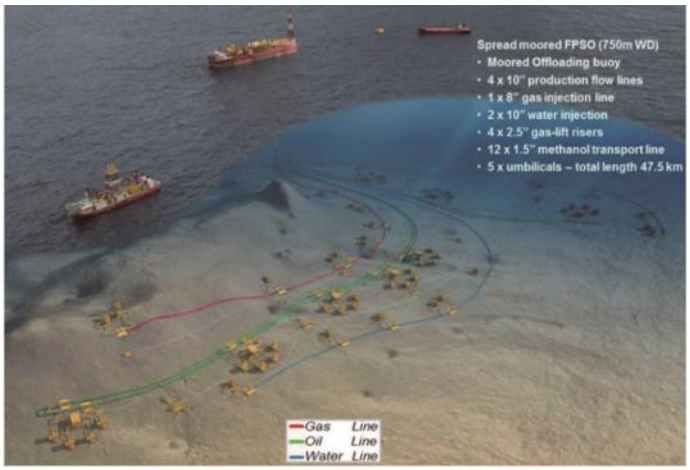

(a) Daisy chain layout of Usan Field in West Africa parrallel distributed manifolds

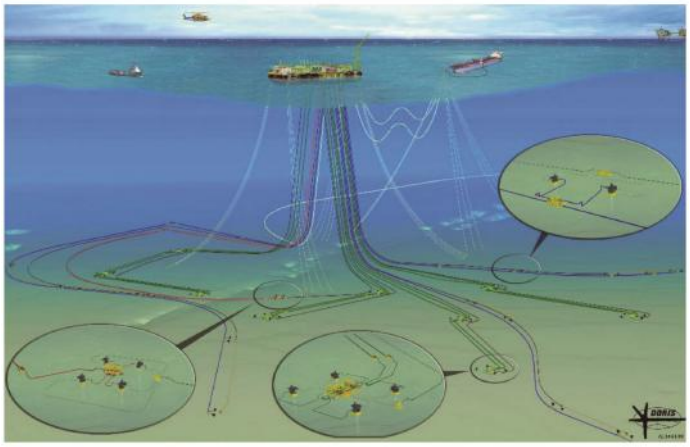

(b) Daisy chain layout of AKPO Field in West Africa series distributed manifolds

Figure 2.6: Layout of daisy chained manifold system in Usan and AKPO field [31, 34]

requires a large number of risers and flowlines (2 risers and 2 flowlines for each wellhead), leading to high cost.

Compared with satellite well system, the total flowline length of both the template system and cluster well system is much lower, and the wellheads are close to each other, reducing the drilling rig movement when changing the drilling site from one well to another, thus improving the drilling operation efficiency. But due to the close spacing between wellheads, directional drilling is usually required in order to reach the target pay zone in the reservoir, which is more expensive than vertical well drilling[38]. Besides, the well locations are not as flexible as the satellite well system because they are related to the positions of templates or manifolds. Figure 2.7 illustrates the template and cluster manifold used in Aasta Hansteen field in Norwegian Sea [19] and in Dalia field of West Africa [33], respectively.

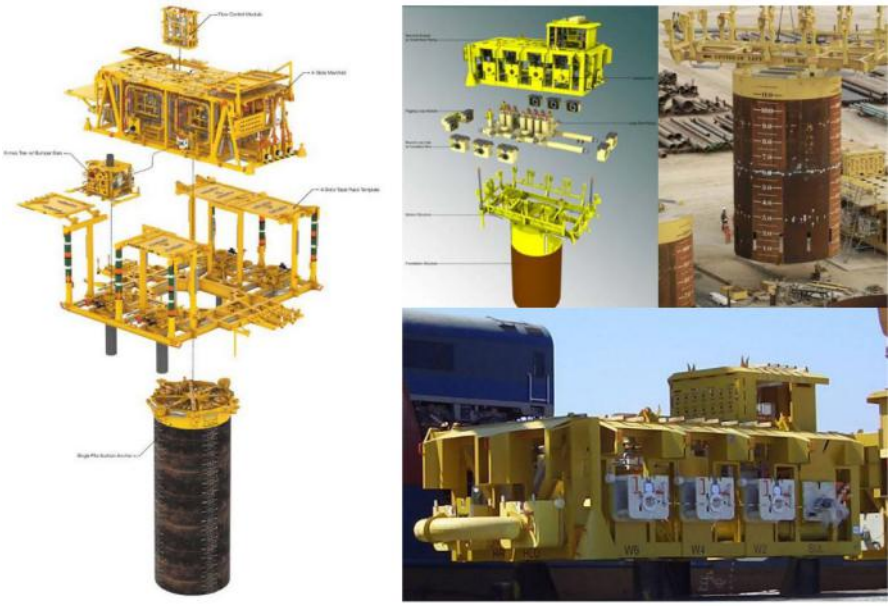

(a) 4-slots template (b) 6-slots manifold

Figure 2.7: Template and cluster manifold [19, 33]

Daisy chain system needs fewer riser connections, and rigid lines are usually selected for the trunk line, which is more reliable than flexible lines [4]. Flowline length and cost are both reduced compared with the other concepts. If the wellheads are daisy-chained, the wells could be vertical which is much cheaper. The closed-loop allows for convenient implementing pigging operation to mitigate flow assurance risk. However, once the daisy chain system has been determined and the trunk line is installed, the wellhead locations could not be changed if new subsurface data is obtained. Besides, since the trunkline gathers the produced fluids from series of wells or manifolds, the flow rate will be very high and large size of rigid pipe is required, which is more difficult and expensive to install.

Therefore, at the early stage of FEED (Front to the end engineering design), to decide which kind of subsea production system should be selected for an offshore project, usually several candidate concepts are provided at first according to the reservoir characteristics, predicted production information, sea environment and other related factors. Then, for each candidate concept, the detailed layout is designed, including the flowline routes, facilities' numbers and locations, pipeline network configurations, and so on, which is an optimization process under given objective and constraints. These concepts and corresponding layouts will be estimated, compared and the final subsea production system will be determined based on the cost, reliability, technical feasibility and other related criteria synthetically. [39–41].

In deep water Brazil, the development experience summarized above indicates that the satellite well system and manifold system are most widely applied. This

thesis will focus on these two concepts, which are satellite well system and manifold system. The optimization models for both concepts are developed respectively, in order to provide an effective tool to determine the subsea production system arrangement quickly with both economic and technical feasibilities. We define the subsea concept together with the corresponding subsea layout under the concept as "subsea arrangement", which is used in the title of the thesis. Related research work about this topic is presented in the next section.

2.2 Related research work

The offshore field development optimization could be dated back to the work of Devine and Lesso [42]. They proposed a mixed-integer model, through which to determine the location and number of the drilling platform, and the correspondence between the wells and the drilling platforms. The sum of drilling cost and platform cost is set as the objective. And the drilling cost is defined to be related to the horizontal distance between the wellhead and the corresponding drilling platform. The optimization model is stated as follows:

$$\begin{aligned} &\text{Minimize} \quad F = \sum_{i=1}^{W}\sum_{j=1}^{L} t_{ij} f(d_{ij}) + \sum_{j=1}^{L} P_j(M_j, x_j, y_j) \\ &\text{subject to} \\ &\qquad \sum_{j=1}^{L} t_{ij} = 1 \\ &\qquad \sum_{i=1}^{W} t_{ij} - M_j = 0 \end{aligned} \tag{2.1}$$

In this model (x_j, y_j) is the location for platform j on the X-Y plane. t_{ij} is a binary variable, $t_{ij} = 1$ means well target i is drilled from plaftform j, otherwise, $t_{ij} = 0$. M_j is the number of wells drilled from platform j. d_{ij} is the horizontal straight distance between well i and platform j. f is the drilling cost function that is related to d_{ij}, and P_j is the cost function of platform j that is related to the location and the number of wells drilled from it. L and W represent the number of drilling platform and the number of wellhead, respectively.

The proposed model is identical in general structure to the well-known "Location-Allocation" problem, which is a kind of operational research topic widely discussed in many areas, such as logistics management [43] and healthcare system optimization[44].

This research work provided the basic method of dealing with offshore field developments and indicated that related theories of operational research could be applied in this area. After that, some other issues related to the field development were

taken into consideration.

Iyer et al. [45] included the reservoir production performance and built up a multiperiod mixed-integer linear programming model, to optimize the planning and scheduling of offshore oil field infrastructure investment and operations, aiming at maximizing the total net present value (NPV). Carvalho and Pinto [46] improved the model, considering the reservoir pressure decay during the development life, through assuming the linear decay as the function of the cumulative oil production. Gupta and Grossman [47] applied non-linear reservoir pressure decay and established an MINLP model (mixed-integer nonlinear programming) to maximize the total NPV for a long-term planning horizon. The production scheduling problem was also discussed in many other research, with different ways of defining the long-term reservoir performance to make the model be more practical [48–50].

But these research work did not discuss how to arrange the subsea facilities and flowline connections between them, which is the detailed subsea layout. It was simplified, through using the horizontal distance between wellheads and platforms, or between reservoirs and platforms, in order to define the drilling and pipeline cost [46], as well as the pressure drop inside flowlines [45]. This simplification does not present the effect of subsea layout, because different subsea layouts provide different flowline lengths and routes, as well as different types and numbers of subsea facilities, which are all related to the cost estimation and production prediction.

In some degree, the subsea layout design is to determine the flowline network that connects the related facilities. This kind of work could be seen in many other areas such as water pipe network optimization and gas transmission network optimization. Dobersek and Goricanec presented an optimization of pipe network with hot water under hydraulics limitations [51]. El-Mahdy et al. [52] optimized the pipe size used in a natural gas pipe network considering cost and pressure drop, the network topology was predefined, and pressure drop was defined through non-linear equations about gas flow. Sanaye and Mahmoudimehr [53] designed a natural gas transmission network layout considering the pipeline length, pressure drop and flow rate. The proposed model was also non-linear due to the related gas flow pressure drop equations. GA (Genetic Algorithm) was used to solve both models to overcome the difficulties brought by the nonlinearity and the discontinuity. Kabirian and Hemmati [54], Üster and Dilaverolu [55], Mikolajková [56] analyzed the extension of an existing gas pipeline network with least operating and capital costs. The connection strategy for the newly added node, as well as the mass flows, compressor duties and changes in the flow directions, were optimized. Mikolajková then developed a method of linearizing the model to accelerate the solving process [57]. The mathematical ways of describing the pipe network, the process of building up the mathematical model, and the solution methods all provided some inspiration for the

subsea production system layout optimization.

Wang [58] discussed the subsea wells partition in the layout of cluster manifolds. The proposed mathematical model is similar to the work of Devine and Lesso [42]. The objective function is the total length of the flowlines which connect wellheads and manifolds. Later another model was developed to optimize the number and position of PLEM (pipeline end manifold), as well as the connections with cluster manifold and FPSO [59]. Then three different types of jumper connections were further considered [60]. These results indicated the subsea layout effect on the total cost. But the positions of the cluster manifolds or the PLEM were set as the geometric center of the facilities directly connected to them, which may not be the optimal positions. In these model, the number and size of the manifolds are the input parameters and location of the manifold in one well group are set as the geometric center of the corresponding wellheads that belongs to the group. This treatment resulted in an integer linear programming model that the decision variables are only the connection relationship between wellheads and manifolds, or between PLEM and FPSO.

Rodrigues [61] proposed a MILP model to obtain the minimum total cost, through determining the numbers and positions of platforms, cluster manifolds and wellheads, and the connection relations between the facilities. The model takes the well trajectory into consideration, by simplifying well trajectory into vertical segments and horizontal segments. The space area between sea level and the reservoir was discrete into a series of rectangular grid nodes. The related facilities' positions are selected from these grid nodes, as well as the routes of flowlines and well trajectories. Therefore, all the discrete grid nodes were the decision variables. The model assumed vertical risers, and one manifold must correspond to one platform which floats on the sea surface just above the manifold. This assumption limited the application of the proposed model to more general situations, in which one platform or FPSO might connect with two or more manifolds, with other kinds of riser configurations [23].

These researches simplified the seabed environment. Practically, there are some restricted areas on the seabed that the flowlines and facilities should avoid, which is like "obstacle areas". The shape of the obstacle varies. For example, the existing flowline that should not be crossed is "line shape", and the closed region corresponds to geotechnical hazard or ecological protection area is "polygon shape" [62]. Besides, the flowline structural issues and multiphase flow are all possible factors that affect layout optimization. Kang and Lee [63] and Xiao [64] optimized the subsea single pipe route considering the presence of obstacles, the seabed was also discrete into rectangular grid nodes. The shortest path algorithm, Dijkstra algorithm, was applied. Xiao [64] also included the effect of multiphase flow on the pipe

route. The pressure drop of multiphase flow was not directly calculated, instead, it was expressed by the ground undulations, considering that high-pressure drops were caused by variations in seabed elevation.

Vieira [62] divided the pipe into a set of straight lines and curves and proposed an optimization model for pipe route selection considering avoiding subsea obstacles. Lucena [65] provided a further discussion of this model, considering different constraint handling methods. Rocha [66] and Baioco [67] improved the model, including the considerations of on-bottom stability, free-span and multiphase flow. The proposed pipe route optimization model was applied to design a satellite well system with one FPSO[68]. The head nodes (wellheads) were fixed and connected to the same end node (FPSO). Optimizing the layout of such a system is actually optimizing the pipe route between each satellite well to the FPSO. But if there are two or more FPSOs for a satellite well system, the assignment between wellheads and FPSOs becomes unknown. Similarly, for the cluster manifold system, if the location of manifolds is also the decision variable, the connection relationships between wellheads, manifolds and FPSOs are also unknown rather than fixed. As a result, the single pipe route optimization is hard to be implemented under these situations. A more general model that for the whole pipe network is needed.

Gong [69] discussed the generalized "Location-Allocation" model considering several polygon obstacles. Genetic Algorithm (GA) was applied to determine the locations of the "service centers", while the connections between "service centers" and "customers" were obtained through linear programming. Many other works related to "Location-Allocation problem" also applied GA to solve the proposed model [44, 70, 71]. Since the process of GA does not require derivatives which are essential for some classical optimization algorithm, the mathematical model could be discontinuous or non-differentiable, providing the possibility for dealing with more complicated problems. But GA is a kind of evolutionary algorithm, and usually results in different solutions from several repeated process. It always provides "good solution" that is close to the optimal one, or sometimes "local optimum" rather than the "global optimum". Therefore, the evolutionary strategy of GA needed to be designed carefully to avoid pre-mature, in order to ensure the algorithm performance [72].

Zhang [73] optimized an offshore oil field gathering system, under given location of the platforms, the connection topology, major parameters of pipelines and facilities were figured out. Similar to the work of Rodrigues [61], the optimization was based on discrete seabed topography, by rectangular grid nodes. This idea was also applied in another work of Zhang [74], in which a topological structure of onshore production well-gathering pipeline network was optimized. Manifold positions, as well as the connections between facilities, were obtained for the minimum total cost.

These works considered flow rate, terrain obstacles, and production techniques. The proposed model providing a way of combining flowline route determination and connection relationship between subsea facilities together. Since the position of facilities and flowline routes were limited to be from the discrete nodes, it was possible that a better solution might exist on the continuous $X-Y$ plane that the discrete nodes did not cover. Denser grid nodes would bring better solutions but result in extremely large numbers of decision variable, making the calculation scale be too large, and difficult to obtain solutions.

Rosa [75] proposed a MILP model to design a subsea production network that accounts for the number of manifolds and platforms to be installed, their location, well assignment to these gathering systems, and pipeline diameters. Reservoir dynamics were considered but not coupled with the optimization model. Instead, several reservoir simulations under different layout configurations were conducted to provide the boundaries of related parameters of the optimization model. Redutskiy [76] proposed an MINLP model, putting the layout design, operation scheduling and production scheduling together, to optimize the total NPV. The proposed model considered the hybrid of cluster manifold system and daisy chain system. The seabed was simplified and subsea obstacle was not considered. Besides, the proposed model assumed a single-phase flow along the flowlines and adopted a nonlinear continuous equation to estimate the frictional pressure loss, which was easy to find the analytical first derivative expressions. If obstacles and multiphase flow were included, the proposed solution method was not applicable, and the model would be difficult to solve.

2.3 Discussions about previous work

These previous research work presented the main issues about the subsea production system layout optimization, which are summarized as follows.

(1) The plan of subsea field development could be divided into two parts, one is the system layout, and the other is scheduling, including the operation scheduling and production scheduling. The two parts are interrelated. Subsea production system layout determines the fluid flow directions and process, which are important for the operation and production scheduling, and also affect the investment. These two parts have ever been put together to become an integrated model, as what Redutskiy did [76], which would be very complicated and hard to solve, even though with some simplifications which are some kind more different with the practical situation, for instance, the assumption of single-phase flow inside the flowlines. It would be better to separately conduct subsea system layout optimization and the operation and production scheduling by order so that the result of the first process could be the input for the second one. Under this condition, more considerations

could be taken for both parts. This thesis will focus on the first part, the subsea production system layout optimization. Different subsea concepts are considered.

(2) The subsea production system layout optimization is similar to "Location-allocation problem", including determining the facilities' location and the pipeline network. The objective is to minimize the total CAPEX of the system. Some factors are taken into consideration such as seabed topography, subsea obstacles, fluid flow behavior and so on, in order to properly reflect the practical situation. Considering more leads to more practical results, but more complicated mathematical models.

(3) Mixed-integer programming is mostly applied to define the optimization model. Due to different considerations about the optimization, some proposed models are linear (MILP), while some are non-linear (MINLP). In this thesis, mixed-integer programming is also used to develop the related mathematical models.

(4) Brand and bound method is the main tool to solve mixed-integer programming [77]. Some MILP solvers have been developed based on this method, such as GUROBI and CPLEX that could be applied for the subsea production system layout optimization [73, 75]. For the MINLP model, usually, some treatments are made to transform it into one or several MILP models, which are easier to be solved. The nonlinear equations could be linearized to approximate the MINLP model to MILP model [57]. Some intelligent algorithms like GA could be applied to design the solution candidates for nonlinear variables, then each candidate corresponds to a MILP sub-model that could be solved conveniently [78]. The treatments are specific depending on the features of the proposed model.

According to the literature review, several points that could be improved to make the optimization model for subsea production system layout more practical are summarized as follows.

(1) The flowlines in the subsea system should avoid intersection with each other. For example, in a cluster manifold system, the jumpers or flowlines between wellheads and manifolds might become the obstacles for the flowlines between manifolds and host facilities. But the connections between wellheads and manifolds are also the decision variables. Therefore, compared with those static obstacles such as restricted region et al., this kind of obstacle needs extra equations to define, which has not been considered in detail.

(2) The floating facilities, such as FPSOs, were always treated as nodes, and risers could connect with the nodes in any direction as long as meeting the proposed constraints. But in practical situation, it is a little different. For example, the riser interfaces on a spread mooring FPSO usually distribute on the starboard or portside, or on them both, so that the risers could only connect to the FPSO on these two sides, which affects the flowline routes. Besides, the mooring lines should also be avoided by the flowlines [79]. These issues should be taken into consideration for

the subsea production system layout design, which most of the previous work have not included yet.

(3) In most of the previous work about layout optimization, there was only one terminal to receive the produced fluid of the whole system. The constraints of capacity were not considered. If the field area is larger and more than one floating platform is required, the processing capacities, as well as the maximum riser number of the floating platform, will become constraints for the subsea production system layout. This issue has not been discussed in detail yet.

(4) Usually, the production zone and well bottom position in the reservoir are predetermined by reservoir engineers. The wellhead locations on the seabed would affect the well trajectory shape and length, thus affecting the drilling cost. As a result, a combination of wellhead locations, well trajectories and subsea system layout are meaningfull to optimize the total cost. Most of the previous research did not take the well drilling into consideration and worked on fixed wellhead locations. Rodrigues [61] did some work about this issue, but the proposed model was only limited to be applicable in the case that one floating platform connected with only one manifold through the vertical riser. the integrated model for more general situations has not been studied yet.

2.4 Thesis structure and main contributions

In this thesis, a unified process for the arrangement optimization of the subsea production system is established, under different subsea system concept. Two different concepts are studied, which are satellite well system and manifold system. For each concept, two different scenarios are considered. For the first concept, we take vertical well and horizontal well into account, respectively, as the two different scenarios. And for the second concept, we consider satellite well-manifold system with vertical wells, and the cluster manifold system with horizontal wells, respectively. Each scenario has its own characteristics, resulting in different optimization models, the decision variables, as well as the solution methods. The points that need further improvements mentioned in section 2.3 are included in this thesis, making the proposed models more practical. The thesis structure is shown in Figure 2.8

First of all, the mathematical descriptions of engineering considerations for the subsea production system arrangement optimization are provided. Then these descriptions are applied to the optimization models for the two major subsea concepts. For each concept, the corresponding optimization model, solution methods, case studies, and parametric studies are included. At last, comparisons of the proposed models are presented.

The main contributions of the thesis are shown below.

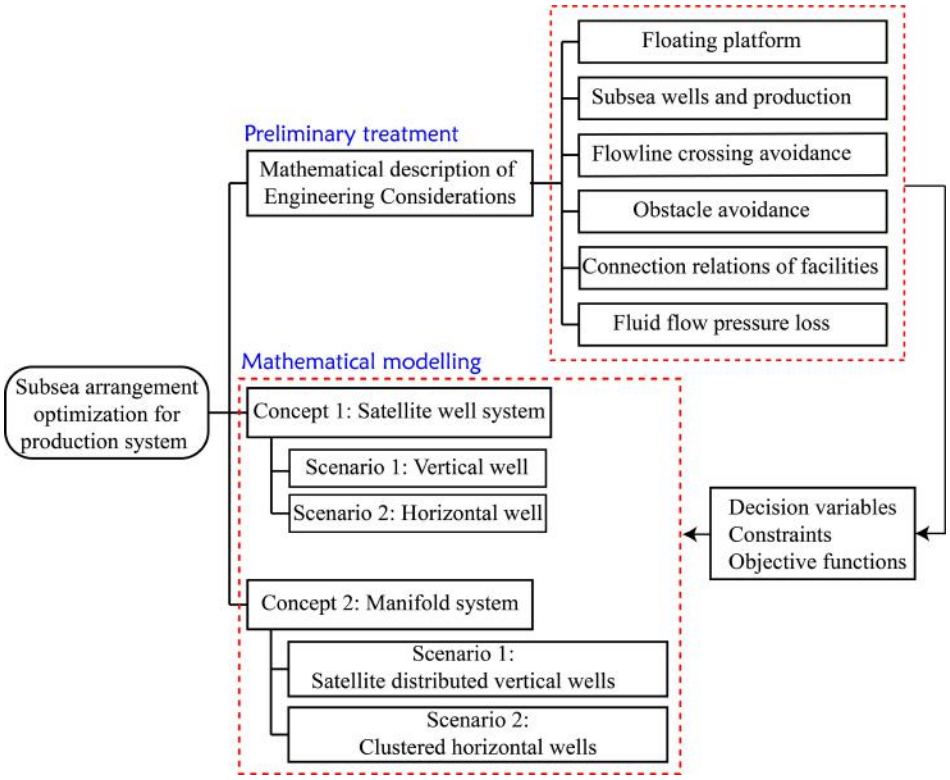

Figure 2.8: Thesis structure

(1) The layout optimization models for satellite well system and manifold system are proposed. They are organized together, providing a convenient and reliable tool for real-world applications.

(2) More technical issues are considered, making the proposed models more practical. Drilling cost is integrated into the system layout optimization, through adding into the effect of wellhead location on the well trajectory and the subsea flowline. Flowline intersection avoidance is set as one of the constraints to ensure that the flowlines will not affect each other. FPSO is selected as the floating facility in this work. The processing capacity of FPSO is considered to limit the connections of the flowlines and risers. Besides, seabed obstacles and fluid flow behaviour are all taken into account when developing the optimization models.

(3) Mixed-integer programming is used to develop the mathematical models, and a new solution process is provided. Some of the proposed models are non-linear (MINLP), which are decomposed into a series of mixed-integer linear programming models (MILP) with the help of the gradient descent method. The Delaunay triangulation is applied to find a good initial solution for the subsequent process, in order to find the global optimum.

(4) The comparisons of different subsea production system concepts are conducted through case studies, which clearly demonstrate the differences between different types of subsea production system arrangements.

Chapter 3

Engineering considerations and mathematical descriptions

When developing a mathematical model to describe one practical problem, it is almost impossible to consider everything of the complex practical situation. Instead, some simplifications or assumptions should be made, in order to reduce the difficulty of mathematical modelling. These simplifications and assumptions should be proper so that they won't change the characteristics of the target problem and affect the potential results too much. In this chapter, some major engineering considerations for the subsea arrangement optimization are simplified to reduce complexity. Besides, some basic mathematical descriptions of these considerations are proposed, as the preliminary treatment of the subsequent optimization models.

3.1 Basic assumptions and simplifications

3.1.1 Seabed topography

Though the seabed is undulating, in the area of an offshore oil field, especially the one in ultradeep water, the seabed slope is very small [79], and the variation of seabed elevation is relatively much smaller compared with the horizontal scale of the area.

As a result, the flowline length between two positions is very close to the straight connection segment, so that using the straight connection segment to represent flowline will not change the cost too much, which is the major objective of the layout optimization. Therefore, considering the small seabed slope, the seabed could be assumed as a flat plane, for the subsea production system layout optimization.

The small variation of seabed elevation and the small slope also indicate that the pressure or temperature distribution along the flowline could be approximately calculated on the assumed straight flowlines on the flat plane, instead of on the

complicated undulating seabed. Of course, this treatment won't be accurate, but this rough estimation could reflect the range and magnitude of the pressure or temperature, which are enough for the related considerations for layout optimization.

3.1.2 Subsea obstacles

Due to the complexity of subsea topography, some restricted areas can act as obstacles that should be avoided by flowlines and facilities. These areas can be divided into two categories: one is line-shaped, such as existed wirelines and umbilical and other flowlines; the other is polygon-shaped, which represents a closed region, such as geohazard regions, regions of environmental protection and other developed fields [80]. These obstacle areas distribute on the sea bottom, and the height is not considered.

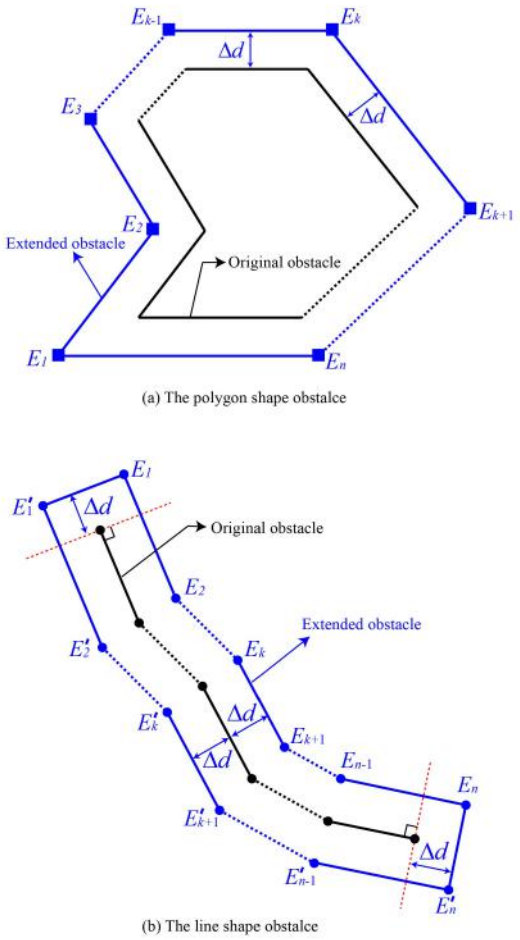

Figure 3.1: Extension of obstacles

The pipe route must also keep some distance away from these obstacles to ensure the safety of the installation and operation [81]. Therefore, the obstacles are extended outwards to achieve this requirement, as shown in Figure 3.1. Figures

3.1(a) and 3.1(b) present the extension of line-shaped obstacles and polygon-shaped obstacles, respectively. For the polygon-shaped obstacles, each edge of the polygon was moved by a distance Δd along its outer normal vector direction. The extended edges form a new polygon for the design of the subsea pipe route. The extension of line-shaped obstacles is similar. The difference is the treatment of the head and end nodes, as shown in Figure 3.1(b). Taking the head node, for instance, the straight line perpendicular to the first edge was moved by a distance Δd along its outer normal vector direction. The same treatment was done for the end node. Then, together with the extended edges of the line, a polygon is formed. The distance Δd is the minimum "safe distance" between the pipe route and the real obstacles. This is a manual set value that can differ between obstacles. Through this process, the two kinds of obstacles were both transformed to polygon-shaped for the subsequent layout design.

It should be noted that the obstacles described here are static obstacles, which are fixed on the seabed. As mentioned in Chapter 2, the possible flowlines between facilities become the extra potential obstacles, which depend on the layout itself during the optimization process, so that this kind of obstacles seem to be "dynamic obstacles", the treatment of this issue will be introduced in Chapter 5 which is about the layout optimization of manifold system.

3.1.3 Subsea Well

The subsea well could be vertical or directional. The directional well, especially the horizontal well, could improve the well production and reach reserves that otherwise might not be developed. But directional well drilling is more difficult and expensive compared with vertical drilling. Besides, the directional wells with long horizontal departure are called extended reach wells and are often defined as wells with the ratio between the total measured depth (TD) and the true vertical depth (VD) more than 2.0 [82]. In deep water Brazil, all these types of well have ever been applied [9, 83]. Of course, due to the technical feasibility, the horizontal displacement of one well is limited, for instance, in deepwater Brazil, the possible maximum horizontal displacement is about 6000-6500m [84].

Directional well drilling could effectively reduce the length of subsea flowlines, which does good to reducing the subsea production system cost [85]. But the increase in drilling cost might balance this reduction. Larger the horizontal displacement is, higher the drilling cost will be. Therefore, the discussion between the relationship between subsea well and the subsea production system layout makes sense. In this thesis, the horizontal well and vertical well are considered, the difference of production rate, drilling cost and horizontal displacement are included in the layout

optimization.

The practical wellbore presents a three-dimensional curved trajectory. For simplification, the well trajectory is presented by the combination of vertical parts and horizontal part. The length of the vertical part is the vertical depth of well bottom, and the length of the horizontal part is the horizontal distance between wellhead and well bottom, as shown in Figure 3.2. Through this way, the drilling cost of one well is represented by

$$COST_{drilling} = P_v L_v + P_h L_h \tag{3.1}$$

where the P_v and P_h are the cost per unit length for vertical part and horizontal part, and L_v, L_h are the length of vertical part and horizontal part.

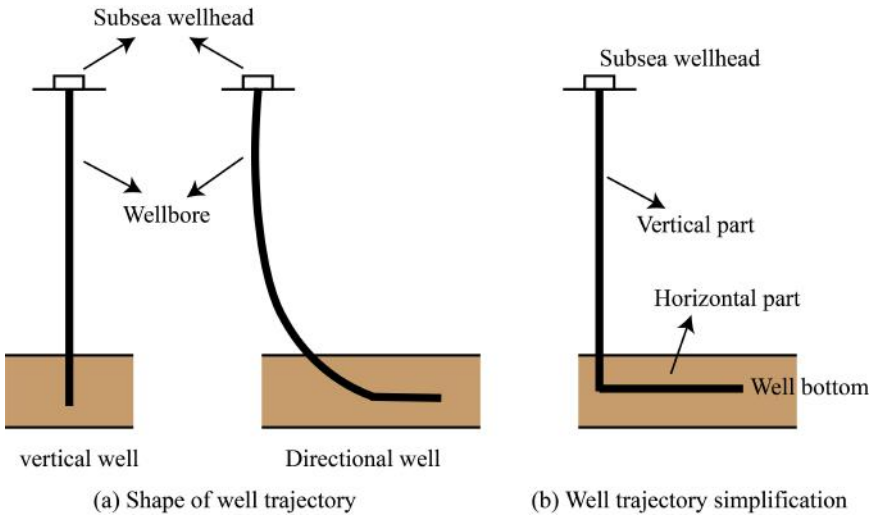

Figure 3.2: Shape of well trajectory and simplification

As for the production rate, the best way is to use the reservoir simulation technique to obtain the well production for different well types or different horizontal displacement. These simulation results are the input information for the subsequent optimization models to obtain the best horizontal displacement. The reservoir simulation is complicated and beyond the scope of this thesis. For simplification, the vertical well productivity and horizontal well productivity are estimated through theoretical equations.

The production rate of vertical well is calculated by

$$Q_v = \frac{2\pi K h \Delta P}{\mu B_o \ln(r_e/r_w)} \tag{3.2}$$

The production rate of horizontal well is calculated by Joshi equation [86].

$$Q_h = \frac{2\pi Kh\Delta P/\mu B_o}{\ln\left[\frac{a+\sqrt{a^2-(L_p/2)^2}}{L/2}\right] + \frac{h}{L}\left(\frac{h}{2r_w}\right)}$$
$$a = (L_p/2)\left[\frac{1}{2} + \sqrt{\frac{1}{4} + \frac{1}{(0.5L_p/r_e)^4}}\right]^{0.5} \tag{3.3}$$

In eq. (3.2) and eq. (3.3), Q_v and Q_h are the production rate for the vertical and horizontal well, respectively. K is the reservoir permeability, h is the oil column thickness, ΔP is the pressure difference between reservoir and well bottom, μ is the fluid viscosity under reservoir condition, r_e and r_w represent the flow radius and wellbore radius, respectively, B_o is the volume factor to transfer the production rate to the surface condition, L_p is the production interval of the horizontal well, and we use a proportion factor β to represent its relationship with the horizontal displacement L_h: $L_p = \beta L_h$. The horizontal production interval length also has a maximum value, which will be set as the input information for the subsequent optimization work.

It should be noted that the calculation of productivity for both vertical well and horizontal well are complicated due to the variation of reservoir characteristics and different well completion method. The above-adopted productivity calculation equations are relatively simple and theoretical, in which the complicated reservoir properties, such as skin factor, the production variation with developing time, and the water flooding influence et al. are not considered. The proposed production calculation equations are just to provide a general view between the horizontal displacement and the production rate, thus presenting the process of how subsea production system layout optimization is linked to the subsea well.

3.1.4 Floating platform

The floating production storage and offloading unit (FPSO) is selected as the floating platform in this thesis, which is widely used in deepwater field development in Brazil [14]. There are mainly two types of FPSO, turret moored FPSO and spread moored FPSO. A spread moored FPSO is a vessel moored by anchor legs from the bow and stern of the vessel in a four-group arrangement. The risers are suspended from "riser porches" on the side of the vessel. This type of mooring system maintains the vessel in a fixed orientation in global coordinates. A turret moored FPSO is designed as a single point mooring (SPM) that allows the FPSO to weathervane about the mooring system, in response to the environment. Riser systems are also supported within the turret structure. Figure 3.3 illustrates the main structure of these two types of FPSO.

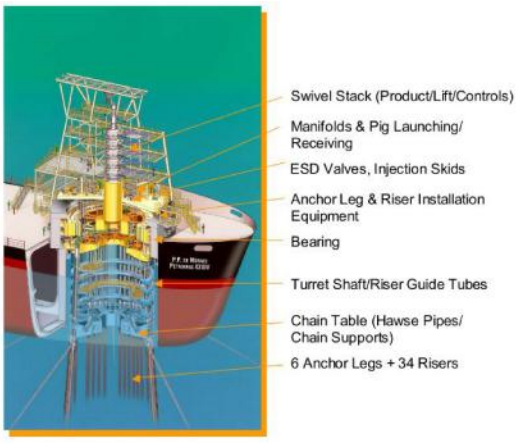

(a) Turret moored FPSO

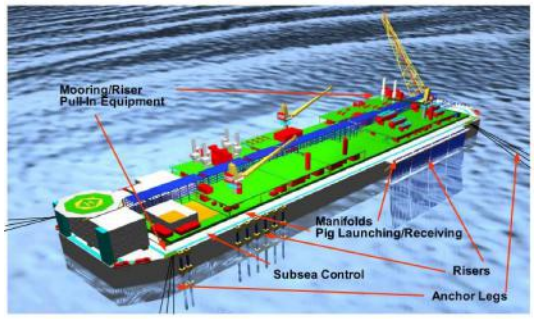

(b) Spread moored FPSO

Figure 3.3: Main structure of turret moored and spread moored FPSO [87]

Three major features are considered and treated for the subsea production system layout optimization.

The first is the FPSO hull. For turret moored FPSO, the risers and mooring lines are all connected to the single point mooring system, therefore the turret FPSO is treated as one single node, representing the single point mooring system which acts as the terminal of the subsea production system. While for the spread moored FPSO, the risers and mooring lines are immediately connected with the hull, so that the hull is treated as one segment with length equal to the FPSO. The two ends of the segment connect with mooring lines.

The second is the mooring lines. For both types of FPSO, the mooring lines are grouped as clusters, and the vertical projection of one cluster on the $X - Y$ plane is approximated by a triangle area form by the projections of the two outside mooring lines. In order to limit the possibility of a mooring line breaking and falling onto a subsea flowline, the flowlines are generally routed around the mooring line clusters. Therefore, these triangle projections are the restricted areas that the wellheads should not be located and the flowlines should not pass through [68].

The third is the risers. Riser configuration is not considered in the optimization model, instead, the length of the riser is given as input information, for the cost

estimation. Practically, enough distance should be left between the riser base and touch down point (TDP) to help absorb the dynamic tension from the riser due to the FPSO motions. This distance is assumed to be constant. And the riser projection length on the plane is constant, either.

The simplification of the riser connection is up to the type of FPSO. Figure 3.4 helps explain. For turret moored FPSO, riser could connect to the turret in any direction except crossing the mooring line cluster projection polygons. Therefore, the possible riser base positions should distribute on a circle centered on the projection of FPSO position, and the radius of the circle is the riser projection length, as shown in Figure 3.4(a).

For spread moored FPSO, usually, the riser interfaces distribute on the starboard or portside, so that the risers could only connect to one of two sides. Besides, since the riser joints on the FPSO are close with each other, and relatively much shorter compared with the riser length and flowline length, the riser joints are simplified as one single node located in the middle of the segment that represents the FPSO hull. Similarly, the possible riser base positions are thought to distribute on a circle centered on this simplified single point, and the radius of the circle is the riser projection length, as shown in Figure 3.4(b).

Under this simplification, the flowline section connects the riser base should be collinear with the riser projection in order to minimize the flowline length. Therefore, on the projection plane, the single node that represents the single point mooring system for turret moored FPSO, or the riser joints for spread moored FPSO, could be set as the terminal node at first for flowline route selection of the subsea production system, and the flowline route to riser base could be obtained by subtracting the riser horizontal projection, thus conveniently determine the location of riser base. Figure 3.4 illustrate the simplification for both types of FPSO.

Through those above assumptions and simplifications, to conveniently describe the subsea production system in the mathematical way, the well system, subsea production system and the terminal system including risers are all vertically projected to the same horizontal plane, as shown in Figure 3.5, which presents an example of manifold system.

As can be seen in Figure 3.5, on this projection plane, the well bottom, wellhead, and manifold are all treated as single nodes, using different types of symbol. The projection of well trajectory is the horizontal displacement, which is represented by the dotted line between wellhead and corresponding well bottom. The obstacles (restricted areas) are treated as polygons, and the vertices of these polygons are also treated as single nodes. In this thesis, we assumed the subsea obstacles to be convex polygons. The flowlines are represented by solid lines between the nodes. The flowline should be close to the obstacle edge if the straight connection is not

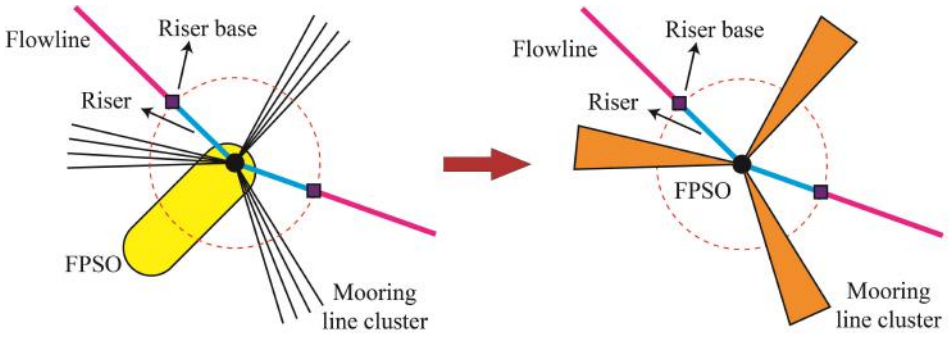

(a) Simplification of turret moored FPSO

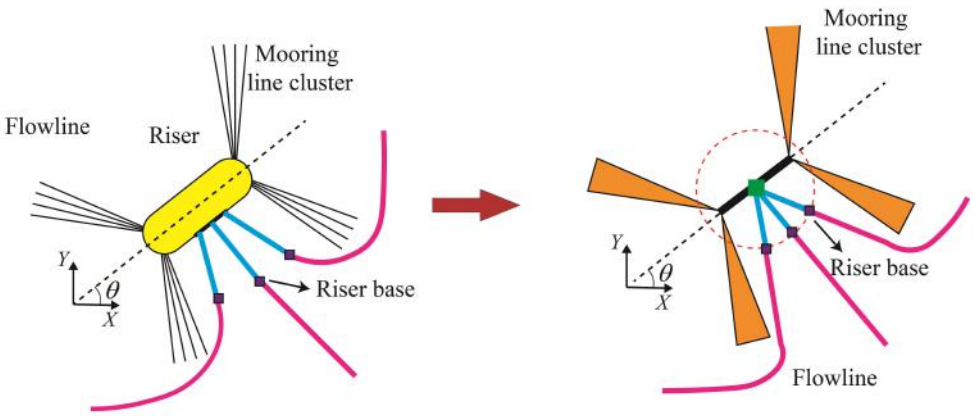

(b) Simplification of spread moored FPSO

Figure 3.4: Simplification of FPSO, mooring lines and riser connections

permitted since the flowline should not cross the obstacle areas, in order to minimize the flowline length. In the projection plane, this condition is represented by the polyline passing by several vertices of obstacle polygons, as shown in Figure 3.5.

The subsequent subsea production system layout optimization is abstracted into a network design problem on the projection plane shown in Figure 3.5, which is a graph with nodes and edges. For different subsea production system concept, the characters of connections between facilities are different, leading to different forms and ways of establishing the mathematical model. But there are several identical considerations, including the flowline crossing avoidance, and pressure loss estimations. The corresponding mathematical descriptions are all based on this vertical projection plane, which is presented in the next section.

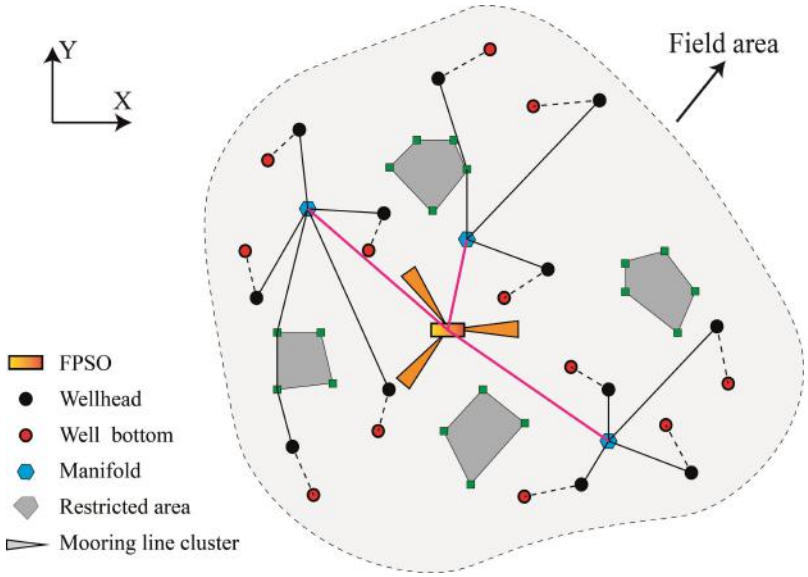

Figure 3.5: Vertical projection of the hydrocarbon flow system

3.2 General engineering considerations

3.2.1 Relation between flowlines

There are two relationships between any two different flowlines: intersected with each other or not. As discussed above, the flowlines are represented by polylines passing series of nodes. Any two consecutive nodes form one segment of the polyline. Therefore, analyzing the relationship between two flowlines could start from analyzing the relationship between two segments which belong to the two polylines respectively.

There are four kinds of relationships between two segments on the $X-Y$ plane: (a) strictly intersected, (b) separated from each other, (c) The two segments share one same vertex, and (d) partially coincide. Figure 3.6 briefly presents these four relationships.

All these four relationships have corresponding engineering meanings. Relationship (a) means that the flowline contains segment AB and flowline contains segment PQ are intersected, which should be avoided when determining the flowline route.

Relationship (b) is always what we desired. If any two segments from two flowlines respectively are separated, the two flowlines must be separated from each other.

Relationship (c) is a little special. Taking the scenario in Figure 3.6 as an example, since node Q is on the segment AB, there are actually three segments: AQ, PQ and QB. This scenario could be regarded as the following situation: The flowline segment PQ and flowline segment AQ share the node Q. If node Q is a kind of receiving node, such as manifold, segment QB will be a new route start from node Q, while if node Q is just an intermediate node, such as the vertices of obstacle

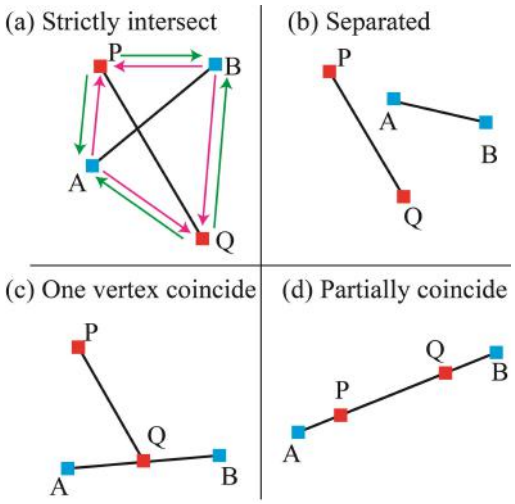

Figure 3.6: Relationship between two different segments

region as mentioned above, the segment QB belongs to both route "$P-Q-B$" and "$A-Q-B$", and could be regarded as two parallel closely laid flowline segments. Under this condition, the length of segment QB should be calculated twice to obtain the flowline lengths of the two different routes. As a result, relationship (c) is also acceptable.

Relationship (d) could also be regarded as that two parallel closely laid flowline segments, which is also acceptable.

Given the x and y coordinates, these relationships could be defined through vector cross product. Let

$$\begin{aligned} c_1 &= \left(\overrightarrow{AP} \times \overrightarrow{AQ}\right)\left(\overrightarrow{BP} \times \overrightarrow{BQ}\right) \\ c_2 &= \left(\overrightarrow{PA} \times \overrightarrow{PB}\right)\left(\overrightarrow{QA} \times \overrightarrow{QB}\right) \end{aligned} \tag{3.4}$$

$c_1 < 0$ AND $c_2 < 0$ reflects relationship (a). According to the above discussion, relationship (a) is defined as "strictly intersected", and the other three are defined as "not intersected". The calculation of eq.3.4 requires the coordinates of node A, B, P, and Q, so that an abstract function C_F related to the node coordinates is defined to represent the relationship between segment AB and PQ:

$$C_F(A,B,P,Q) = \begin{cases} 1, & AB \quad \text{strictly intersects with} \quad PQ \\ 0, & AB \quad \text{does not intersect with} \quad PQ \end{cases} \tag{3.5}$$

A,B,P,Q represents the corresponding node coordinates. The value of this function is either 0 or 1, which is a binary. This way of definition is for the purpose of combining with the optimization model to represent avoiding flowline intersection. In subsequent chapters, the detailed application process will be introduced.

3.2.2 Relation between flowline and obstacles

There are also two relationships between one flowline and one restricted area (or obstacle), intersected or not. Similarly, the relationship between segment and obstacle polygon should be discussed first. Based on the projection plane shown in Figure 3.5, the nodes on a flowline is either outside the obstacle polygon or belong to the vertices of the obstacle polygon, and all the possible relationship between the flowline segment and obstacle polygon could be exhausted, as shown in Figure 3.7.

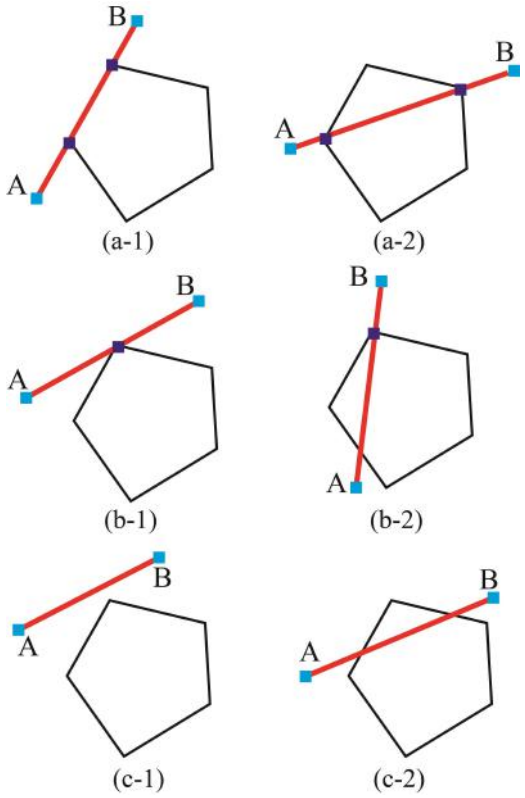

Figure 3.7: Different relationships between segment and obstacle polygon

Based on the relationship between segment vertices and polygon vertices, totally six different relationships are listed.

(a) The segment passes two of the polygon vertices. If the two vertices are adjacent, the segment coincides one of the polygon edges, which is defined as "not intersected" and is acceptable, as shown in Figure 3.7 (a-1), otherwise, the segment intersects the polygon. which is unfeasible, as shown in Figure 3.7.

(b) The segment passes only one of the polygon vertices. Under this condition, the segment is possible to be outside the polygon, as shown in Figure 3.7 (b-1), which is defined as "not intersected", or intersect one of the polygon edges, which is unfeasible, as shown in Figure 3.7 (b-2). Relationship (a) and (b) include the condition that the segment vertices coincide the polygon vertices.

(c) The segment does not pass any vertex of the polygon. Again, there are two

possibilities, one is that the segment separates from the polygon, which is defined as "not intersected", as shown in Figure 3.7 (c-1), and the other is that the segment intersects two of the polygon edges, which is unfeasible, as shown in Figure 3.7 (c-2).

Suppose the vertices of polygon are represented by $A_1, A_2, ..., A_k, ..., A_n, A_{n+1}$, where node A_{n+1} is coincide with node A_1, representing a closed polygon, and the vertices of segment AB are $A(x_A, y_A)$, $B(x_B, y_B)$. The process of mathematically describe these scenarios is shown below, using the function C_F which is proposed in the above section for the relationship of two segments.

① k from 1 to n, calculate $c_k = C_F(A, B, A_k, A_{k+1})$. If $c_k = 1$, the relationship corresponds to scenario (b-2) or (c-2) in Figure 3.7, AB intersects the polygon, BREAK. Else, turn to ②;

② k from 1 to n, set $N = 0$, determine whether node A_k is on the segment AB. If so, $N = N + 1$. Turn to ③;

③ Check the value of N. $N = 0$ and $N = 1$ correspond to scenario (c-1) and (b-1), respectively. Under both situation, AB does NOT intersect the polygon. If $N = 2$, check whether these two nodes are consecutive and if so, AB does NOT intersect the polygon, corresponding to scenario (a-1), otherwise, AB intersects the polygon, corresponding to scenario (a-2).

Let's use Ω to represent the polygon. An abstract function C_R is defined to represent the above process for the determination of the relationship between segment AB and polygon Ω:

$$C_R(A, B, \Omega) = \begin{cases} 1, & AB \quad \text{intersects} \quad \Omega \\ 0, & AB \quad \text{does not intersect} \quad \Omega \end{cases} \tag{3.6}$$

Similarly, A and B in eq. (3.6) represents the node coordinates, and the value of this function is also either 0 or 1, which is a binary. This way of definition is for the purpose of combining with the optimization model to represent the avoidance of restricted areas. In subsequent chapters, the detailed application process will be introduced.

3.2.3 Pressure and Temperature loss

The process of fluid flow from the wellhead to the topside through flowlines and risers is with both pressure and temperature loss due to the long distance of flowline and the low temperature of seawater. If the pressure loss is too high, the energy of the fluid itself might not be enough to maintain the flow process toward the topside, resulting in the need of measurements of energy compensation, such as

subsea pump and compressor, which brings extra expenditure. Therefore, we always prefer a layout with relatively lower pressure loss. And if the temperature loss is too high, the risk of wax deposition or hydrate formation will increase, leading to flow assurance problems. Some extra positive measurements could be implemented to prevent or remediate the problems, such as chemical injection, pipe heating, and pigging operations, bringing extra expenditure. Therefore, the temperature loss along the flowline should also be carefully considered.

Due to the variation of pressure and temperature along a flowline, the phase of the oil flowing inside keeps changing, presenting multiphase flow, usually considered as "gas-liquid" flow, or sometimes "gas-water-oil" flow. The hydraulic calculation of multiphase flow is complicated [88]. Considering that the temperature also affects the oil PVT properties besides pressure, the temperature and pressure drop should be calculated simultaneously, making it even more complicated and time-consuming.

In this thesis, the pressure loss is included to the optimization models, but we don't obtain the exact value, instead, since we prefer the low pressure loss system, the relative magintude of pressure loss is enough to identify whether it is high or not. As a result, some simpler equations are applied for convenient combining with the layout optimization.

The pressure loss of single phase flow in circular tube is relatively simple, as shown in eq. 3.7.

$$\Delta P = f_D \frac{\rho v^2 L}{2D} \tag{3.7}$$

where f_D is the friction factor, L is the flowline length, D is the flowline internal diameter, v is the flow velocity, and ρ is the fluid density. For laminar flow, the friction factor is inversely proportional to the Reynolds number, which is

$$f_D = \frac{64}{Re} \tag{3.8}$$

Considering that

$$Re = \frac{\rho v D}{\mu} \tag{3.9}$$

and

$$v = \frac{4Q}{\pi D^2} \tag{3.10}$$

where Q is the volume flow rate.

Substitute eq.(3.8)-eq.(3.10) into eq.(3.7), there is

$$\Delta P = \frac{128 \mu Q \Delta L}{\pi D^4} \tag{3.11}$$

Though eq. (3.11) reflects the pressure drop of single phase flow, it reveals the general relationship between pressure drop, flow rate, flowline length and size, so that the complex multiphase flow could be an analogy with the single phase flow for a simplification, and the term "QL/D^4" in eq.(3.11) is used to indirectly represent the level of pressure loss, instead of immediately calculating it. The term "QL/D^4" reflects the basic relationship between the pressure loss and the flow rate, pipe length as well as pipe diameter. Higher the value of this term is, higher the pressure loss will be. We use symbol "E" to represent the term "QL/D^4" in order to distinguish from the real pressure loss:

$$E = \frac{Q\Delta L}{D^4} \tag{3.12}$$

Different system layout results in different flowline length L and corresponding flow rate Q, leading to different values of "E", which reflects the magnitude of pressure loss. Eq. (3.12) is applied to build up the objective function for optimization models, which will be detailed presented in the subsequent chapter.

The temperature loss is an important aspect related to flow assurance. For the satellite well system, the wellheads are connected with the FPSO immediately through two flowlines and two risers, providing the flow loop for potential pigging operation for possible flow assurance problems. Under this condition, temperature loss is not the major consideration that affects the subsea layout, besides, since the flowlines of each wellhead are relatively independent of each other, the temperature drop tends to be minimized if the shortest flowline route is obtained, which is an important part for reducing the cost, so that it is feasible not to consider temperature loss for the optimization model.

For the manifold system, if wellheads are clustered, the wellheads and manifolds are connected through short jumpers, the temperature loss is very small, and the flowline loop could be built between manifolds and FPSOs, providing the capacity of pigging operation, so that the temperature loss for the cluster manifold system is not the major factor that affects the layout optimization, and is not included in the optimization model.

If wellheads are satellite distributed in the manifold system, the distances between wellheads and manifolds require longer flowlines. Considering that the pigging operation is not available between wellheads and manifolds (the flowline loop could only be built between manifolds and FPSOs) [89], the temperature along the flowline between wellheads and manifolds should not be too long in case of the wax or hydrate deposition. Insulation and inhibitor injection are the most common ways of avoiding these flow assurance problems. We do not include the temperature loss calculation in the optimization model, because the flow assurance measurements are

inevitable during the development of life. The optimized results could be further analyzed or verified, for example, software OLGA could be applied to simulate the temperature distribution throughout the whole pipeline network to help identify whether there is a risk of wax deposition or hydrate formation, as one of the additional notes for evaluating the proposed subsea arrangement. The optimization work in this thesis mainly provides several options for the subsequent further evaluation and offers an initial understanding of the cost level for the subsea system. Therefore, the subsequent evaluation process is not included.

In summary, the pressure loss will be included in the proposed models by using the term "QL/D^4" to represent the magnitude. The temperature loss is not included in the proposed models, and the flow assurance risks could be identified through further analysis of the optimized results, which is about another topic and not included in the thesis.

3.3 Chapter summary

In this chapter, the basic assumptions and simplifications are proposed, as the preparation for establishing the mathematical model for subsea production system layout optimization. The assumptions and simplifications are summarized below.

Assumptions:

1. The seabed topography and slope are assumed to be neglected so that the seabed is assumed to be a flat plane.
2. Seawater temperature around the subsea flowlines is assumed to be constant.
3. Restriction areas on the seabed are assumed to be polygons on the flat plane, acting as obstacles.
4. Riser configuration is not considered, and the length of risers are assumed to be equal, as well as the projection length of the seabed, which are all given as input information.
5. Well trajectory is assumed to be the combination of vertical part and horizontal part.

Simplifications:

1. Well production rate calculation is simplified, using simple theoretical equations.
2. FPSO hull is simplified to be a single node (for turret moored) or a short segment (for spread moored), and the projection of mooring line clusters are treated to be triangles, as the subsea obstacles.

3. The subsea production system, well system and floating platform all vertically project on the horizontal $X-Y$ plane, simplifying the layout optimization problem to be a network design on a graph.

4. The pressure loss along the flowline is represented by simple formulas, to simplifying the complicated calculation, while reflecting the magnitude of the pressure for the layout optimization.

There might be some extra assumptions or simplifications besides these ones for different concepts specifically, which are included in the subsequent chapters.

Chapter 4

Layout optimization of Satellite well system

4.1 Problem statement

There is a deepwater oil field to be developed, as shown in Figure 4.1. As discussed in Chapter 3, the layout optimization will be on the horizontal $X-Y$ plane where all the components of the system vertically project on, so that the related positions are represented by x and y coordinates.

N_W wells are designed to be deployed across the field area, for well W_l, the well bottom position is (x_l^{wb}, y_l^{wb}), the top depth of the reservoir from the seabed is H_l, and the reservoir thickness is h_l. The reservoir is considered uniform, and the permeability is K, and the oil viscosity is μ. The corresponding production rate is Q_l^w, $l = 1, 2, 3, ..., N_W$, which could be calculated through eq. (3.2) or eq.(3.3), depending on the well type.

In the field area, there are several restricted areas that the flowlines should avoid intersecting. The number of these areas is R. Restricted area A_r is treated as a convex polygon and represented by a sequence of vertices $(x_1^r, y_1^r), (x_2^r, y_2^r), ..., (x_{t_r}^r, y_{t_r}^r), (x_1^r, y_1^r)$. The last and first vertices are the same, indicating a closed polygon. The segment between any two consecutive vertices represents one of the polygon edges. The vertex number of area A_r is t_r (the last vertex is not included becasue it is the same with the first one), $r = 1, 2, ..., R$. Before being input into the optimization model, these restricted areas will be first of all extended considering the safety distance as discussed in section 3.1.2.

Spread-moored FPSO is chosen to be the terminal of the production system. The mooring lines' information such as orientations and lengths are predetermined and provided as input parameters. The number of FPSO designed to receive the production of the field is N_{fpso}. The positions of the FPSOs are (x_t^{fpso}, y_t^{fpso}), and

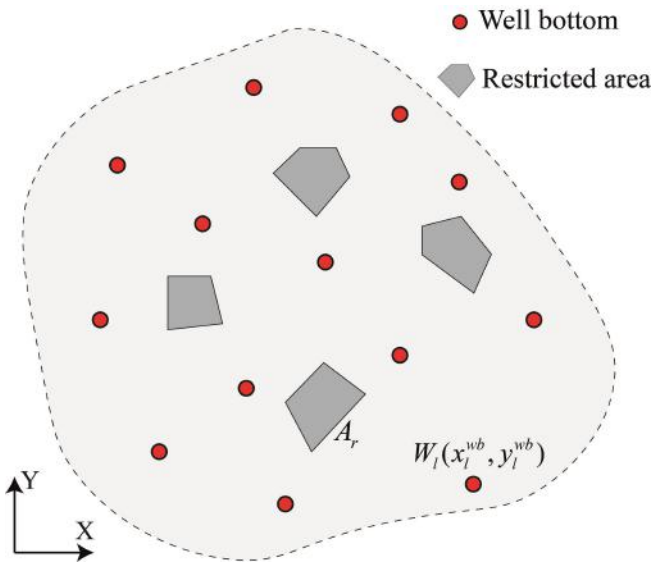

Figure 4.1: Schematic view of input information: Well bottom and restricted area distribution

each FPSO has four mooring line clusters. The projections of these clusters on the horizontal plane are also the obstacles that should be avoided, as shown in Figure 4.1.

The number of available sizes is N_{fpso}^{ava}, for size s, the processing capacity is $Q_s^{process}$, and the maximum riser number is N_s^{riser}, and the corresponding price is CP_s^{fpso}. Larger FPSO is with higher price. Since the inital production of the field is with low water cut, we consider the oil processing capacity as the restriction, in order to ensure the FPSOs could handle the production during the high oil production period.

Considering that for deepwater field development, it is preferred to use standardized flowlines [85], the sizes of all the flowlines that connecting wellhead and riser base, and the risers from the riser base to the FPSO are the same. The price of riser and flowline are considered the same, either, which is presented by CP^{line}

To establish a subsea production system under the concept of satellite well system for the field production, there are three points that should be determined:

1. *The assignment between the wells and FPSOs, that is, to determine which FPSO should one well be connected.*

2. *The size of the FPSO for the field production, depending on the production rate and the number of the wells that are connected.*

3. *The flowline routes between wells and FPSOs, which should avoid the subsea obstacles. The wellhead locations and the length of the horizontal part if the horizontal well is to be used.*

The objectives include the following three aspects.

1. *The total cost should be as low as possible.*
2. *The payback period should be as short as possible*
3. *The pressure losss should be as low as possible*

For the concept of satellite well system, two different scenarios are considered, the first is that all wells are vertical, which means that the wellhead positions coincide with the corresponding well bottom positions on the flat plane, and the second is that horizontal wells are considered for production, under which the wellhead positions become decision variables. The mathematical models for both scenarios are developed, respectively.

4.2 Mathematical model

4.2.1 Scenario 1: Vertical well

Adjacent matrix

As discussed above, on the flat plane, there are three types of nodes:

(1) Riser porch nodes. For spread moored FPSO, the riser porch node is the middle point of the assumed segment which represents the FPSO hull. The node set is $\mathcal{I}_{\mathcal{F}}$, and the element number is equal to the designed number of FPSO.

(2) Wellhead nodes. For vertical well, the wellhead position coincides with the corresponding well bottom position on the flat plane. The node set is $\mathcal{I}_{\mathcal{W}}$, and the element number is equal to the number of wells.

(3) Obstacle nodes. The obstacle regions will first of all be extended as mentioned in section 3.1.2, and the vertices of the extended obstacle polygons are defined as set $\mathcal{I}_{\mathcal{O}}$. The vertices of each obstacle are arranged by the order in this node set, which are represented as

$$\mathcal{I}_{\mathcal{O}} = \{\mathcal{I}_{\mathcal{O}1}, \mathcal{I}_{\mathcal{O}2}, ..., \mathcal{I}_{\mathcal{O}r}, ..., \mathcal{I}_{\mathcal{O}R+4N_{fpso}}\} \tag{4.1}$$

The subsea restricted areas and the mooring line clusters projections are all included in the obstacle node set, since each FPSO has four mooring line clusters, the total number of obstacles is $R + 4N_{fpso}$. In this node set, the r^th subset denotes the r^{th} obstacle, Ω_r

To design the layout for the concept of satellite well system is actually to find a way of connecting the above defined nodes. Wellheads are the start nodes while the riser porches are the end nodes. The obstacle nodes act as the intermediate nodes,

which the flowline routes might pass by in order to avoid crossing with the obstacle regions. Therefore, we could define an integral node set that put all the kind of nodes together, let

$$\mathcal{I} = \{\mathcal{I}_{\mathcal{F}}, \mathcal{I}_{\mathcal{W}}, \mathcal{I}_{\mathcal{O}}\} \tag{4.2}$$

The coordinates of node i in set $\mathcal{I}$ is represented by ND_i. The adjacent matrix V,is defined to indicate the connectivity between any two nodes, node i, $j \in \mathcal{I}$. If the two nodes could be connected, $V(i,j) = 1$, otherwise, $V(i,j) = 0$. The connectivity depends on whether their connection intersects with any of the obstacles, which could be calculated through function C_R shown in eq.(3.6) defined in Chapter 3, therefore,

$$V(i,j) = \begin{cases} 1, & \sum_{r=1}^{R+4N_{fpso}} C_R(ND_i, ND_j, \Omega_r) = 0 \\ 0, & \sum_{r=1}^{R+4N_{fpso}} C_R(ND_i, ND_j, \Omega_r) > 0 \end{cases} \tag{4.3}$$

The positions of all related nodes as well as the obstacles are known, the adjacent matrix M is fixed for the layout optimization. The adjacent matrix is used to develop the layout optimization model.

Decision variables

Binary variable x_{ij} is introduced to indicate the connection relationship between the nodes for the subsea layout. If node i is connected to node j, $x_{ij} = 1$, otherwise, $x_{ij} = 0$.

Continuous variable Q_{ij} is introduced to indicate the flow rate between node i and node j.

Binary variable z_{ts} is introduced to indicated the selection of FPSO from the available options. If the size s is selected for FPSO t, $z_{ts} = 1$, otherwise, $z_{ts} = 0$.

Due to the existence of subsea obstacles, the wellheads and FPSO could not be connected with straight lines directly, instead, the vertices of obstacle polygons might become the intermediate nodes of flowline route, in order to avoid crossing with the obstacles, as shown in Figure 4.2(a). Under this condition, it is possible that two or more flowline routes pass by the same intermediate node, which is then like a "shared node". Considering that usually the routes passing by the same intermediate node area close with each other, they should be toward the same terminal (FPSO) to achieve shorter flowline length, thus reducing cost, therefore, from the "shared node" to the same terminal (FPSO), the route should be with the shortest, which is unique, as shown in Figure 4.2(b). As a result, these flowline routes after the "shared node" are overlapped, which could be regarded as parallelly laid. For example in

Figure 4.2 (b), the routes start from node A and node B overlap from node C to the terminal node F. Therefore, these overlapped segments need to be calculated twice for the total flowline length.

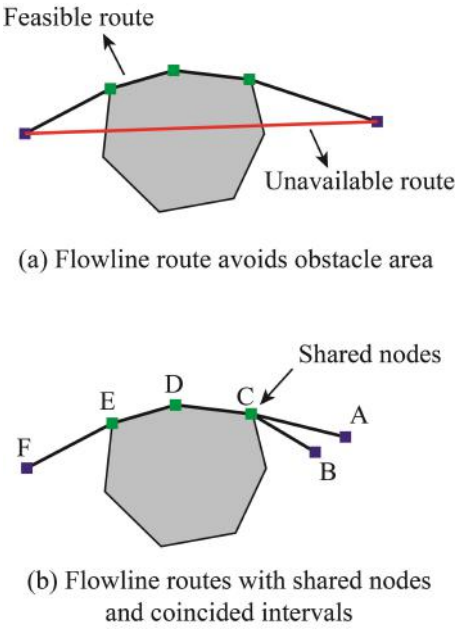

Figure 4.2: Flowline routes that avoid obstacles

Using the binary variable x_{ij} could only represent the connection relationship, but the times that one segment is selected for different routes could not be reflected simply through x_{ij}. So non-negative integer variable q_{ij} is introduced, which represent that segment from node i to node j is selected for q_{ij} times.

Cost components

The components of the total cost could be represented by these defined decision variables.

Drilling cost:

$$COST_{drilling} = P_v L_v = \sum_{l=1}^{N} P_v (H_l + h_l) \tag{4.4}$$

The term $H_l + h_l$ represents the reservoir bottom depth, which means that the vertical well bottom locates at the reservoir bottom.

Flowline cost:

$$COST_{flowline} = 2P^{line} \sum_{i \in \mathcal{I}} \sum_{j \in \mathcal{I}} d_{ij} q_{ij} \tag{4.5}$$

The term d_{ij} is the distance between node i and node j, which should be calculated according to the adjacent matrix, as shown in eq. (4.6). The number "2" means each wellhead has two flowlines to form a loop, so that the length should be calculated twice to represent the total length, as discussed in Chapter 2. For the

same reason, the riser cost expression is also with the factor "2". The same condition will occur for the manifold system, when calculating the export line lengths between manifolds and FPSOs and the riser lengths.

$$d_{ij} = \begin{cases} \sqrt{(NDx_i - NDy_i)^2 + (NDx_j - NDy_j)^2}, & V_{ij} = 1 \\ +\infty, & V_{ij} = 0 \end{cases} \tag{4.6}$$

NDx and NDy represents the x and y coordinates, respectively. When $V(ij) = 0$, the $+\infty$ could be denoted by a very large number for the purpose of computer programming.

Riser cost:

$$COST_{riser} = 2P^{riser}NL_{riser} \tag{4.7}$$

L_{riser} is the riser length, which is assumed to be constant. Similarly, to each wellhead requires two risers, so that the total riser number is 2 times of well number N_W.

FPSO cost:

$$COST_{fpso} = \sum_{t=1}^{N_{fpso}} \sum_{s=1}^{N_{fpso}^{ava}} P_s^{fpso} z_{ts} \tag{4.8}$$

The total cost is

$$COST_{total} = COST_{drilling} + COST_{flowline} + COST_{riser} + COST_{fpso} \tag{4.9}$$

Here the cost of X-trees is not taken into considerations for the total cost. This is because the number of wells are provided for the layout optimization, and the cost for X-trees keeps constant, which will not affect the optimization results. Besides, under different scenarios and concepts, the cost of the X-trees are the same, therefore, for the subsequent models for different scenarios, the cost of X-trees is also not taken into account.

Pressure loss

Through eq.(3.12), the total pressure loss of the whole system from wellheads to FPSOs is represented by

$$E_{total} = \sum_{i\in\mathcal{I}} \sum_{j\in\mathcal{I}} \frac{Q_{ij}d_{ij}}{D^4} + \sum_{j\in\mathcal{I}_\mathcal{F}} \sum_{i\in\mathcal{I}} \frac{Q_{ij}L_{riser}}{D^4} \tag{4.10}$$

At the right side of the equal sign, the first term reflects the pressure loss level between wellheads and riser bases, and the second term reflects the pressure loss level in the risers. Note that the decision variable Q_{ij} represent the flow rate in any two nodes of the whole node-set, and we choose the nodes that belong to FPSO

node-set $\mathcal{I}_{\mathcal{F}}$ to represent the flow toward the FPSO nodes, which is set as the range for the outer summation in the second term.

Payback period

The payback period refers to the amount of time it takes to recover the cost of an investment. In this thesis, the static payback period that does not consider the discount rate is used, and besides, we assumed that all the produced fluid is oil, and the income equals to the oil sales, therefore, the payback period PB is

$$PB = \frac{COST_{total}}{P^{oil} \sum_{l=1}^{N} Q_l^w} \tag{4.11}$$

P^{oil} is the oil price, which is assumed constant. Q_l^w could be obtained through eq.(3.2). This payback period expression won't be very accurate, and is relatively rough and simple, which does not consider the OPEX (operating expense) and the possible variation of oil price, but the value reflects the link between the total cost and the production rate and providing a rough consideration for the time length that balancing the total cost through selling the produced oil. As a result, it is set to be one of the objective functions.

Constraints

Following constraints should be satisfied, for a feasible layout of the satellite well system.

$$x_{ij} \leq V(i,j) \quad \forall i,j \in \mathcal{I} \tag{4.12}$$

$$\psi x_{ij} \leq q_{ij} \leq \Psi x_{ij} \quad \forall i,j \in \mathcal{I} \tag{4.13}$$

$$\psi q_{ij} \leq Q_{ij} \leq \Psi q_{ij} \quad \forall i,j \in \mathcal{I} \tag{4.14}$$

$$x_{ij} + x_{ji} \leq 1 \quad \forall i,j \in \mathcal{I} \tag{4.15}$$

$$\sum_{j \in \mathcal{I}} x_{ij} = 1, \quad \sum_{j \in \mathcal{I}} x_{ji} = 0 \quad \forall i \in \mathcal{I}_{\mathcal{W}} \tag{4.16}$$

$$\sum_{j \in \mathcal{I}} q_{ij} = 1, \quad \sum_{j \in \mathcal{I}} q_{ji} = 0 \quad \forall i \in \mathcal{I}_{\mathcal{W}} \tag{4.17}$$

$$\sum_{j\in\mathcal{I}} Q_{ij} = Q^{w}_{i_w}, \quad \sum_{j\in\mathcal{I}} Q_{ji} = 0, \quad i_w = i - N_{fpso} \quad \forall i \in \mathcal{I}_{\mathcal{W}} \tag{4.18}$$

$$\sum_{j\in\mathcal{I}} x_{ij} = 0, \quad \sum_{j\in\mathcal{I}} x_{ji} \leq \frac{1}{2} \sum_{s=1}^{N^{ava}_{fpso}} (N^{riser}_{s} z_{ts}), \quad t = i, \quad \forall i \in \mathcal{I}_{\mathcal{F}} \tag{4.19}$$

$$\sum_{j\in\mathcal{I}} q_{ij} = 0, \quad \sum_{j\in\mathcal{I}} q_{ji} \leq \frac{1}{2} \sum_{s=1}^{N^{ava}_{fpso}} (N^{riser}_{s} z_{ts}) \quad t = i, \quad \forall i \in \mathcal{I}_{\mathcal{F}} \tag{4.20}$$

$$\sum_{j\in\mathcal{I}} Q_{ij} = 0, \quad \sum_{j\in\mathcal{I}} Q_{ji} \leq \sum_{s=1}^{N^{ava}_{fpso}} (Q^{riser}_{s} z_{ts}), \quad t = i, \quad \forall i \in \mathcal{I}_{\mathcal{F}} \tag{4.21}$$

$$\sum_{i\in\mathcal{I}_{\mathcal{F}}} \sum_{j\in\mathcal{I}} x_{ji} \leq N_W, \quad \sum_{i\in\mathcal{I}_{\mathcal{F}}} \sum_{j\in\mathcal{I}} q_{ji} = N_W, \quad \sum_{i\in\mathcal{I}_{\mathcal{F}}} \sum_{j\in\mathcal{I}} Q_{ji} = \sum_{i_w=1}^{N} Q^{w}_{i_w}, \quad \forall i \in \mathcal{I}_{\mathcal{F}} \tag{4.22}$$

$$\sum_{j\in\mathcal{I}} q_{ij} - \sum_{j\in\mathcal{I}} q_{ji} = 0, \quad \sum_{j\in\mathcal{I}} Q_{ij} - \sum_{j\in\mathcal{I}} Q_{ji} = 0, \quad \sum_{j\in\mathcal{I}} x_{ij} \leq 1, \quad \forall i \in \mathcal{I}_{\mathcal{O}} \tag{4.23}$$

Eq.(4.12) shows that node i and node j must be connectable, if not, $x_{ij} = 0$;

Eq.(4.13) and (4.14) clarify the relationship between the variable x_{ij}, q_{ij}, and Q_{ij}: if $x_{ij} = 0$, the other two variables are equal to zero, indicating that there is no flow between node i and node j if they are not connected, and if $x_{ij} = 1$, the other two variables are larger than zero and must not be equal to zero, indicating that if node i and node j are connected, the flow must exist. Here ψ is a very small number to limit the variable won't be equal to zero when $x_{ij} = 1$, and Ψ is a large number.

Eq.(4.15) means that the flow between node i and node j should only be in one single direction.

Eq.(4.16) and (4.17) presents that one well should only have one route, and the wellhead nodes are the start of the flowline routes, no path exists from anywhere toward the wellhead nodes.

Eq. (4.18) defines the flow rate at wellhead nodes. Since the wellhead nodes are the start nodes, the flow rates equal to the production rates of corresponding wells, which are obtained through eq.(3.2), and no other flow enters these nodes.

Eq. (4.19) and (4.20) describe the connection requirements at the riser porches nodes. These nodes are the terminals of flowline routes, and for each riser porch node, the number of connected flowlines should not exceed the maximum number of the selected size of FPSO.

Eq. (4.21) is the requirement that no flow exits the riser porch nodes, indicating

that these nodes are the end of flowlines. And for each riser porch node, the total flow rate from the connected flowlines should not exceed the maximum processing capacity of the selected size of FPSO.

Eq. (4.22) is the constraints for the whole system, which is that the total number of the flowlines connected to riser porch nodes should equal to the number of wells, and the total flow rate should equal to the total production rate of the wells.

Eq. (4.23) includes the constraints for the intermediate nodes, which belongs to the obstacle vertices. According to the discussions above, it is possible that two or more route have some part overlapped, though the routes are regarded parallelly laid, the total flow rate in these overlapped flowlines is equal to the sum of the flow rate before the shared node, which presenting conservative, as shown by the first two equalities. Besides, starting from node i, at most one node could be connected, which is described by the third term of eq. (4.23).

General form of the mathematical model

The above discussions have already proposed the three key aspects of an optimization model: decision variables, objective functions, and constraints. Three objective functions are defined: the minimum total cost, the minimum pressure loss, and the minimum payback period. In the subsequent sections, these three objective functions are studied separately and the optimization results are compared.

No matter which objective function is considered, it is the function of the decision variables, and the constraints are also the function of the decision variables. On the other hand, the adjacent matrix, and the oil production rate of each well could be obtained through the input information, indicating that they are independent of the decision variables. Therefore, the simplified representation of this model could be written as:

$$\begin{aligned} &\min \quad f(\boldsymbol{x}, \boldsymbol{z}, \boldsymbol{q}, \boldsymbol{Q}) \\ &\text{subject to} \\ &\begin{cases} g(\boldsymbol{x}, \boldsymbol{z}, \boldsymbol{q}, \boldsymbol{Q}) = 0 \\ h(\boldsymbol{x}, \boldsymbol{z}, \boldsymbol{q}, \boldsymbol{Q}) <= 0 \end{cases} \end{aligned} \tag{4.24}$$

The objective function could be the total cost or pressure loss. The constraint functions g and h represents the equality constraint set, and the inequality constraint set, respectively. $\boldsymbol{x}$, $\boldsymbol{z}$, $\boldsymbol{q}$, $\boldsymbol{Q}$ are the decision variable sets, and each stands for the corresponding variable matrix defined above.

Obviously, the objective function and the constraints are all linear, and the decision variables include both integer variables and continuous variables, therefore, the proposed model is mixed-integer linear programming problem (MILP).

4.2.2 Scenario 2: Horizontal well

Treatment of wellhead locations and adjacent matrix

The longer length of horizontal displacement leads to the shorter length of flowline, thus reducing the flowline cost, but at the same time, the cost for drilling increases, making the total cost varies, while the well production rate increases, which brings more income. Therefore, it makes sense to find proper horizontal displacements for the wells in order to balance the cost and income, which means the wellhead locations become the extra decision variables besides the mentioned ones in Scenario 1. Figure 4.3 helps explain how to deal with these newly added decision variables.

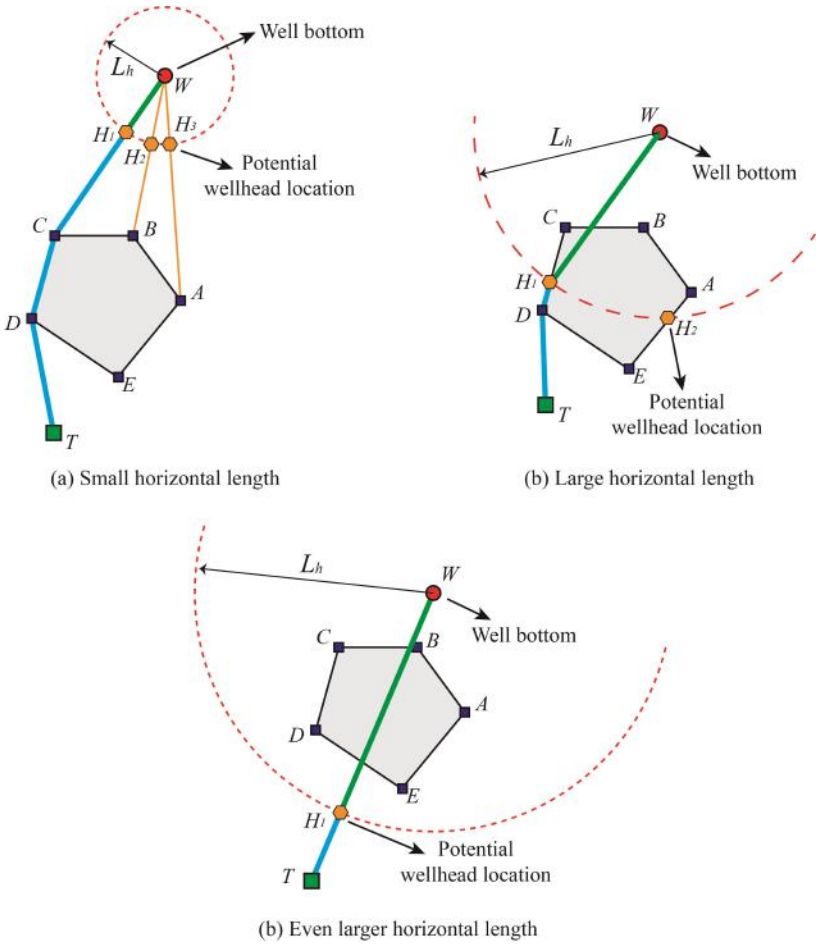

Figure 4.3: Potential wellhead locations under different scale of horizontal displacements

To decide the wellhead location of one well, there are two parameters, one is the horizontal displacement, and the other is the orientation relative to the well bottom. As shown in Figure 4.3, the well bottom is node W and the horizontal length of the well is L_h. On one hand, the possible wellhead position should be located on the circle centered on node W with radius L_h. Assuming that the vertical depth around the well bottom is constant, according to eq. (3.1), with the horizontal length L_h,

the drilling cost is fixed.

On the other hand, the flowline route will pass through a series of nodes. Considering the possible wellhead location described in the above paragraph, the flowline route length should be as small as possible to reduce the cost. For example, in Figure 4.3(a), initially we do not know where the wellhead is and what the route between wellhead node and the terminal node T will be like. But it could be inferred that, if the route pass through node A, to minimize the flowline route length, the wellhead should be located at node H_3, which makes flowline segment AH_3 and well trajectory projection H_3W be collinear. For the same reason, the node H_2 and H_1 are also potential wellhead locations in case that node B and node C are selected for the flowline route, respectively.

As long as the horizontal displacement is given, the orientation could be obtained based on the above-proposed idea. Therefore, the decision variables could be simplified to be horizontal displacements of all the wells, instead of the wellhead locations. We could first of all set the well bottom node as the start node for the flowline route on the flat plane, after obtaining the best flowline route, the wellhead location could be achieved by subtracting the length of horizontal displacement of the well along the determined flowline route.

When applying this method, according to the value of the horizontal displacement L_h, there are several situations that should be carefully treated.

1. ***Situation 1:*** The horizontal displacement is relatively small, as shown in Figure 4.3(a). Through the above-mentioned method, the route $W-C-D-T$ is with the shortest length when initially setting well bottom node W to be the start, and wellhead location should be H_1, making the final flowline route be "$W-C-D-H_1$" and the well trajectory projection be "H_1-W". Under this condition, the original nodes and connection relationships are not affected, meaning that the adjacent matrix obtained through eq. (4.3) could stay the same while applying the above-described rule for determining the wellhead locations. The distance matrix d_{ij} need to be modified in order to represent the flowline cost through eq. (4.25)

$$d_{ij} = \begin{cases} d_0, & V_{ij}=1, \quad i \notin \mathcal{I}_{\mathcal{W}}, \quad j \notin \mathcal{I}_{\mathcal{W}} \\ d_0 - L_{hl}, & V_{ij}=1, \quad i \in \mathcal{I}_{\mathcal{W}}, \quad l = i - N_{fpso} \quad \text{or} \\ & \qquad\quad j \in \mathcal{I}_{\mathcal{W}}, \quad l = j - N_{fpso} \\ +\infty, & V_{ij}=0 \end{cases} \tag{4.25}$$

$$d_0 = \sqrt{(NDx_i - NDy_i)^2 + (NDx_j - NDy_j)^2}$$

L_{hl} is the horizontal displacement of the l_{th} well.

2. ***Situation 2:*** As shown in Figure 4.3(b) and (c), the horizontal displacement is large enough so that some nodes are inside the circle region and the circle intersects with some of the segments between node. In Figure 4.3(b), node A, node B and node C are inside the circle area, and the circle intersect with segment CD and AE, at node H_1 and H_2, respectively. Under this situation, the flowline route will not pass through the nodes inside the circle because the distance to the well bottom is smaller than the horizontal displacement. Instead, node H_1 and H_2 could be included to the node set for the flowline route, and once anyone of them is passed through, it will be the wellhead location. As shown in the figure, route "$T - D - H_1$" is the flowline route, H_1 is the wellhead location, and "H_1W" is the projection of the well trajectory.

   In Figure 4.3(c), the horizontal displacement is even larger so that all the vertices of the obstacle polygon are inside the circle area, for the same reason with Figure 4.3(b), the flowline route should be $T - H_1$, H_1 is the wellhead location, and "H_1W" is the projection of the well trajectory. Note that the well trajectory projection intersects with the obstacle area, which is feasible because the underground well trajectory is not affected by the seabed obstacles.

   Therefore, according to the analysis, different from ***Situation 1***, the adjacent matrix obtained through eq.(4.3) needs to be modified. First, the nodes that are inside the circle area will not be connectable with well bottom nodes, therefore, the corresponding element in the adjacent matrix V_{ij} should be set to 0. And second, the intersections should be included in the node set for the adjacent matrix, and the corresponding connectivity with other nodes should be determined.

   After modifying the adjacent matrix, the distance matrix d_{ij} should then be obtained, through eq.(4.25).

Actually, in a field with many wells, these above situations usually occur simultaneously, depending on the horizontal displacement of each well, and the distribution of well bottoms, seabed obstacles and the FPSO locations. Therefore, given a set of horizontal displacement L_{hl} of the well bottom, the general process of establishing the adjacent matrix and the distance matrix is as follows:

① Generate initial adjacent matrix through according to eq. (4.3);

② For each well, say well l, draw the circle centered on the well bottom W_l with radius L_{hl}. Update the adjacent matrix and the distance matrix through the processes described for ***Situation 1*** and ***Situation 2***.

The adjacent matrix V_{ij} and the distance matrix d_{ij} are the prerequisites for establishing the subsea layout optimization model. When considering horizontal well type, these two matrices are related to the horizontal displacement L_{hl}, which could be represented by

$$\boldsymbol{V} = f_a(\boldsymbol{L_h}) \tag{4.26}$$

$$\boldsymbol{d} = f_d(\boldsymbol{L_h}) \tag{4.27}$$

Where $\boldsymbol{V}$, $\boldsymbol{d}$ and $\boldsymbol{L_h}$ represent for the adjacent matrix elements set, distance matrix elements set, and the horizontal displacement set, respectively, for convenient description.

Decision variables

Besides the horizontal displacements of the wells, the other decision variables are defined the same as scenario 1. The decision variables are listed below, and the detailed definitions and explanations are in section 4.2.1.

1. Binary variable x_{ij}, indicating the connection relationship between the nodes for the subsea layout.
2. Non-negative integer variable q_{ij}, representing the times for which the segment between node i and j is selected.
3. Binary variable z_{ts}, indicating the selection of FPSO.
4. Continuous variable Q_{ij}, indicating the flow rate in the segment between node i and j
5. Continuous variable L_{hl}, indicating the horizontal displacement of well l.

Cost components

The components of the total cost could be represented by these defined decision variables.

Drilling cost:

$$COST_{drilling} = \sum_{l=1}^{N} P_v \frac{H_l + h_l + H_l}{2} + \sum_{l=1}^{N} P_h L_{hl} \tag{4.28}$$

At the right side of the equal sign, the first term is the drilling cost for the vertical part, and we consider the well bottoms are located in the middle of the reservoir,

in order to provide enough flow area around the well, which is different from the vertical well type. The second term is the drilling cost for the horizontal part.

The flowline cost is

$$COST_{flowline} = 2P^{line} \sum_{i \in \mathcal{I}} \sum_{j \in \mathcal{I}} d_{ij} q_{ij} \tag{4.29}$$

The riser cost is

$$COST_{riser} = 2P^{riser} N L_{riser} \tag{4.30}$$

The FPSO cost is

$$COST_{fpso} = \sum_{t=1}^{N_{fpso}} \sum_{s=1}^{N_{fpso}^{ava}} P_s^{fpso} z_{ts} \tag{4.31}$$

The total cost is

$$COST_{total} = COST_{drilling} + COST_{flowline} + COST_{riser} + COST_{fpso} \tag{4.32}$$

Pressure loss

Through eq.(3.12), the total pressure loss of the whole system from wellheads to FPSOs is represented by

$$E_{total} = \sum_{i \in \mathcal{I}} \sum_{j \in \mathcal{I}} \frac{Q_{ij} d_{ij}}{D^4} + \sum_{j \in \mathcal{I}_{\mathcal{F}}} \sum_{i \in \mathcal{I}} \frac{Q_{ij} L_{riser}}{D^4} \tag{4.33}$$

Payback period

The same as scenario 1 for vertical well type, the payback period is

$$PB = \frac{COST_{total}}{P^{oil} \sum_{l=1}^{N} Q_l^w} \tag{4.34}$$

Q_l^w could be obtained through eq.(3.3) for the horizontal well production rate.

Constraints

Constraints from eq.(4.12) to eq.(4.23) for the scenario 1 are also the constraints for scenario 2, which considers the horizontal well type. In addition, since the horizontal displacement is the total length of the well trajectory projection, the actual interval for production should be shorter, and in this thesis, we define the ratio between the length of production interval and the horizontal displacement as β, and $L_{pl} = \beta L_{hl}$. When calculating the oil production rate through eq.(3.3) for Q_l^w, the horizontal length should use L_{pl}. Besides, usually due to the technical

requirements and limitations, the production interval length could not be infinite and has an upper bound, which is represented by

$$L_{pl} = \begin{cases} \beta L_{hl}, & \beta L_{hl} \leq L_{upper}, \quad l = 1, 2, ..., N \\ L_{upper}, & \beta L_{hl} > L_{upper}, \quad l = 1, 2, ..., N \end{cases} \tag{4.35}$$

The relation between horizontal displacement and the production rate could also be schematically presented through Figure.4.4.

Furthermore, the adjacent matrix V_{ij} and the distance matrix d_{ij} are both related to the horizontal displacement, as shown in eq.(4.26) and eq.(4.27).

As a result, eq.(4.12) to eq.(4.23), eq.(4.35), eq.(4.26) and eq.(4.27) together form the constraints for the layout optimization for satellite well system considering horizontal well type.

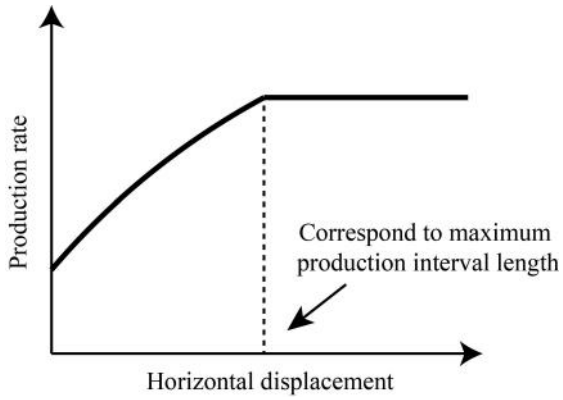

Figure 4.4: Schematical view of the relationship between horizontal displacement and production rate of one well

General form of the mathematical model

Based on the above analysis, the general form of the optimization model could be written as

$$\begin{aligned} &\min \quad f(\boldsymbol{x}, \boldsymbol{z}, \boldsymbol{q}, \boldsymbol{Q}, \boldsymbol{L_h}, \boldsymbol{V}, \boldsymbol{d}) \\ &\text{subject to} \\ &\begin{cases} g(\boldsymbol{x}, \boldsymbol{z}, \boldsymbol{q}, \boldsymbol{Q}, \boldsymbol{L_h}, \boldsymbol{V}, \boldsymbol{d}) = 0 \\ h(\boldsymbol{x}, \boldsymbol{z}, \boldsymbol{q}, \boldsymbol{Q}, \boldsymbol{L_h}, \boldsymbol{V}, \boldsymbol{d}) <= 0 \\ \boldsymbol{V} = f_a(\boldsymbol{L_h}) \\ \boldsymbol{d} = f_d(\boldsymbol{L_h}) \end{cases} \end{aligned} \tag{4.36}$$

Eq.(4.26) and eq.(4.27) are regarded as the auxiliary equations, so that the decision variables are $\boldsymbol{x}$, $\boldsymbol{z}$, $\boldsymbol{q}$, $\boldsymbol{Q}$, $\boldsymbol{L_h}$. Different from the model for vertical well type,

the introduction of horizontal displacement $\boldsymbol{L_h}$ brings nonlinearity to the model, making it become mixed-integer nonlinear programming problem (MINLP).

4.3 Solution method

Two models are proposed considering vertical well and horizontal well, respectively, which are named **MODEL 1** and **MODEL 2** to distinguish from each other.

GUROBI Optimizer is applied to help solve these models. GUROBI Optimizer is a commercial optimization solver for linear programming (LP), quadratic programming (QP), quadratically constrained programming (QCP), mixed-integer linear programming (MILP), mixed-integer quadratic programming (MIQP), and mixed-integer quadratically constrained programming (MIQCP). Branch and bound algorithm is the basic method for solving these problems [77], which is the built-in part of the optimizer. GUROBI could find both feasible and proven optimal solutions very fast. As discussed, **MODEL 1** is a MILP model, so that it could be solved through GUROBI immediately.

However, **MODEL 2** is nonlinear due to the introduction of the variable "$\boldsymbol{L_h}$", and it is not quadratic so that it is unavailable to use GUROBI immediately. Therefore, a decomposition process through gradient descent for **MODEL 2** is proposed in order to find the solution.

Suppose the $\boldsymbol{L_h}$ was known, $\boldsymbol{V}$ and $\boldsymbol{d}$ would aslo be known, and **MODEL 2** would degenerate to a MILP model, named **MODEL 2d**, which is alomost the same with **MODEL 1**. Obviously, **MODEL 2d** could be solved by GUROBI. If we use y to represent the solution of **MODEL 2d** under given value of $\boldsymbol{L_h}$, then different $\boldsymbol{L_h}$ correspond to different y, which could be written as the form of function: $y = F(\boldsymbol{L_h})$. The function F represent the solution of **MODEL 2d**. Therefore, finding the minimum value of objective function for the original **MODEL 2** could be transformed to find the minimum value of $F(\boldsymbol{L_h})$. And the original model is decomposed to two part, as shown in the eq.(4.37). This equation is just for an overview of the decomposed models and the constraints are not presented.

$$\begin{cases} \min \quad y \\ y = F(\boldsymbol{L_h}) \\ F(\boldsymbol{L_h}) = \min\{f(\boldsymbol{x}, \boldsymbol{z}, \boldsymbol{q}, \boldsymbol{Q})\} \end{cases} \tag{4.37}$$

Note that for function $F(\boldsymbol{L_h})$, $\boldsymbol{L_h}$ is a vector that contains the horizontal displacement of all the wells. For convenient description, we use $X = [x_1, x_2, ..., x_n]$ to represent these unknown variables, then what we need to do is to find the minimum value of $F(X)$.

Gradient descent is a first-order iterative optimization algorithm for finding the minimum of a function. For this case, the iteration form of gradient descent is written as

$$X_{k+1} = X_k - \alpha \frac{\nabla F(X_k)}{\|\nabla F(X_k)\|} \tag{4.38}$$

The subscript k represents the k_{th} iteration step, the term $\nabla F(X_k)$ represents the gradient of function $F(X)$ at point X_k, while α is the descent step length, and $\alpha > 0$.

According to eq.(4.37), the function $F(X)$ represents the result of MILP solution, which does not have explicit analytical expressions so that $\nabla F(X)$ could not be calculated through conventional derivatives. Instead, the gradient at point X is approximated through

$$\begin{cases} \nabla F(X) = \left[\dfrac{\partial F}{\partial x_1}, \dfrac{\partial F}{\partial x_2}, ..., \dfrac{\partial F}{\partial x_i}, ..., \dfrac{\partial F}{\partial x_N}\right] \\ \dfrac{\partial F}{\partial x_i} = \dfrac{F(x_1, x_2, ...x_i + \delta x_i, ...x_n) - F(x_1, x_2, ..., x_i, ...x_n)}{\delta x_i} \\ i = 1, 2, ..., N \end{cases} \tag{4.39}$$

Where δx_i is a small perturbation of element x_i.

Suppose in the iteration step k, $\nabla F(X_k)$ has been determined through eq.(4.39), the next step is to find the best step length factor α, in order to achieve the decrement from $F(X_k)$ to $F(X_{k+1})$ as much as possible, therefore, $F(X_{k+1})$ becomes the function of α, which could be written as $F(X_{k+1}) = \Phi(\alpha)$. The best α corresponds to the minimum value of $\Phi(\alpha)$. Here we will not find the exact best α, instead, the "**Back and Forth**" strategy is applied to find a good α, which makes the decrement from $F(X_k)$ to $F(X_{k+1})$ be large enough. Through this way, the convergence speed is fast (though not the fastest), while the calculation consumption for α will not be much. The "**Back and Forth**" strategy is described as follows.

At the iteration step k:

① Set $\alpha_1 = 0$, $h = h_0$, $A_1 = X_k$, $\Phi_1 = F(X_k)$, turn to ②;

② If $h \leq \varepsilon$, stop and output $\alpha = \alpha_1$, ε is a very small number; Else let $\alpha_2 = \alpha_1 + h$, $A_2 = A_1 + \alpha_2 \nabla F(X_k)$, $\Phi_2 = F(A_2)$, turn to ③;

③ If $\Phi_2 > \Phi_1$, set $h = h/2$, turn back to ②; If $\Phi_2 <= \Phi_1$, set $\Phi_1 = \Phi_2$, $A_1 = A_2$, $\alpha_1 = \alpha_2$, $h = 2h$, turn to ④;

④ Let $\alpha_2 = \alpha_1 + h$, $A_2 = A_1 + \alpha_2 \nabla F(X_k)$, $\Phi_2 = F(A_2)$, turn to ⑤;

⑤ If $\Phi_2 <= \Phi_1$, turn back to ③; If $\Phi_2 > \Phi_1$, stop and output $\alpha = \alpha_1$;

Once α has been obtained, X_{k+1} could be achieved through eq.(4.38), and $F(X_{k+1})$ could be calculated, the iteration continues until the convergence criterias are satisfied, as shown in eq.(4.40).

$$\begin{aligned} &\| X_{k+1} - X_k \| \leq \varepsilon_1 \\ &\| F(X_{k+1}) - F(X_k) \| \leq \varepsilon_2 \end{aligned} \tag{4.40}$$

The whole solution flow chart is shown in Figure 4.5

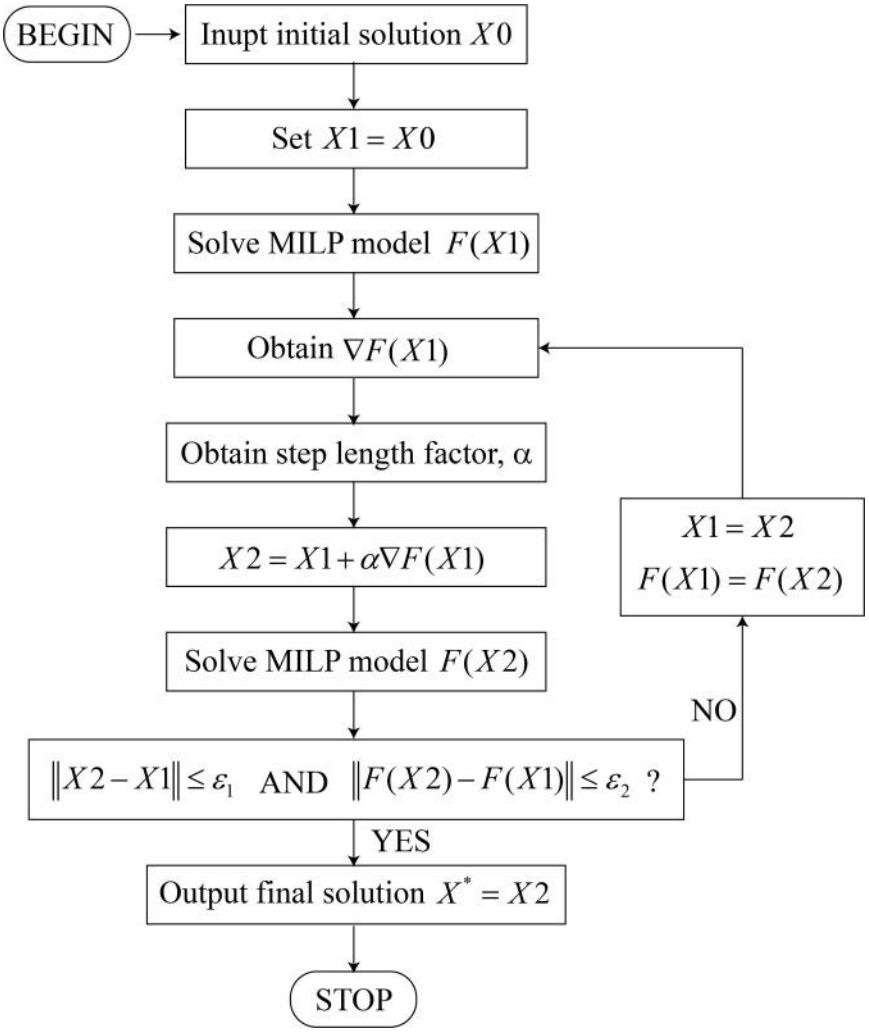

Figure 4.5: Overall solution process of MINLP model considering horizontal wells

4.4 Case studies

4.4.1 Basic information

An offshore field with 19 wells are to be developed, and two spread-moored FPSOs are designed to receive the produced fluid, as shown in Figure 4.6. The water depth is 2300m. The locations of FPSO, mooring line projection lengths and orientations are presented in Table 4.1. There are four different sizes of FPSO for selection, each with different processing capacities and the maximum number of riser connections, as well as the price, as shown in Table 4.2. The well bottom positions and the corresponding reservoir top depth, net thick, and permeability are shown in Table 4.3. The well bottoms are designed based on reservoir engineering theories and the FPSO locations are determined considering the sea state. Both of them are determined and provided as the input information for the subsea layout optimization.

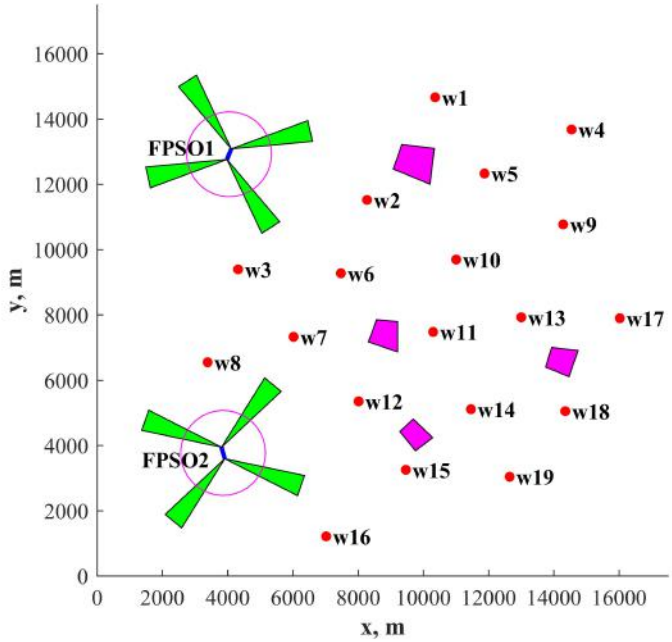

Figure 4.6: Distribution of FPSO, obstacles and wells

Table 4.1: FPSO locations and orientations

FPSO No.	Hull length (m)	Hull center Coordinates, (m)	Head orientation, (relative to x-axis,^{o})	Mooring line projection, (m)
FPSO1	350	(4046.88,12920.67)	67.79	2500
FPSO2	350	(3863.43,3768.91)	105.59	2500

Table 4.2: Available types of FPSO

	Type 1	**Type 2**	**Type 3**	**Type 4**
Processing Capacity (bbl/d)	120000	160000	180000	200000
Maximum riser number	16	20	24	28
Price ($\times 10^6$\$)	400	500	600	700

Table 4.3: Well bottom locations and reservoir properties

Well No.	Coordinates (m)	Top depth to the seabed, (m)	Net thick (m)	Permeability ($\times 10^{-3}\mu m^2$)
w1	(10365.58,14665.04)	3050.36	267.88	87.39
w2	(8273.85,11521.65)	3058.09	292.29	122.77
w3	(4321.11,9393.17)	3123.42	259.42	134.52
w4	(14545.27,13678.33)	3053.06	309.85	109.64
w5	(11874.81,12328.64)	3164.88	297.09	86.36
w6	(7471.96,9273.36)	3196.53	319.59	98.65
w7	(6023.25,7324.6)	3146.05	319.99	90.76
w8	(3386.83,6545.8)	3068.78	313.85	99.67
w9	(14288.06,10771.05)	3116.81	253.36	110.81
w10	(11008.61,9692.71)	3021.55	256.88	116.9
w11	(10301.28,7476.13)	3181.26	281.96	112.02
w12	(8016.64,5347.65)	3175.93	303.09	141.28
w13	(13002,7923.67)	3163.55	315.44	116.26
w14	(11458.73,5108.02)	3052.15	290.76	146.05
w15	(9465.34,3250.88)	3118.87	332	124.64
w16	(7021.84,1214.02)	3004.5	321.84	147.04
w17	(16024.24,7895.48)	3085.05	346.86	96.85
w18	(14352.36,5048.11)	3062.54	303.13	127.33
w19	(12646.44,3039.44)	3032.3	282.51	100.23

There are four subsea restriction areas, which are represented by polygons. These

restriction areas distribute on the sea bottom, and the height is not considered. As mentioned in section 3.1.2, these polygons should be extended in order to keep the safety distance with the flowlines. In this case, the safety distance is 20m, and the coordinates of these polygon vertices after extension are listed in Table 4.4. In the related figures, the presented obstacle areas are the ones after extension. The extension process is one of the preliminary treatment processes, which is the input information. It will not affect the form of the mathematical model, and the purpose of this process is to make the results more practical.

Table 4.4: Coordinates of seabed restriction areas (m)

Area 1	Area 2	Area 3	Area 4
(9344.3,13220.21)	(8568.89,7849.67)	(13932.5,7000.39)	(9692.3,4808.48)
(10339.11,13096.87)	(9211.92,7789.76)	(14745.74,6908.77)	(10289.93,4237.6)
(10206.72,12000.91)	(9211.92,6862.96)	(14465.84,6105.3)	(9760.38,3835.86)
(9079.53,12466.08)	(8319.24,7169.54)	(13750.94,6397.79)	(9280,4424.37)
(9742.41,12696.02)	(8827.99,7417.98)	(14223.76,6603.06)	(9755.65,4326.58)

8in flowline is selected to transport fluid from wellhead to the riser base, and 8in flexible riser is installed to connect the flowline with the FPSO. Riser length is assumed to be constant, which is 3000m, and the riser projection length is 1300m. The corresponding prices are listed in Table 4.5. Drilling cost for the horizontal part and vertical part are also included in Table 4.5.

Table 4.5: Flowline price and drilling cost

Item	Price
8in Flowline	\$2300/m
8in Riser	\$3500/m
Vertical Drilling	\$7500 /m
Horizontal Drilling	\$21000 /m

The subsea arrangement of satellite well system for both scenarios are obtained through the proposed models.

4.4.2 Result and Discussions

Scenario 1: Vertical well

As mentioned above, three kinds of objective functions are used for the layout optimization: minimum total cost, shortest payback period, and minimum pressure loss.

Oil price is \$60/*bbl*. The optimization results are shown in Figure 4.7 and Table 4.6. The three objective functions result in the same subsea layout as shown in Figure 4.7, because all these objective functions tend to achieve shorter flowline length.

As can be seen in Table 4.6, results from objective 1 and objective 2 are exactly the same, because the objective 2 is the objective 1 divided by oil price and total production rates, which are all constant values, according to eq.(4.9) and eq.(4.11).

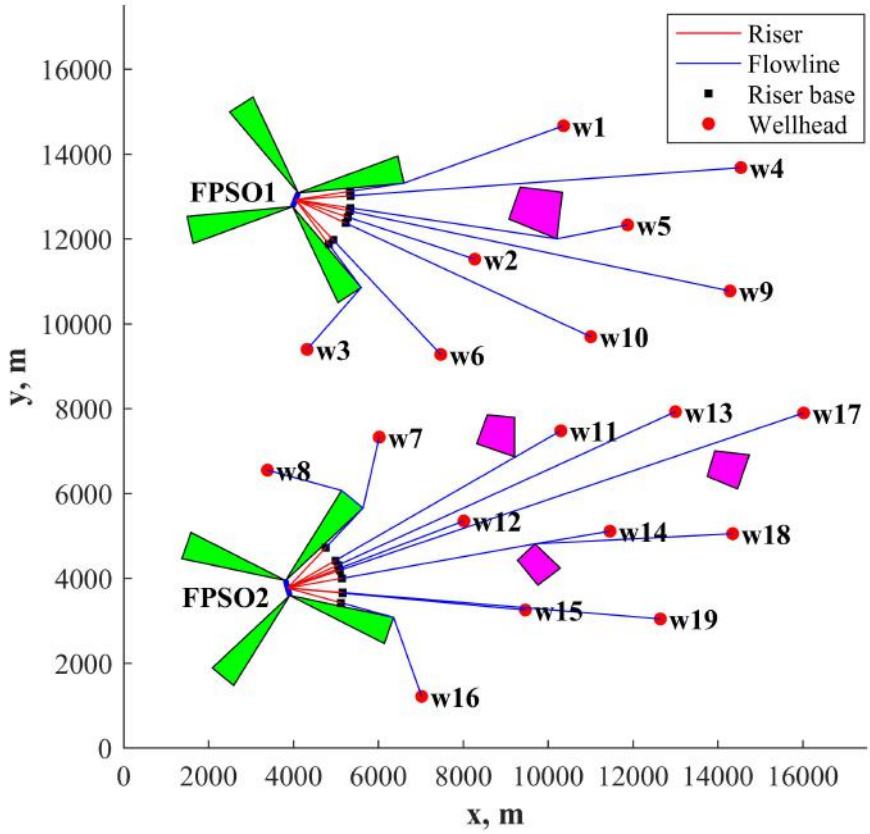

Figure 4.7: Layout of satellite well system considering vertical well

As for objective 3 (minimum pressure loss), the FPSO processing capacities are different from the other two, resulting in different FPSO cost. This is because the objective function shown by eq.(4.10) does not include the FPSO processing capacities, making it not affect the final objective value. Any processing capacities are available as long as they satisfied the capacity constraint shown by eq.(4.21). The defined parameter E which represents the level of pressure loss are the same of the three objectives because all these three objectives tend to find the layout with flowline length as short as possible, not only for reducing the cost but also reducing the pressure loss. As a result, the objective 2 (shortest payback period) could more comprehensively estimate the subsea arrangement, which no matter reflect the level of cost, but also reflect the level of pressure loss, as well as the level of the payback

Table 4.6: Optimization results of the scenario considering vertical well

	Objective 1: Total Cost	Objective 2: Payback period	Objective 3: Pressure loss
Flowline length, m	277146.37	277146.37	277146.37
Processing capacity (FPSO1), bbl	120000	120000	200000
Processing capacity (FPSO2), bbl	180000	180000	200000
Flowline cost, $\times 10^6$\$	637.44	637.44	637.44
Riser cost,$\times 10^6$\$	399	399	399
Drilling cost,$\times 10^6$\$	484.08	484.08	484.08
FPSO cost,$\times 10^6$\$	1000	1000	1400
Total cost, $\times 10^6$\$	2520.51	2520.51	2920.51
Payback period, day	219.51	219.51	254.35
Pressure loss E, $\times 10^{12} d^{-1}$,	1.15	1.15	1.15

period. It will be used as the major objective function for the layout optimization considering horizontal well.

Scenario 2: Horizontal well

For this scenario, there are two more input parameters: first is the maximum length of the production interval, which is 600m in this case, and the other is the ratio between production interval length and the horizontal displacement, β, which is 0.6 in this case. The production rate of each well could be calculated combining eq.(3.3), eq.(4.35) and related reservoir properties shown in Table 4.3.

According to the discussions in section 4.2.2, when considering horizontal drilling, if we use the minimum total cost as the objective function, the results will be the same with scenario 1 because the horizontal drilling cost is much more expensive than the flowline cost, which makes the system tend to reduce the horizontal drilling length as possible. Therefore, the minimum total cost could not reflect the performance of scenario 2. Because horizontal drilling also brings higher production rate, the shortest payback period is selected as the objective function for the optimization model, which takes both cost and revenue into account. Applying the proposed solution strategy for this MINLP problem, we choose the initial horizontal displacement to be 500m for all the wells, and the subsea arrangement could be obtained,

as shown in Figure 4.8.

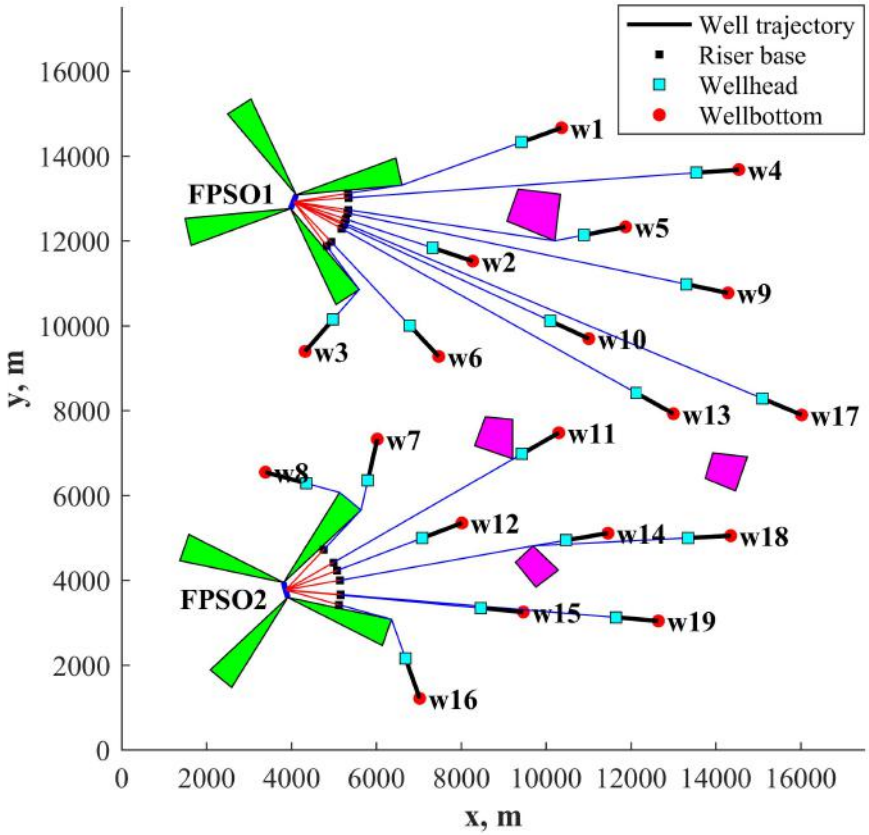

Figure 4.8: Layout of satellite well system considering horizontal well

Figure 4.9 presents the iteration process about the objective function and the step length factor. Beginning from the initial solution, the objective function drops quickly and then generally approach to the optimization results, and the step length factor becomes 0 at the end of the iteration, indicating that no better solutions could be found, and the iteration is stopped.

According to the case information, the maximum production interval length is 600m, and the ratio of β is 0.6. According to eq.(4.35), if the horizontal displacement is larger than 1000m, the production rate will no longer increase, while the cost will be higher, leading to a longer payback period.

When the horizontal displacement is lower than 1000m, increasing the length leads to higher production rate. In this case, the income increment resulting from higher production rate is larger than the cost increment due to longer horizontal drilling, making the payback period shorter.

Furthermore, the drilling cost per unit length is the same for all of the wells, so does the maximum production interval length. As a result, the effect of all the wells' horizontal displacements on the payback period follow the same trend, which

Table 4.7: Optimization results of the scenario considering horizontal well

	Proposed model	Theoretical optimal solution
Flowline length, m	190459.06	190472.77
Processing capacity (FPSO1), bbl	160000	160000
Processing capacity (FPSO2), bbl	160000	160000
Flowline cost, $\times 10^6$\$	438.06	438.09
Riser cost, $\times 10^6$\$	399	399
Drilling cost, $\times 10^6$\$	861.97	861.82
FPSO cost, $\times 10^6$\$	1000	1000
Total cost, $\times 10^6$\$	2699.02	2698.91
Payback period, day	142.23	142.22
Pressure loss E $\times 10^{12} d^{-1}$	1.83	1.83

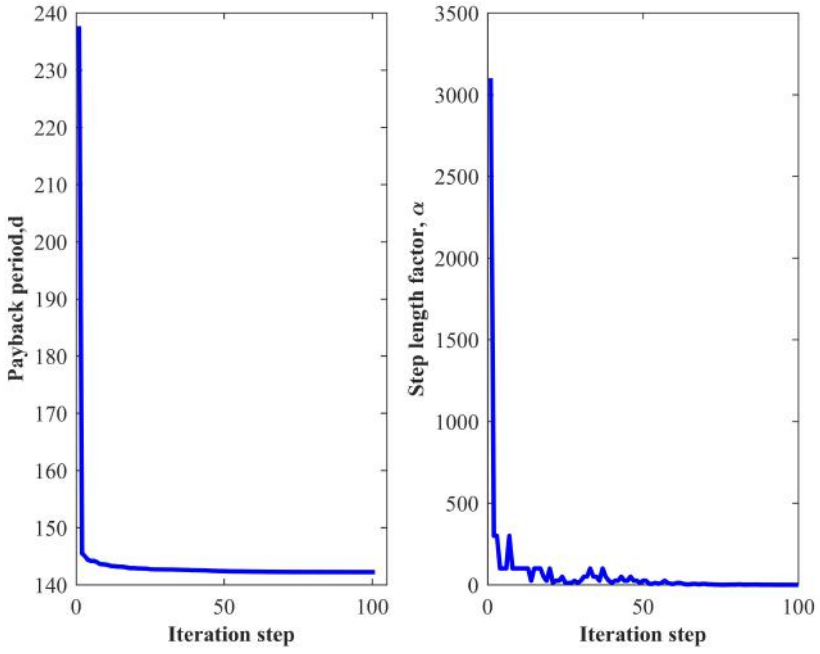

Figure 4.9: Iteration process of the optimzation for scenario 2

means that the optimal horizontal displacements of all the wells will be the same.

Therefore, based on the above discussions, for this case, the theoretical horizontal displacement should be 1000m, for all of the wells.

The optimized horizontal displacement through the proposed model is shown in

Table 4.8. As can be seen in the table, the horizontal displacements are all very close to 1000m. Besides, table 4.7 presents the comparison between the results from the proposed optimization model and the theoretical values. Obviously, results from both are very close, indicating that the proposed model and solution method are valid and feasible. The small differences result from the numerical error related to the convergence criteria.

Table 4.8: Optimized horizontal displacement of each well

Well name	Horizontal displacement,m	Well name	Horizontal displacement,m
w1	1000.01	w11	999.99
w2	999.99	w12	1000.02
w3	999.99	w13	1000
w4	1000.08	w14	1000.16
w5	1000	w15	1000.05
w6	1000.02	w16	1000.62
w7	999.99	w17	999.98
w8	1000.01	w18	999.99
w9	999.99	w19	999.98
w10	999.98		

The case is relatively simple, which assumed the same constant drilling cost per unit length and the same maximum production interval length for all the wells, leading to the result that the optimal horizontal displacements of all the wells are the same. Under more complicated conditions, the complex reservoir characteristics will bring different requirements of the production interval length, and the drilling cost might be a function of horizontal length, indicating that longer horizontal length will be more expensive. Under these complicated conditions, the horizontal displacements of the wells might not be equal, and each well has its own best horizontal displacement. The proposed model is established for these more general conditions, and related parameters are convenient to be input to the model. In this thesis, we provide a simpler case to show how the proposed model and solution method work, as well as presenting the reliability and feasibility of the model. More complex situations are not included.

Comparison of the two scenarios

The first difference between the two scenarios is the well assignment to the FPSOs. For the scenario considering vertical well, well 13 and well 17 are connected to FPSO 2, as shown in Figure 4.7, while for the scenario considering horizontal well, well 13 and well 17 are connected to FPSO 1, as shown in Figure 4.8. This is because of the higher production rate that results from horizontal drilling. Table 4.9 provides the production rates of the wells with considering the vertical well type and horizontal well type. If the well assignment of the scenario kept the same with scenario, since the production rates are higher, the total flow rate to FPSO 1 and FPSO 2 would be 124392.77 bbl/d, 191879.52 bbl/d, requiring the FPSO with processing capacity of 160000 bbl/d and 200000 bbl/d, respectively, while for the optimized well assignment for scenario 2, the flow rates to FPSO 1 and FPSO 2 are 156290.71 bbl/d and 159981.58 bbl/d, requiring two FPSOs with processing capacity of 160000 bbl/d, which reduces the cost of FPSO. Therefore, the proposed model could effectively find the best arrangement based on the provided information.

Table 4.9: Production rate of the wells considering different well types

Well No.	Production rate bbl/d		Well No.	Production rate bbl/d	
	Vertical well	Horizontal well		Vertical well	Horizontal well
w1	6929.54	12393.37	w11	9349.1	16119.07
w2	10621.4	17839.25	w12	12674.27	20724.8
w3	10329.3	18894.79	w13	10855.63	17227.4
w4	10055.84	16174.42	w14	12570.07	21193.53
w5	7594.17	12602.93	w15	12248.41	18694.97
w6	9332.5	14664.57	w16	14007.28	21893.83
w7	8596.03	13494.63	w17	9943.65	14670.54
w8	9259.35	14750.34	w18	11424.77	18679.42
w9	8309.78	15452.26	w19	8381.97	14430.99
w10	8888.61	16371.18			

Table 4.10 provides a further comparison of the FPSO sizes and production distributions. For FPSO 1, in scenario 1 considering vertical well, the selected FPSO is with 120000 bbl/d of processing capacity, and the maximum riser number is 16, and the production distributed to FPSO 1 is 72061.15 bbl/d, from 8 wells, using 16 risers. We could find that only 60% of the processing capacity is used since

there are no riser connections for more wells. About 40% of the processing capacity is left unused, which is a kind of "waster". In scenario 2, the selected FPSO is with 160000 bbl/d of processing capacity, and the maximum riser number is 20. The production distributed to FPSO 1 is 156290.71 bbl/d, from 10 wells, using 20 risers, which also reach the FPSO's maximum riser number, but 97.7% of the processing capacity is used. The same condition happens for FPSO 2. 66.28% and 99.99% of the processing capacity are used in scenario 1 and scenario 2, respectively, while the riser numbers both reach close to the maximum value.

This comparison indicates that using horizontal well for satellite well system is more **cost effective** comparing with using vertical well, because the higher production rate due to horizontal drilling makes the processing capacity of the FPSOs to be more effectively used.

The maximum number of riser connections also plays an important role in the optimization process. If there are more riser connections, more wells could be tied in to make the best use of the FPSO processing capacity. But more risers will increase the weight of the hull, as well as enhancing the complexity of control and maintenance. Therefore, when designing an FPSO, the riser number, the processing capacity, the hull, as well as other related issues on the topside should be synthetically analyzed. But for this case, the comparison is based on the provided available FPSO sizes. We could conclude that when the number of riser connections is limited, for satellite well system, horizontal drilling leads to higher production rate and contributes to making full use of the FPSO's processing capacity.

Table 4.10: Comparison of the FPSO capacities and production conditions

	FPSO1		FPSO2	
	Scenario 1	Scenario 2	Scenario 1	Scenario
Processing Capacity, bbl/d	120000	160000	180000	160000
Maximum riser number	16	20	24	20
Flow rate, bbl/d	72061	156290	119310	159981
Riser number	16	20	22	18

Figure 4.10 presents an overall comparison of the optimization results of scenario 1 and scenario 2. Due to the drilling of horizontal wells, the drilling cost for scenario 2 is 78.03% higher than scenarios 1, while the flowline cost is reduced by 31.27%. The total cost is 7.08% higher compared with scenario 1. But the total production rate increases by 65.27% higher, leading to a significant decrease in the payback

period, from 219.51 days of scenario 1 to 142.22 days of scenario 2. The pressure loss of scenario 2 increases by 65.27% compared with scenario 1.

The results indicate that the total cost of scenario 2 is higher, but the payback period is shorter, which means that fewer days are needed to balance the investment by selling the produced oil. Therefore, horizontal drilling is more promising than vertical drilling for economic performance.

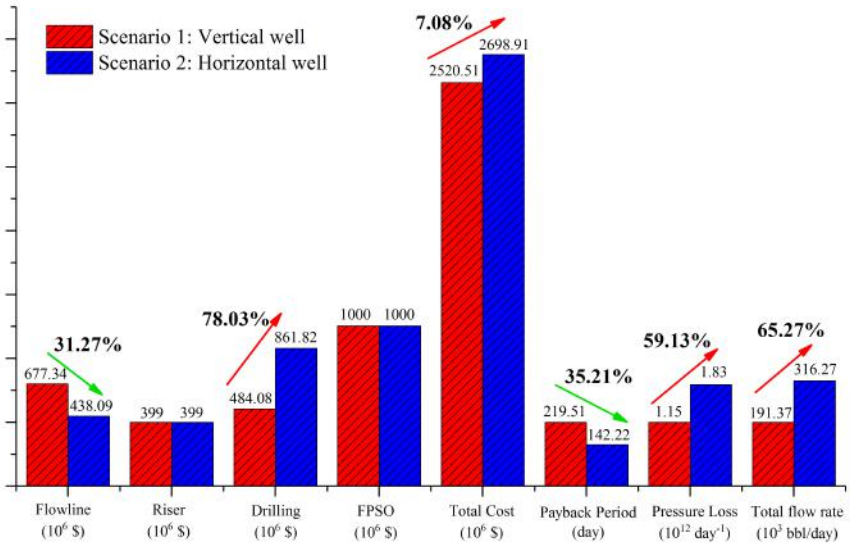

Figure 4.10: Overall comparison for the optimization results

The flexiblity of the proposed models

In the above discussions, the proposed **MODEL 1** and **MODEL 2** both include the information of wells as the decision variables. They are also applicable if some decision variables have already been given. For instance, if the well trajectories have already been designed in advance considering the underground formation and the reservoir characteristics [90], the wellhead positions, as well as the production rates, will be known, the descriptions about the well trajectories and production rates could be removed, then both **MODEL 1** and **MODEL 2** will degenerate into the scenario that finding the proper assignments between wellheads and FPSO, which is similar to the ones proposed by many researchers [42, 58].

Besides, for the case study results of **MODEL 2**, the optimal displacement is 1000m, the optimized wellhead locations were not affected by the subsea obstacles, because the optimal displacement is not large enough so that not all the situations discussed in Figure 4.3 were presented. But in practical application, those compli-

cated situations might occur. In order to show the model's capacity of dealing with different complicated situations, we randomly generated a set of horizontal displacement ranging from 2000m-2500m for all the wells and optimize the corresponding subsea layout through **MODEL 2**, in order to cover the possible situations shown in Figure 4.3. Once input the horizontal displacements, **MODEL 2** becomes a MILP problem. The optimized layout is shown in Figure 4.11.

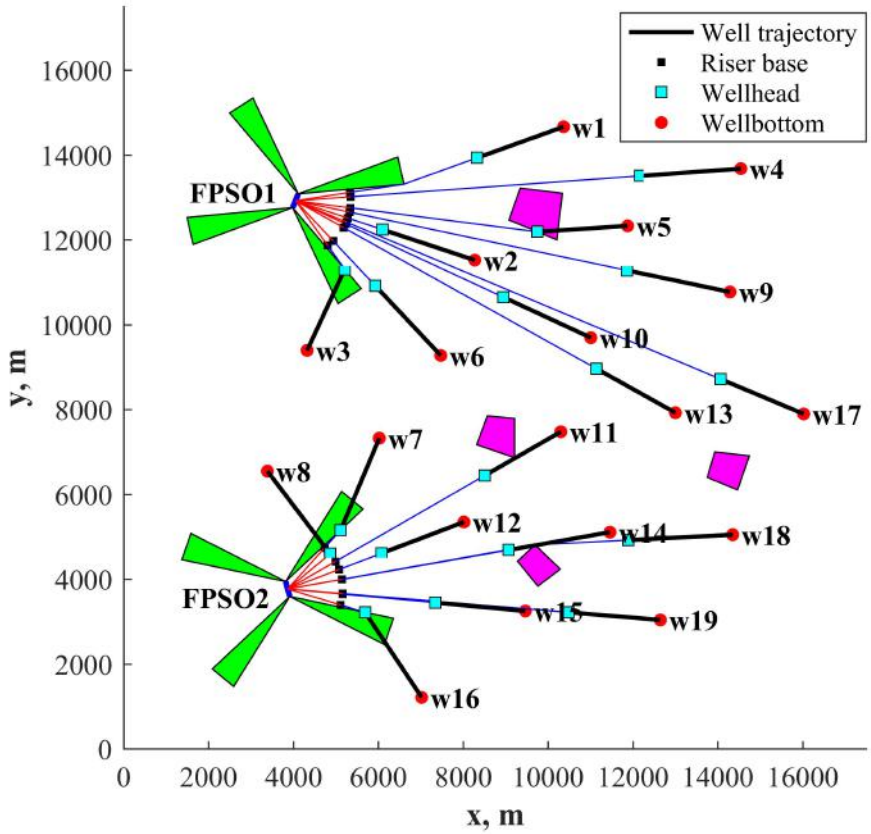

Figure 4.11: The layout under given long horizontal displacements of the wells

The example which is shown in Figure 4.11 presents all the possibilities shown by Figure 4.3 about potential wellhead locations. For instance, the trajectory of well $w19$ represents the situation of Figure 4.3(a), the trajectory of well $w5$, $w3$, $w7$ all cross with the subsea obstacles, corresponding to Figure 4.3(b), the trajectory of well $w14$ reflects the situation of Figure 4.3(c) since its horizontal displacement is large enough that makes the wellhead be located behind the near obstacle area and connected to FPSO 2 by straight line. The results in Figure 4.11 indicates that the proposed **MODEL 2** is capable to deal with different complicated situations. Therefore, the proposed **MODEL 1** and **MODEL 2** could be both flexibly applied according to the actual conditions.

4.5 Chapter summary

(1) In this chapter, we focused on the concept of satellite well system and proposed optimization models for the subsea layout design. Two scenarios are considered, scenario 1 considers vertical wells, and scenario 2 considers horizontal wells. For scenario 1, the proposed layout optimization model is a Mix-integer linear programming problem (MILP), and for scenario 2, the proposed model is a Mix-integer nonlinear programming problem (MINLP).

(2) GUROBI solver is applied to solve the MILP problem. For MINLP problem, the decomposition strategy based on gradient descent is proposed to transform the original model into a series of MILP problems that are convenient to be solved by GUROBI, and the final optimal solution is obtained through iteration process.

(3) An offshore field with 19 wells, 2 FPSOs, and 4 subsea restriction areas is taken for the case study. The layouts of both scenarios are optimized through the proposed models. The results indicate that the proposed models are valid and feasible. And the proposed solution strategy is with good performance.

(4) The optimization results of the two scenarios are compared. it is found that under the given available options of FPSO, scenario 2 uses almost all of the processing capacities of FPSO, while for scenario 1, a large percentage of the processing capacities are left unused, which is a kind of "waste". Therefore, scenario 2 is more cost-effective. Besides, though the total cost of scenario 2 is higher than scenario 1, shorter payback period and higher production rate could be obtained, indicating better economic performance.

(5) The proposed models could be both flexibly applied according to the actual conditions.

Chapter 5

Layout optimization of manifold system

5.1 Problem statement

In the manifold system, the wellheads are divided into several groups, wellheads in one group will be connected to one manifold, and the produced fluids commingle here, then flow to the FPSO or other kinds of receiving terminals. Figure 5.1 illustrates a schematic view of a manifold system.

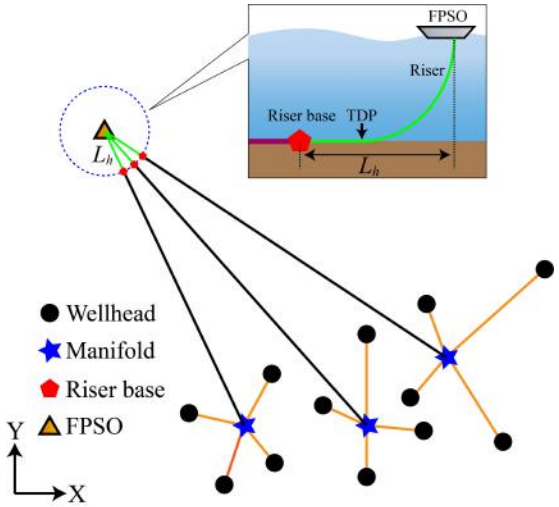

Figure 5.1: Schematic view of a manifold system

For the layout optimization, the input information is almost the same with what has been presented in chapter 4 for the satellite well system, besides three aspects of differences:

(1) Two different flowline sizes are required. The smaller size of flowline/jumper between wellheads and manifolds, and the larger size of flowline and riser between manifold and FPSOs. Because the commingling of produced fluid at manifold leads

to higher pressure drop, requiring a larger size of the flowline. The internal diameters are represented by D_{wm} and D_{mf}, respectively, and the corresponding prices per unit length are P_{wm}^{line} and P_{mf}^{line}.

(2) There are N_M^{ava} different types of manifold for selection, for the type t manifold, the slots number is S_t, and the corresponding cost is $P_t^{manifold}$. $t = 1, 2, ..., N_M^{ava}$.

(3) The designed number of the manifold is N_M, which is provided as a known parameter for the layout design and could be adjusted to determine the best number.

The flow process of the manifold system is different from the satellite well system. The produced fluids from wellheads firstly arrive at the manifolds and then flow to the riser bases. Therefore, the layout is different, leading to different ways for the description of the optimization model, compared with what has been done in chapter 4. Following points should be determined for the layout of the manifold system.

1. *The locations of the manifolds, and the assignment between wells and manifolds, which means which manifold should one well be connected with.*

2. *The assignment between the manifolds and FPSOs, that is, to determine which FPSO should one manifold be connected with.*

3. *The size of each manifold, that is, the slots number of each manifold, depending on the number of wells that are connected.*

4. *The size of the FPSO for the field production, depending on the production rate and the number of manifolds that are connected.*

5. *The flowline routes between wells and manifolds and the routes between manifolds and FPSOs, which should avoid the subsea obstacles.*

6. *The wellhead locations and the length of the horizontal part if the horizontal well is to be used.*

The objectives include the following three aspects, which are the same as the satellite well system.

1. *The total cost should be as low as possible.*

2. *The payback period should be as short as possible.*

3. *The pressure loss should be as low as possible.*

For the concept of the manifold system, two different scenarios are considered, the first is the satellite well-manifold system, with vertical wells. Wellheads distribute as the satellite pattern, and flowlines are required to connect the manifolds and wellheads. The second scenario is the cluster manifold system, with horizontal

wells. The wellheads are grouped as clusters, and one manifold is installed for one cluster, wellheads and manifold are connected through short jumpers. The engineering considerations for these two scenarios are different, which will be presented in subsequent text. The optimization models for both scenarios are developed, respectively.

5.2 Mathematical models

5.2.1 Scenario 1: Satellite well manifold system

Adjacent matrix and segment intersection matrix

Similar with the satellite well system considering vertical well, on the flat plane, there are three basic types of nodes: riser porch nodes $\mathcal{I}_{\mathcal{F}}$, Wellhead nodes $\mathcal{I}_{\mathcal{W}}$, and obstacle nodes $\mathcal{I}_{\mathcal{O}}$. Besides, the manifold node set should also be included, which is represented by $\mathcal{I}_{\mathcal{M}}$.

As indicated in chapter 2, the flowline segments might become obstacles of the other flowline routes. Let's take Figure 5.2 as an example to explain. Due to the flowline between node C and D, the straight connection between node A and node B is unfeasible due to flowline intersection. Instead, the feasible route should go around CD. The shortest path should be the route that starts from A and then to node D, and finally connects node B, which in the practical situation could be regarded as a route that inflects at node D. Of course, the practical route could not exactly pass through node D because this node is the position of Xtree and usually is laid some distance away. But the overall route and length are very close so that for simplification, the route is assumed to exactly pass through node D.

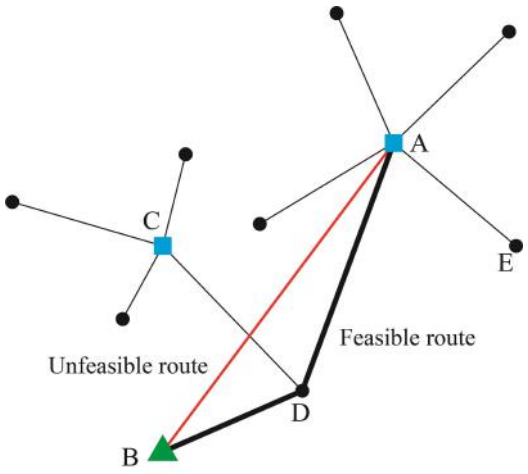

Figure 5.2: Possible intersection between the flowline routes

This simplification indicates that node D not only belongs to the wellhead node

set which is the start of the flowline route, but also the possible intermediate node set which some flowline route might pass by in order to avoid flowline crossing. For the purpose of building up mathematical model, a new node set is introduced: these nodes coincide with the wellhead nodes on the $X-Y$ plane, but for anyone wellhead node and its corresponding coincided newly introduced node, they are not connectable. Through this way, the role of wellhead node keeps unique, as the start of flowline route, and these newly introduced nodes act as the intermediate nodes. These nodes actually do not exist and are imaginary for mathematical modelling, so that this node set is named "Virtual node set", which is represented by $\mathcal{I}_{\mathcal{V}}$

The whole node set could be organized as

$$\mathcal{I} = \{\mathcal{I}_{\mathcal{F}}, \mathcal{I}_{\mathcal{O}}, \mathcal{I}_{\mathcal{V}}, \mathcal{I}_{\mathcal{W}}, \mathcal{I}_{\mathcal{M}}\} \tag{5.1}$$

Again, the adjacent matrix V could be obtained, through the following rules that representing the basic characteristics of the manifold system.

1. *Rule 1: Any two nodes from the manifold node set are not connectable*
2. *Rule 2: The node from the wellhead node set and the corresponding coincided virtual node from the virtual node set are not connectable*
3. *Rule 3: The node could not be connected with itself*
4. *Rule 4: Connection between any two nodes should not intersect with any obstacles*

The above rules could be represented through eq. (5.2)

$$V_{ij} = \begin{cases} 0, & \forall i, j \in \mathcal{I}_{\mathcal{M}} \\ 0, & \forall i \in \mathcal{I}_{\mathcal{W}}, \quad j \in \mathcal{I}_{\mathcal{V}}, \quad NDx_i = NDx_j, \quad NDy_i = NDy_j \\ 0, & i = j \\ 0, & \sum_{r=1}^{R+4N_{fpso}} C_R(ND_i, ND_j, \Omega_r) > 0, \quad \forall i, j \in \mathcal{I} \\ 1, & \sum_{r=1}^{R+4N_{fpso}} C_R(ND_i, ND_j, \Omega_r) = 0, \quad \forall i, j \in \mathcal{I} \end{cases} \tag{5.2}$$

To avoid the flowline intersection, we need to know whether any two segments intersect. Note that two segments totally include four nodes (two nodes for each), therefore, to determine whether the segment between node i and node j intersects with the segment between node h and node k, a binary variable $C_X(i, j, h, k)$ is introduced, which form a 4D matrix, called the "intersection matrix" in this thesis.

Through eq. (3.5), the value of $C_X(i,j,h,k)$ could be determined, as shown in eq.(5.3)

$$C_X(i,j,h,k) = \begin{cases} 1, & C_F(N_i,N_j,N_h,N_k) = 1 \\ \\ 0, & C_F(N_i,N_j,N_h,N_k) = 0 \end{cases} \tag{5.3}$$

It should be noted that, for the manifold system, the manifold positions are decision variables, therefore, the adjacent matrix and the intersection matrix are all related to the position of manifolds.

Decision variables

The definition of decision variables is similar to the satellite well system:

Binary variable x_{ij}, $\forall i,j \in \mathcal{I}$, $x_{ij} = 1$ indicates that node i is connected with node j, while $x_{ij} = 0$ means there is no flowline between node i and node j.

Binary variable $p_{k,tm}$, $p_{k,tm} = 1$ indicates that the kth manifold selects type tm from the avaible ones. $k = 1,2,...,N_M$, $tm = 1,2,...,Tm$.

Binary variable z_{st}, is introduced to indicate the selection of FPSO from the available options. If the size s is selected for FPSO t, $z_{ts} = 1$, otherwise, $z_{ts} = 0$.

Non-negative integer variable q_{mij} and $q_{f_{ij}}$, $\forall i,j \in \mathcal{I}$, represent the number of flowlines between node i and node j toward manifold and FPSO, respectively.

The continuous variable Q_{mij} and $Q_{f_{ij}}$, $\forall i,j \in \mathcal{I}$, represent the total flow rates from node i to node j toward manifold and FPSO, respectively.

The manifold positions (x_k^m, y_k^m), $k = 1,2,...,N_M$, which could be arranged as a row vector $M = [x_1^m, y_1^m, ..., x_k^m, y_k^m, ..., x_{N_M}^m, y_{N_M}^m]$. The elements are continuous variables.

Cost components

The components of the total cost could be represented by these defined decision variables.

The drilling cost is

$$COST_{drilling} = P_v L_v = \sum_{l=1}^{N} P_v(H_l + h_l) \tag{5.4}$$

The term $H_l + h_l$ represents the reservoir bottom depth, which means that the vertical well bottom locates at the reservoir bottom.

The flowline cost is

$$COST_{flowline} = P_{wm}^{line} \sum_{i\in\mathcal{I}} \sum_{j\in\mathcal{I}} d_{ij} q_{mij} + 2P_{mf}^{line} \sum_{i\in\mathcal{I}} \sum_{j\in\mathcal{I}} d_{ij} q_{f_{ij}} \tag{5.5}$$

The term d_{ij} is the distance between node i and node j, which should be calculated according to the adjacent matrix, as shown in eq. (5.6). As the right side of the equal sign, the first term in the cost of flowlines between wellheads and manifolds. Since there is no flowline loop, there is only one single flowline between one wellhead and the corresponding manifold. The second term is the flowline cost between manifolds and FPSOs. The flowline loop is required so that the total length should be multiplied by number "2", as discussed in Chapter 2.

$$d_{ij} = \begin{cases} \sqrt{(NDx_i - NDy_i)^2 + (NDx_j - NDy_j)^2}, & V_{ij} = 1 \\ +\infty, \quad V_{ij} = 0 \end{cases} \tag{5.6}$$

NDx and NDy represents the x and y coordinates, respectively. When $V_{ij} = 0$, the $+\infty$ could be denoted by a very large number for the purpose of computer programming.

The riser cost is

$$COST_{riser} = 2P^{riser} N_M L_{riser} \tag{5.7}$$

L_{riser} is the riser length, which is assumed to be constant. Similarly, each wellhead requires two risers, so that the total riser number is 2 times of well number N.

The FPSO cost is

$$COST_{fpso} = \sum_{t=1}^{N_{fpso}} \sum_{s=1}^{N_{fpso}^{ava}} P_s^{fpso} z_{ts} \tag{5.8}$$

The manifold cost is

$$COST_{manifold} = \sum_{k=1}^{N_M} \sum_{tm=1}^{N_M^{ava}} P_{tm}^{manifold} p_{k,tm} \tag{5.9}$$

The total cost is

$$COST_{total} = COST_{drilling} + COST_{flowline} + COST_{riser} + COST_{fpso} + COST_{manifold} \tag{5.10}$$

Pressure loss

Through eq.(3.12), the total pressure loss of the whole system from wellheads to FPSOs is represented by

$$E_{total} = \sum_{i\in\mathcal{I}} \sum_{j\in\mathcal{I}} \frac{Q_{mij} d_{ij}}{D_{wm}^4} + \sum_{i\in\mathcal{I}} \sum_{j\in\mathcal{I}} \frac{Q_{f_{ij}} d_{ij}}{D_{mf}^4} + \sum_{j\in\mathcal{I}_{\mathcal{F}}} \sum_{i\in\mathcal{I}} \frac{Q_{f_{ij}} L_{riser}}{D_{mf}^4} \tag{5.11}$$

At the right side of the equal sign, the first term reflects the total pressure loss in the flowlines between wellheads and manifolds, and the second term is for the flowlines between manifolds and riser bases, while the third term reflects the pressure loss in the risers.

Payback period

Similar to the models for the concept of satellite well system, the payback period is

$$PB = \frac{COST_{total}}{P^{oil} \sum_{i_w=1}^{N_W} Q_{i_w}^{w}} \tag{5.12}$$

Constraints

Following constraints should be satisfied, for a feasible layout of the satellite well system.

Eq.(5.13) shows that node i and node j must be connectable, if not, $x_{ij} = 0$.

$$x_{ij} \leq V(i,j) \quad \forall i,j \in \mathcal{I} \tag{5.13}$$

Eq.(5.14) indicates that there is at most only one flow direction between node i and node j.

$$x_{ij} + x_{ji} \leq 1, \quad \forall i,j \in \mathcal{I} \tag{5.14}$$

Eq.(5.15), eq.(5.16) and eq.(5.17) indicates that the flow only and must happens between node i and j when they are connected. ψ is a very small positive number used to ensure the flow won't be zero when node i, j are connected. Ψ is a large number.

$$\psi x_{ij} \leq q_{mij} \leq \Psi x_{ij}, \quad \psi x_{ij} \leq q_{f_{ij}} \leq \Psi x_{ij}, \quad \forall i,j \in \mathcal{I} \tag{5.15}$$

$$q_{mij} + q_{f_{ij}} \geq \psi x_{ij}, \forall i,j \in \mathcal{I} \tag{5.16}$$

Eq.(5.16)

$$\psi q_{mij} \leq Q_{mij} \leq \Psi q_{mij}, \quad \psi q_{f_{ij}} \leq Q_{f_{ij}} \leq \Psi q_{f_{ij}}, \quad \forall i,j \in \mathcal{I} \tag{5.17}$$

Eq.(5.18) is used to ensure that any two segments between the nodes won't cross with each other. When $x_{ij} = 1$ which means node i, j are connected, the node pairs that the segments will cross with the segment between i and j should not be selected

as part of the flowline route.

$$\sum_{h\in\mathcal{I}}\sum_{k\in\mathcal{I}} C_X(i,j,h,k) \leq (1-x_{i,j})\Psi, \quad \forall i,j \in \mathcal{I} \tag{5.18}$$

Eq.(5.19) means that only one size of FPSO could be selected for one designed FPSO position.

$$\sum_{s=1}^{N_{fpso}^{ava}} z_{ts} = 1, \quad t = i, \quad \forall i \in \mathcal{I}_{\mathcal{F}} \tag{5.19}$$

Eq.(5.20)-eq.(5.25)) describe the requirements for the riser porch nodes. First, the riser porch nodes are the ends of the system, and there will be no flow exits the riser porch nodes. At the same time, for each FPSO, the risers connected with it should not exceed its maximum available riser numbers, and the total flow rate enters one FPSO should not exceed its processing capacity. These requirements are represented by eq.(5.20), eq.(5.22) and eq.(5.24). Note that the factor "1/2" is due to the consideration of flowline loop, which requires two risers for the connection between one manifold and the corresponding FPSO.

Second, the flow toward manifolds is defined separately from the flow toward the FPSOs, and only the latter one could arrive at FPSOs, which are represented by eq.(5.21) and eq.(5.23).

Third, the total number of the risers connected to the FPSOs should equal to two times of the manifold number, considering the requirements of flowline loop, and the total flow rate enters FPSOs should equal to the total production rate of all the wells, which are described by eq.(5.25).

$$\sum_{j\in\mathcal{I}} x_{ij} = 0, \quad \sum_{j\in\mathcal{I}} x_{ji} \leq \frac{1}{2}\sum_{s=1}^{N_{fpso}^{ava}} (N_s^{riser} z_{ts}), \quad t = i, \quad \forall i \in \mathcal{I}_{\mathcal{F}} \tag{5.20}$$

$$\sum_{j\in\mathcal{I}} q_{mij} = 0, \quad \sum_{j\in\mathcal{I}} q_{mji} = 0, \quad \forall i \in \mathcal{I}_F \tag{5.21}$$

$$\sum_{j\in\mathcal{I}} q_{f\,ij} = 0, \quad \sum_{j\in\mathcal{I}} q_{f\,ji} \leq \frac{1}{2}\sum_{s=1}^{N_{fpso}^{ava}} (N_s^{riser} z_{ts}) \quad t = i, \quad \forall i \in \mathcal{I}_{\mathcal{F}} \tag{5.22}$$

$$\sum_{j\in\mathcal{I}} Q_{mij} = 0, \quad \sum_{j\in\mathcal{I}} Q_{mji} = 0, \quad \forall i \in \mathcal{I}_F \tag{5.23}$$

$$\sum_{j\in\mathcal{I}} Q_{f\,ij} = 0, \quad \sum_{j\in\mathcal{I}} Q_{f\,ji} \leq \sum_{s=1}^{N_{fpso}^{ava}} (Q_s^{process} z_{ts}), \quad t = i, \quad \forall i \in \mathcal{I}_{\mathcal{F}} \tag{5.24}$$

$$\sum_{i\in\mathcal{I}_\mathcal{F}}\sum_{j\in\mathcal{I}} x_{ji} \leq N_M, \quad \sum_{i\in\mathcal{I}_\mathcal{F}}\sum_{j\in\mathcal{I}} q_{f_{ji}} = N_M, \quad \sum_{i\in\mathcal{I}_\mathcal{F}}\sum_{j\in\mathcal{I}} Q_{ji} = \sum_{i_w=1}^{N} Q^w_{i_w}, \quad \forall i \in \mathcal{I}_\mathcal{F} \tag{5.25}$$

Eq.(5.26)-Eq.(5.30) describes the requirements for the wellhead nodes. The wellheads are the start of the whole system so that there will be no flow enters, and one wellhead should and must be connected with only one flowline. These requirements are presented by eq.(5.26), eq.(5.27) and eq.(5.29). Since the flow toward FPSO starts from the manifolds, there will be no flow toward FPSO starts from the wellheads, which are defined by eq.(5.28) and eq.(5.30). In eq.(5.29), the third term defines the relationship between the index i_w in well node set $\mathcal{I}_\mathcal{W}$ and integral node set $\mathcal{I}$ based on the arrangement order of different type of nodes. Here since the virtual nodes and obstacle nodes all act as the intermediate nodes, we put them together named set $\mathcal{I}_\mathcal{B}$, and the corresponding total node number is N_B.

$$\sum_{j\in\mathcal{I}} x_{ij} = 1, \quad \sum_{j\in\mathcal{I}} x_{ji} = 0, \quad \forall i \in \mathcal{I}_W \tag{5.26}$$

$$\sum_{j\in\mathcal{I}} q_{mij} = 1, \quad \sum_{j\in\mathcal{I}} q_{mji} = 0, \quad \forall i \in \mathcal{I}_W \tag{5.27}$$

$$\sum_{j\in\mathcal{I}} q_{f_{ij}} = 0, \quad \sum_{j\in\mathcal{I}} q_{f_{ji}} = 0, \quad \forall i \in \mathcal{I}_W \tag{5.28}$$

$$\sum_{j\in\mathcal{I}} Q_{mij} = Q^w_{i_w}, \quad \sum_{j\in\mathcal{I}} Q_{mji} = 0, \quad i_w = i - N_F - N_B \quad \forall i \in \mathcal{I}_W \tag{5.29}$$

$$\sum_{j\in\mathcal{I}} Q_{f_{ij}} = 0, \quad \sum_{j\in\mathcal{I}} Q_{f_{ji}} = 0, \quad \forall i \in \mathcal{I}_W \tag{5.30}$$

Eq.(5.31)-Eq.(5.33) describe the requirements for the intermediate node set $\mathcal{I}_\mathcal{B}$ as mentioned above, including the obstacle nodes and the virtual nodes. First, the flow is conserved, which means that for any node, the inflow rate should be equal to the outflow rate, as represented by eq.(5.31) and eq.(5.32). And second, since there should be at most one segment connect with any of the nodes at the outflow side, as discussed in section 4.2.1 about the possible route overlapping, eq.(5.33) is provided.

$$\sum_{j\in\mathcal{I}} q_{mij} - \sum_{j\in\mathcal{I}} q_{mji} = 0, \quad \sum_{j\in\mathcal{I}} q_{f_{ij}} - \sum_{j\in\mathcal{I}} q_{f_{ji}} = 0 \quad \forall i \in \mathcal{I}_B \tag{5.31}$$

$$\sum_{j\in\mathcal{I}} Q_{mij} - \sum_{j\in\mathcal{I}} Q_{mji} = 0, \quad \sum_{j\in\mathcal{I}} Q_{fij} - \sum_{j\in\mathcal{I}} Q_{fji} = 0 \quad \forall i \in \mathcal{I}_B \tag{5.32}$$

$$\sum_{j\in\mathcal{I}} x_{ij} <= 1 \quad \forall i \in \mathcal{I}_B \tag{5.33}$$

Eq.(5.34)-Eq.(5.40) define the requirements for the manifold nodes. The manifolds are the start of the flowline routes toward FPSOs, and at the same time, they are the end of the flowline routes connecting wellheads. Therefore, for each manifold, there is only one and must be only one flowline route toward FPSO, and the flow between wellheads and manifolds will not exit the manifold node, according to the definition of q_m and q_f. Besides, the flowline routes toward FPSO should not pass by the manifold nodes. These three requirements are defined by the first terms of eq.(5.34), eq.(5.35) and eq.(5.36), respectively.

Furthermore, the flowlines connecting one manifold and the corresponding wellheads should not exceed the maximum slots number of the selected manifold size, which are represented by the second terms of eq.(5.34) and eq.(5.35), respectively. Considering the requirement of flowline loop for the connection between manifolds and FPSOs, we assume that the flowline routes in one loop are overlapped and are regarded as one route for the layout description, and the route length will be multiplied by 2 to obtain the total flowline length.

For each manifold, the flow is conserved, which means the total inflow rate should be equal to the total outflow rate, as shown by eq.(5.37). The second term and third term indicate that the flow toward the FPSO should not enter the manifold node, while the flow toward the manifold should not exit the manifold node.

The total flow rate arrives at the manifolds should be equal to the total production rate of the wells, and the total number of flowlines connected with manifolds should be equal to the number of wells. These requirements are represented by eq.(5.38).

We have a series manifold sizes for selection, and only one size could be selected for one manifold, which is shown by eq.(5.39).

Eq.(5.40) defines the relationship between the node index in the manifold node set $\mathcal{I}_\mathcal{M}$ and the integral node set $\mathcal{I}$, based on the node arrangement order of different type of nodes.

$$\sum_{j\in\mathcal{I}} x_{ij} = 1, \quad \sum_{j\in\mathcal{I}} x_{ji} \leq \sum_{tm=1}^{Tm} p_{k,tm} S_{tm}, \forall i \in \mathcal{I}_M \tag{5.34}$$

$$\sum_{j\in\mathcal{I}} q_{mij} = 0, \quad \sum_{j\in\mathcal{I}} q_{mji} \leq \sum_{tm=1}^{Tm} p_{k,tm} S_{tm}, \forall i \in \mathcal{I}_M \tag{5.35}$$

$$\sum_{j\in\mathcal{I}} q_{f\,ij} = 1, \quad \sum_{j\in\mathcal{I}} q_{f\,ji} = 0, \forall i \in \mathcal{I}_M \tag{5.36}$$

$$\sum_{j\in\mathcal{I}} Q_{f\,ij} - \sum_{j\in\mathcal{I}} Q_{m\,ji} = 0, \quad \sum_{j\in\mathcal{I}} Q_{f\,ji} = 0 \quad \sum_{j\in\mathcal{I}} Q_{m\,ij} = 0 \quad \forall i \in \mathcal{I}_M \tag{5.37}$$

$$\sum_{i\in\mathcal{I}_M}\sum_{j\in\mathcal{I}} x_{ji} \leq N_W, \quad \sum_{i\in\mathcal{I}_M}\sum_{j\in\mathcal{I}} q_{m\,ji} = N_W, \quad \sum_{i\in\mathcal{I}_M}\sum_{j\in\mathcal{I}} Q_{m\,ji} = \sum_{h\in\mathcal{I}_M} Q_h, \forall i \in \mathcal{I}_M \tag{5.38}$$

$$\sum_{tm=1}^{Tm} p_{k,tm} = 1, \quad \forall k \in 1, 2, ..., N_M \tag{5.39}$$

$$k = i - N_F - N_B - N_W \quad \forall k \in 1, 2, ..., N_M, \quad \forall i \in \mathcal{I}_M \tag{5.40}$$

Objective functions

The above discussions have already proposed the three key aspects of an optimization model: decision variables, objective functions, and constraints. Three basic objective functions are defined: the minimum total cost, the minimum pressure loss, and the shortest payback period. For the vertical well type, the production rate of each well is input information, and oil price is assumed to be constant, the shortest payback period also brings the minimum total cost. Therefore, the minimum cost is selected as the first objective function, as shown by eq.(5.41).

$$\begin{aligned} COST_{total} = \quad & COST_{drilling} + COST_{flowline} + COST_{riser} \\ & + COST_{fpso} + COST_{manifold} \end{aligned} \tag{5.41}$$

Eq.(5.41) does not include information about pressure loss. To minimize the total cost, the flowline length tends to be as short as possible, which also lead to lower pressure loss according to the definition of pressure loss shown by eq.(3.12): $E = QL/D^4$. But if we want to know the effect of pressure loss on the subsea layout, only using eq.(5.41) is not enough. At the same time, simply using the total pressure loss shown by eq.(5.11) lacks the information about the cost for FPSOs and manifolds. As a result, in order to comprehensively include all aspects together, we combine the total cost and the total pressure loss together, as well as the result of the satellite well system concept through weighted average, as the second objective function:

$$\begin{aligned} \min \quad & \mathcal{Z} = \beta_1 \frac{E_{total}}{E_0} + \beta_1 \frac{COST_{total}}{COST_0} \\ & \beta_1 + \beta_2 = 1, \quad \beta_1, \beta_2 \in [0, 1] \end{aligned} \tag{5.42}$$

E_0 and $COST_0$ are the optimization results of the concept of satellite well system considering vertical well type. Through this way, the cost and pressure loss are both represented as the dimensionless forms, which could be added together, in order to present the collective effect of the two objective functions on the layout optimization, as well as the comparison with the satellite well system concept. To minimize the objective function, both total cost and pressure loss tend to be as small. To study the effect of pressure loss, the factor β_2 could be larger. In the case studies, the two objective functions are compared and discussed.

General form of the mathematical model

No matter which objective function is considered, it is the function of the decision variables, as well as the constraints, with both equalities and inequalities.

We use the bold symbols $\boldsymbol{x}$, $\boldsymbol{z}$, $\boldsymbol{p}$, $\boldsymbol{q_m}$, $\boldsymbol{q_f}$, $\boldsymbol{Q_m}$, $\boldsymbol{Q_f}$, $\boldsymbol{M}$ to represent the corresponding matrices or vectors. Besides, the adjacent matrix V_{ij}, segment intersection matrix C_X, and the distance matrix d_{ij} are all related to the manifold positions, which are represented by

$$\begin{aligned} \boldsymbol{V} &= f_v(\boldsymbol{M}) \\ \boldsymbol{C_X} &= f_c(\boldsymbol{M}) \\ \boldsymbol{d} &= f_d(\boldsymbol{M}) \end{aligned} \tag{5.43}$$

Therefore, the general form of the proposed optimization model could be written as

$$\begin{aligned} \min \quad & f(\boldsymbol{x}, \boldsymbol{z}, \boldsymbol{p}, \boldsymbol{q_m}, \boldsymbol{q_f}, \boldsymbol{Q_m}, \boldsymbol{Q_f}, \boldsymbol{M}, \boldsymbol{V}, \boldsymbol{d}, \boldsymbol{C_X}) \\ \text{subject to} \quad & \begin{cases} g(\boldsymbol{x}, \boldsymbol{z}, \boldsymbol{p}, \boldsymbol{q_m}, \boldsymbol{q_f}, \boldsymbol{Q_m}, \boldsymbol{Q_f}, \boldsymbol{M}, \boldsymbol{V}, \boldsymbol{d}, \boldsymbol{C_X}) = 0 \\ h(\boldsymbol{x}, \boldsymbol{z}, \boldsymbol{p}, \boldsymbol{q_m}, \boldsymbol{q_f}, \boldsymbol{Q_m}, \boldsymbol{Q_f}, \boldsymbol{M}, \boldsymbol{V}, \boldsymbol{d}, \boldsymbol{C_X}) <= 0 \\ \boldsymbol{V} = f_v(\boldsymbol{M}) \\ \boldsymbol{C_X} = f_c(\boldsymbol{M}) \\ \boldsymbol{d} = f_d(\boldsymbol{M}) \end{cases} \end{aligned} \tag{5.44}$$

The function set f and g represents all the constraints which describe the subsea

layout characteristics, from eq.(5.14) to eq.(5.40). And the last four sets are related to manifold positions, which bring nonlinearity to the optimization model so that the proposed optimization model belongs to the MINLP problem.

5.2.2 Scenario 2: Cluster manifold

Description of the main characteristics

Different from the satellite well-manifold system, for cluster manifold system, wellheads are clustered, and the reservoir targets are reached through directional drilling or extended reach drilling. The wellheads are connected with the manifolds through short jumpers. Figure 5.2.2 presents a schematic view for a cluster manifold system. The jumpers are considered standardized and the lengths are the same, represented by L_J.

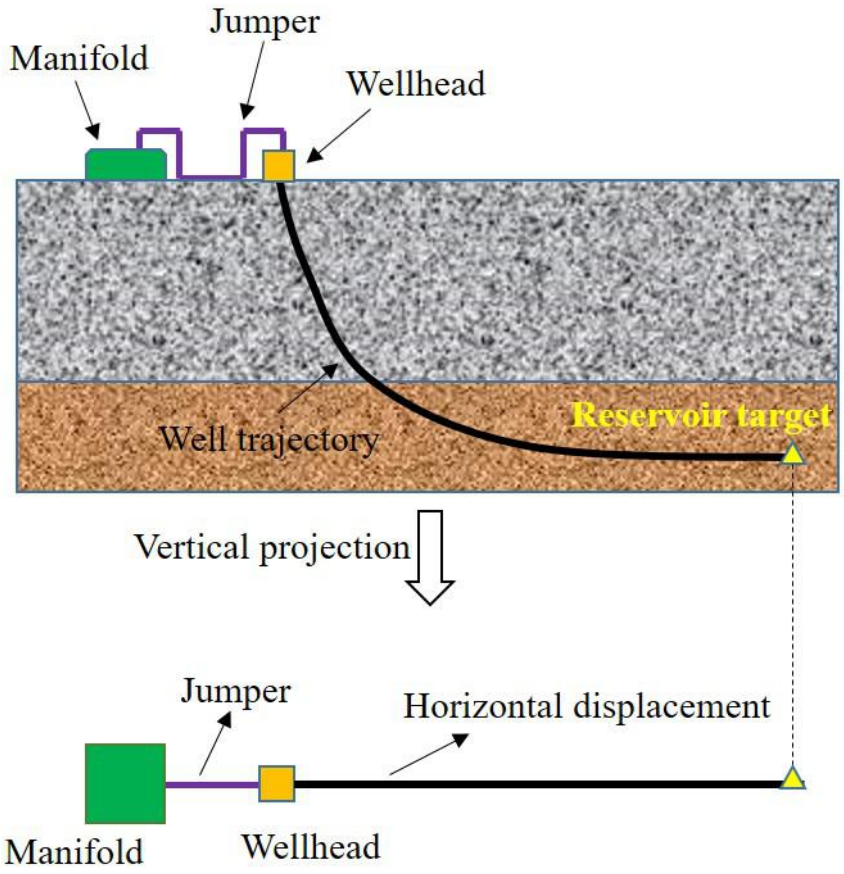

Figure 5.3: Schematic view of a simple cluster manifold system

Similar to what has been discussed in section 4.2.2, when the projection of jumper and well trajectory are collinear, the horizontal displacement is the minimum. Therefore, when building up the layout optimization model, we could assume the straight connection between reservoir target and the manifold on the projection

$X-Y$ plane, and the wellhead location as well as the well horizontal displacement could be obtained through subtracting the length of jumper, just like how we determine the riser base locations as mentioned in section 3. Besides, since each well cluster and the corresponding manifold are close with each other compared with the width and length of the whole offshore field, and the cluster manifolds usually distribute far away from each other for the purpose of covering the whole offshore field area, the short jumpers will not affect the flowline routes between manifolds and FPSOs.

Therefore, the subsea layout of the cluster manifold system could be divided into two parts. The first part is the well assignments to the manifolds, in which the connection between wellheads and manifolds represents well trajectory projections together with the jumpers, as shown in Figure 5.2.2. The seabed obstacles and riser porch nodes are not included in this part.

The second part is the manifold assignments to the FPSOs, in which the flowline routes between manifolds and FPSOs should be determined. The manifold nodes, obstacle nodes and the riser porch nodes are considered in this part. It is easy to find that this part is almost the same with satellite well system described in chapter 4, here the manifold nodes are like "big satellite wellheads". Therefore, the optimization model for the satellite well system could be applied here, only with some minor modifications.

The definition of node set is similar to previous models in this thesis. On the flat plane, there are four basic types of nodes: riser porch nodes $\mathcal{I}_{\mathcal{F}}$, obstacle nodes $\mathcal{I}_{\mathcal{O}}$, well bottom node set $\mathcal{I}_{\mathcal{W}}$, and the manifold node $\mathcal{I}_{\mathcal{M}}$. node set $\mathcal{I}_{\mathcal{W}}$ and $\mathcal{I}_{\mathcal{M}}$ are used for the first part of the layout. Node set $\mathcal{I}_{\mathcal{F}}$, $\mathcal{I}_{\mathcal{O}}$, and $\mathcal{I}_{\mathcal{M}}$ are used for the second part, which is put together as the overall node set shown by eq.(5.45).

$$\mathcal{I} = \{\mathcal{I}_{\mathcal{F}}, \mathcal{I}_{\mathcal{O}}, \mathcal{I}_{\mathcal{M}}\} \tag{5.45}$$

The adjacent matrix V_{ij} and distance matrix d_{ij} could be obtained through eq.(4.3) and eq.(4.6).

Another important issue is about the production rate. For well j connected to manifold i, the horizontal displacement is $L_{ij} - L_J$, the horizontal production interval length could be obtained through eq.(4.35), and the production rate could be calculated through eq.(3.3). As a result, this feature makes the scenario different from all the others, because the production rate of the well become to relate to both the manifold position and the assignment to the manifold. Therefore, a production rate matrix Q_{ij}^w is introduced, to represent the possible production rate if well j is assigned to manifold i. Given the manifold positions, the Q_{ij}^w could be obtained. The same with distance matrix d_{ij}, the element in the production matrix is effective

only when node i and j are connected.

Decision variables

The definition of decision variables is as follows.

Binary variable y_{ij}, $i \in \mathcal{I}_{\mathcal{M}}$, $j \in \mathcal{I}_{\mathcal{W}}$, indicates the connection relationship between manifolds and wells. $y_{ij} = 1$ means well j is connected to manifold i.

Binary variable x_{ij}, $\forall i, j \in \mathcal{I}$, $x_{ij} = 1$ indicates that node i is connected with node j, while $x_{ij} = 0$ means there is no flowline between node i and node j.

Binary variable $p_{k,tm}$, $p_{k,tm} = 1$ indicates that the kth manifold selects type tm from the avaible ones. $k = 1, 2, ..., N_M$, $tm = 1, 2, ..., Tm$.

Binary variable z_{st}, is introduced to indicate the selection of FPSO from the available options. If the size s is selected for FPSO t, $z_{ts} = 1$, otherwise, $z_{ts} = 0$.

Non-negative integer variable $q_{f_{ij}}$, $\forall i, j \in \mathcal{I}$, represent the number of flowlines between node i and node j toward FPSO.

The continuous variable $Q_{f_{ij}}$, $\forall i, j \in \mathcal{I}$, represent the total flow rates from node i to node j toward FPSO.

The manifold positions (x_k^m, y_k^m), $k = 1, 2, ..., N_M$, which could be arranged as a row vector $\boldsymbol{M} = [x_1^m, y_1^m, ..., x_k^m, y_k^m, ..., x_{N_M}^m, y_{N_M}^m]$. The elements are continuous variables.

Cost components

The components of the total cost could be represented by these defined decision variables.

The drilling cost is

$$COST_{drilling} = P_v L_v + P_h L_h = \sum_{l=1}^{N_W} P_v \frac{H_l + h_l + H_1}{2} + \sum_{i \in \mathcal{I}_{\mathcal{M}}} \sum_{j \in \mathcal{I}_{\mathcal{W}}} y_{ij}(L_{ij} - L_J) \quad (5.46)$$

At the right side of the equal sign, the first term is the drilling cost for the vertical part, and we consider the well bottoms are located in the middle of the reservoir, in order to provide enough flow area around the well. The second term is the cost of the drilling cost for the horizontal part. L_{ij} means the distance between manifold i and well j on the $X - Y$ plane.

The flowline cost is

$$COST_{flowline} = 2P_{mf}^{line} \sum_{i \in \mathcal{I}} \sum_{j \in \mathcal{I}} d_{ij} q_{f_{ij}} \quad (5.47)$$

The riser cost is

$$COST_{riser} = 2P^{riser} N_M L_{riser} \quad (5.48)$$

The FPSO cost is

$$COST_{fpso} = \sum_{t=1}^{N_{fpso}} \sum_{s=1}^{N_{fpso}^{ava}} P_s^{fpso} z_{ts} \tag{5.49}$$

The manifold cost is

$$COST_{manifold} = \sum_{k=1}^{N_M} \sum_{tm=1}^{N_M^{ava}} P_{tm}^{manifold} p_{k,tm} \tag{5.50}$$

The jumper cost is

$$COST_{jumper} = N_W L_J \tag{5.51}$$

The total cost is

$$\begin{aligned} COST_{total} = \quad & COST_{drilling} + COST_{flowline} + COST_{riser} \\ & + COST_{fpso} + COST_{manifold} + COST_{jumper} \end{aligned} \tag{5.52}$$

Pressure loss

Through eq.(3.12), the total pressure loss of the whole system from manifolds to FPSOs is represented by

$$E_{total} = \sum_{i \in \mathcal{I}} \sum_{j \in \mathcal{I}} \frac{Q_{f_{ij}} d_{ij}}{D_{mf}^4} + \sum_{j \in \mathcal{I}_{\mathcal{F}}} \sum_{i \in \mathcal{I}} \frac{Q_{f_{ij}} L_{riser}}{D_{mf}^4} \tag{5.53}$$

Payback period

The production rates of the wells are related to the well assignment to the manifolds, the total production rate could be represented by $\sum_{i=1}^{N_M} \sum_{j=1}^{N_W} Q_{ij}^w y_{ij}$, and the payback period is

$$PB = \frac{COST_{total}}{\sum_{i=1}^{N_M} \sum_{j=1}^{N_W} Q_{ij}^w y_{ij}} \tag{5.54}$$

Constraints

Following constraints should be satisfied, for a feasible layout of the cluster manifold system.

Each well must be connected with one manifold, and the total number of well connected to the same manifold should not exceed the maximum slots number of this manifold. The slots number depends on which size of manifold we select from the available ones. These requirements are defined by eq.(5.55), eq.(5.56) and eq.(5.57).

$$\sum_{i \in \mathcal{I}_{\mathcal{M}}} y_{ij} = 1, \quad \forall j \in \mathcal{I}_{\mathcal{W}} \tag{5.55}$$

$$1 \leq \sum_{j \in \mathcal{I}_{\mathcal{M}}} y_{ij} \leq \sum_{tm=1}^{Tm} p_{i,tm} S_{tm}, \quad \forall i \in \mathcal{I}_{\mathcal{M}} \tag{5.56}$$

$$\sum_{tm=1}^{Tm} p_{i,tm} = 1, \quad \forall i \in 1, 2, ..., N_M \tag{5.57}$$

For the nodes on the seabed, first of all, node i and node j must be connectable, if not, $x_{ij} = 0$, which is described by eq.(5.58). Eq.(5.59) and eq.(5.60) indicate that the flow only and must happens between node i and j when they are connected. ψ is a very small positive number used to ensure the flow won't be zero when node i, j are connected. Ψ is a large number. Eq.(5.61) ensures that there is at most only one flow direction between node i and node j.

$$x_{ij} \leq V_{ij} \quad \forall i, j \in \mathcal{I} \tag{5.58}$$

$$\psi x_{ij} \leq q_{f_{ij}} \leq \Psi x_{ij} \quad \forall i, j \in \mathcal{I} \tag{5.59}$$

$$\psi q_{f_{ij}} \leq Q_{f_{ij}} \leq \Psi q_{f_{ij}} \quad \forall i, j \in \mathcal{I} \tag{5.60}$$

$$x_{ij} + x_{ji} \leq 1 \quad \forall i, j \in \mathcal{I} \tag{5.61}$$

Eq.(5.62)-eq.(5.64) describe the requirements for the manifold nodes. First of all, the cluster manifold could be regarded as the start of the subsea system, therefore, there will be no flow enters, and one wellhead should and must be connected with only one flowline, which is shown by eq.(5.62) and eq.(5.63).

It should be noted that when we consider the manifolds as the flow sources of the subsea system, there is no flow enters as mentioned. But these flow sources receive the fluid from wells, and the flow rate at each manifold should be equal to the total production rate of the wells that are connected with this manifold, which is described by eq.(5.64). This requirement is very important because it connects the descriptions of the first part (wells and manifolds) and the second part (manifolds and FPSOs), resulting in a whole system from well bottoms to the FPSOs.

$$\sum_{j \in \mathcal{I}} x_{ij} = 1, \quad \sum_{j \in \mathcal{I}} x_{ji} = 0 \quad \forall i \in \mathcal{I}_{\mathcal{M}} \tag{5.62}$$

$$\sum_{j \in \mathcal{I}} q_{f_{ij}} = 1, \quad \sum_{j \in \mathcal{I}} q_{f_{ji}} = 0 \quad \forall i \in \mathcal{I}_{\mathcal{M}} \tag{5.63}$$

$$\begin{cases} \sum\limits_{j\in\mathcal{I}} Q_{f_{ij}} = \sum\limits_{j_w\in\mathcal{I}_\mathcal{W}} Q^w_{i,j_w} y_{i,j_w} & \forall i \in \mathcal{I}_\mathcal{M} \\ \sum\limits_{j\in\mathcal{I}} Q_{f_{ji}} = 0 & \forall i \in \mathcal{I}_\mathcal{M} \end{cases} \tag{5.64}$$

Eq.(5.65)-Eq.(5.68) indicate the requirements for riser porch nodes.

The riser porch nodes are the ends of the system, and there will be no flow exits the riser porch nodes. At the same time, for each FPSO, the risers connected with it should not exceed its maximum available riser numbers, and the total flow rate enters one FPSO should not exceed its processing capacity. These requirements are represented by eq.(5.65), eq.(5.66) and eq.(5.67). Note that the factor "1/2" is due to the consideration of flowline loop, which requires two risers for the connection between one manifold and the corresponding FPSO.

The total number of the risers connected to the FPSOs should equal to two times of the manifold number, considering the requirements of flowline loop, and the total flow rate enters FPSOs should equal to the total production rate of all the wells, which are described by eq.(5.68).

$$\sum_{j\in\mathcal{I}} x_{ij} = 0, \quad \sum_{j\in\mathcal{I}} x_{ji} \leq \frac{1}{2} \sum_{s=1}^{N^{ava}_{fpso}} (N^{riser}_s z_{i,s}), \quad \forall i \in \mathcal{I}_\mathcal{F} \tag{5.65}$$

$$\sum_{j\in\mathcal{I}} q_{f_{ij}} = 0, \quad \sum_{j\in\mathcal{I}} q_{f_{ji}} \leq \frac{1}{2} \sum_{s=1}^{N^{ava}_{fpso}} (N^{riser}_s z_{i,s}), \quad \forall i \in \mathcal{I}_\mathcal{F} \tag{5.66}$$

$$\sum_{j\in\mathcal{I}} Q_{f_{ij}} = 0, \quad \sum_{j\in\mathcal{I}} Q_{f_{ji}} \leq \sum_{s=1}^{N^{ava}_{fpso}} (Q^{fpso}_s z_{i,s}), \quad \forall i \in \mathcal{I}_\mathcal{F} \tag{5.67}$$

$$\sum_{i\in\mathcal{I}_\mathcal{F}} \sum_{j\in\mathcal{I}} x_{ji} \leq N_M, \quad \sum_{i\in\mathcal{I}_\mathcal{F}} \sum_{j\in\mathcal{I}} q_{f_{ji}} = N_M, \quad \sum_{i\in\mathcal{I}_\mathcal{F}} \sum_{j\in\mathcal{I}} Q_{f_{ji}} = \sum_{i_w=1}^{N_M} \sum_{j_w=1}^{N_W} Q^w_{i_w,j_w} y_{i_w,j_w} \tag{5.68}$$

Eq. (5.69) includes the constraints for the intermediate nodes, which are the obstacle polygons' vertices. According to the discussions above, it is possible that two or more routes have some part overlapped, which are regarded parallelly laid. This point means that starting from node i, at most one node could be connected. Besides, though these routes are regarded parallelly laid, the total flow rate in these overlapped flowlines is equal to the sum of the flow rate before the shared node, which indicates that the flow is conserved. These requirements are shown by eq.(5.69).

$$\sum_{j\in\mathcal{I}} q_{f_{ij}} - \sum_{j\in\mathcal{I}} q_{f_{ji}} = 0, \quad \sum_{j\in\mathcal{I}} Q_{f_{ij}} - \sum_{j\in\mathcal{I}} Q_{f_{ji}} = 0, \quad \sum_{j\in\mathcal{I}} x_{ij} \leq 1, \quad \forall i \in \mathcal{I}_\mathcal{O} \tag{5.69}$$

Objective fucntions

The objective functions are the same with scenario 1 that considering manifold system with satellite distributed vertical wells, including the minimum total cost, and the hybrid objective combining total cost and pressure loss, as shown by eq.(5.52), and eq.(5.42), respectively. The payback period is not selected as the objective function, for one reason, we intend to keep the objective functions the same with scenario 1 for comparison, and for the other, the payback period presents serious nonlinearity since the decision variable y_{ij} appears on the denominator, as shown by eq.(5.54), making it hard to be solved. In the case studies, the payback period will be discussed as one of the indeces to evaluate the optimization results.

General form of the mathematical model

The same with the previous models in this text, no matter which function is selected, it is the function of defined decision variables. And so are the constraints, with both equalities and inequalities.

We use the bold symbols $\boldsymbol{x}$, $\boldsymbol{y}$,$\boldsymbol{z}$, $\boldsymbol{p}$, $\boldsymbol{q_f}$, $\boldsymbol{Q_f}$, $\boldsymbol{M}$ to represent the corresponding matrices or vectors. Besides, the adjacent matrix V_{ij}, and the distance matrix d_{ij} are all related to the manifold positions, which are represented by

$$\begin{aligned} \boldsymbol{V} &= f_v(\boldsymbol{M}) \\ \boldsymbol{d} &= f_d(\boldsymbol{M}) \end{aligned} \tag{5.70}$$

Furthermore, as discussed above, the production rate matrix is also related to the manifold positions, which is represented by

$$\boldsymbol{Q^w} = f_Q(\boldsymbol{M}) \tag{5.71}$$

Therefore, the general form of the proposed optimization model for the layout of cluster manifold could be written as

$$\begin{aligned} &\min \quad f(\boldsymbol{x}, \boldsymbol{z}, \boldsymbol{p}, \boldsymbol{q_f}, \boldsymbol{Q_f}, \boldsymbol{M}, \boldsymbol{V}, \boldsymbol{d}, \boldsymbol{Q^w}) \\ &\text{subject to} \\ &\begin{cases} g(\boldsymbol{x}, \boldsymbol{z}, \boldsymbol{p}, \boldsymbol{q_f}, \boldsymbol{Q_f}, \boldsymbol{M}, \boldsymbol{V}, \boldsymbol{d}, \boldsymbol{Q^w}) = 0 \\ h(\boldsymbol{x}, \boldsymbol{z}, \boldsymbol{p}, \boldsymbol{q_f}, \boldsymbol{Q_f}, \boldsymbol{M}, \boldsymbol{V}, \boldsymbol{d}, \boldsymbol{Q^w}) \leq 0 \\ \boldsymbol{V} = f_v(\boldsymbol{M}) \\ \boldsymbol{d} = f_d(\boldsymbol{M}) \\ \boldsymbol{Q^w} = f_Q(\boldsymbol{M}) \end{cases} \end{aligned} \tag{5.72}$$

The function set f and g represents all the constraints which describe the subsea layout characteristics, from eq.(5.55) to eq.(5.69). And the last three sets, $\boldsymbol{V}$, $\boldsymbol{d}$, $\boldsymbol{Q^w}$ are related to manifold positions, which bring nonlinearity to the optimization model so that the proposed optimization model belongs to the MINLP problem.

5.3 Solution method

5.3.1 Overall solution strategy

For convenient description, we name the optimization models for satellite well-manifold system and the cluster manifold system **MODEL 1** and **MODEL 2**, respectively, to distinguish from each other. Both **MODEL 1** and **MODEL 2** are MINLP problems.

Suppose the $\boldsymbol{M}$ was known, for **MODEL 1**, $\boldsymbol{V}$, $\boldsymbol{d}$ and $\boldsymbol{C_X}$ would be obtained, and for **MODEL 2**, $\boldsymbol{V}$, $\boldsymbol{d}$ and $\boldsymbol{Q_w}$ would be obtained, then the original models would become linear, which could be solved by GUROBI solver. This is exactly the same with the proposed solution strategy for the layout optimization model of the satellite well system considering horizontal drilling, which is discussed in chapter 4. Again the gradient descent method is applied to build up the iteration framework to find the best manifold positions. The proposed solution process in section 4.3 could be applied here, just by replacing the $\boldsymbol{L_h}$ in section 4.3 with $\boldsymbol{M}$. The detailed equations and flow chart have already been presented in section 4.3 and here we will not repeat.

5.3.2 Initial solution candidates

Given the number of the manifold, we need to determine the initial manifold positions to start the iteration. According to the work by Cooper et al.[43, 91], these "Location-allocation" problems always have a series of local optimums. Therefore, the initial solution is very important to achieve high-quality results.

In the work of Zhang et al. [73, 74] and Rodrigues et al. [61], the space was discrete into grids, and the facilities' positions were selected through these discrete grid nodes. This way of treatment provides some inspirations for finding an initial solution: we could distribute a series of nodes on the $X-Y$ plane as candidate nodes, and select the manifolds from these candidates. Through proper ways of distribution, the nodes will cover most of the solution space, and the resulted initial solution will be close to the optimum, which is good for the subsequent iteration to achieve the optimal solution.

In this thesis, the Delaunay triangulation is applied to distribute the candidate nodes. Delaunay triangulation (also known as a Delone triangulation) for a given

set P of discrete points in a plane is a triangulation $DT(P)$ such that no point in P is inside the circumcircle of any triangle in $DT(P)$ [92]. Figure 5.4 illustrate a simple example to help illustrate this concept. As shown in the figure, there are four discrete nodes, A, B, C and D. Obviously, there are two ways of dividing them into two triangles, which are ΔABD and ΔBCD, in Figure 5.4(a), and ΔABC and ΔACD in Figure 5.4(b). Circle 1, 2, 3, and 4 are the circumcircles of these triangles, respectively. For the first scenario in (a), node C lies outside circle 1 of ΔABD, and node A lies outside circle 2 of ΔBCD, but the second scenario in (b) is different, in which node D is inside the circumcircle of ΔABC and node B is inside the circumcircle of ΔACD. Therefore, scenario (a) is the Delaunay triangulation for node A, B, C and D.

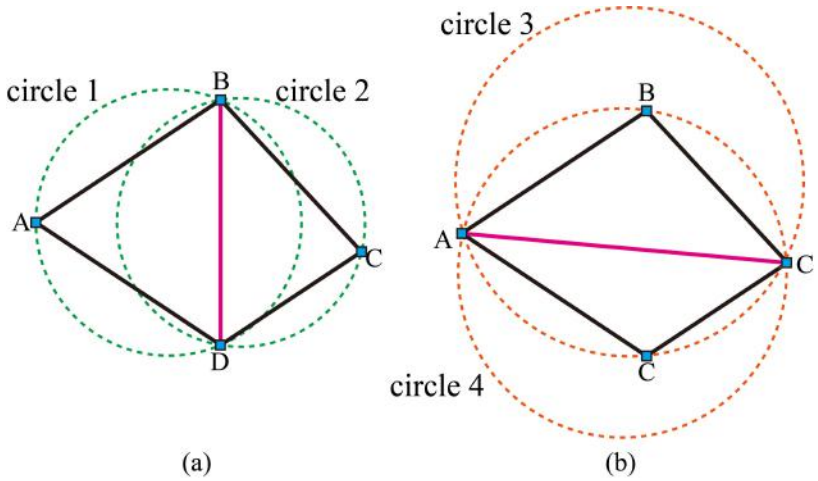

Figure 5.4: Basic concept of Delaunay triangulation

Figure 5.5 is an example of Delaunay triangulation for the more general situation when there are many discrete nodes distributing on the plane. For each triangle, the geometric center locates inside, and the distribution density is related to the density of discrete nodes. Besides, all these geometric centers are inside the convex hull formed by these discrete nodes, as shown by the red line in the figure. And the distribution of the gravity center almost covers the whole area of the convex hull. Considering reducing cost, manifolds are always located inside the convex hull formed by the given facilities' nodes, such as wells, obstacle polygons' vertices and so on. And the candidate nodes are expected to be distributed throughout the field area. The characteristics of geometric centers based on Delaunay triangulation become very effective and fit for the seeking of manifold positions.

Therefore, for a given offshore field, the Delaunay triangulation is applied to the defined several types of nodes, and the geometric centers of all the triangles are taken as the candidate positions for the manifolds, for the determination of the initial solution. The geometric centers located inside the subsea restricted areas

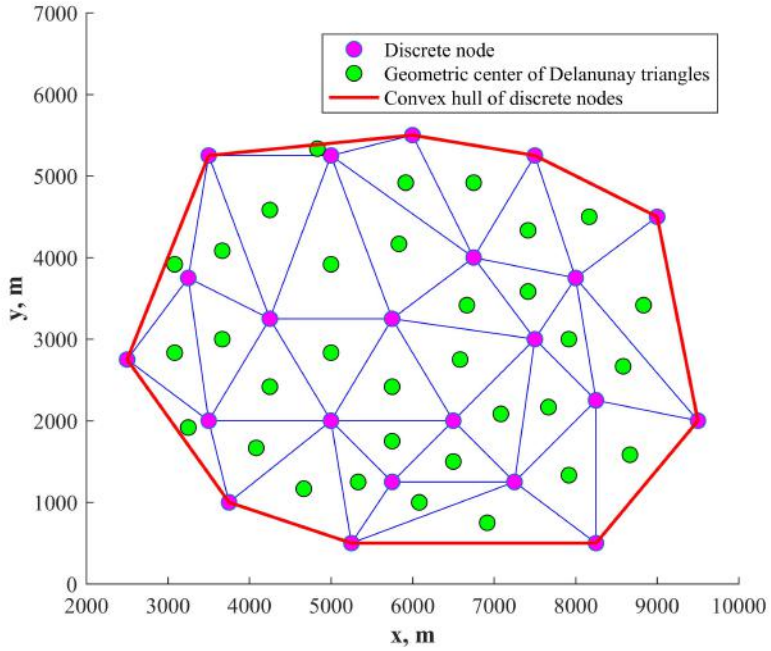

Figure 5.5: A general example of Delaunay triangulation

or the riser laying regions will be eliminated. Figure 5.6 presents the Delaunay triangulation for the case provided in chapter 4.

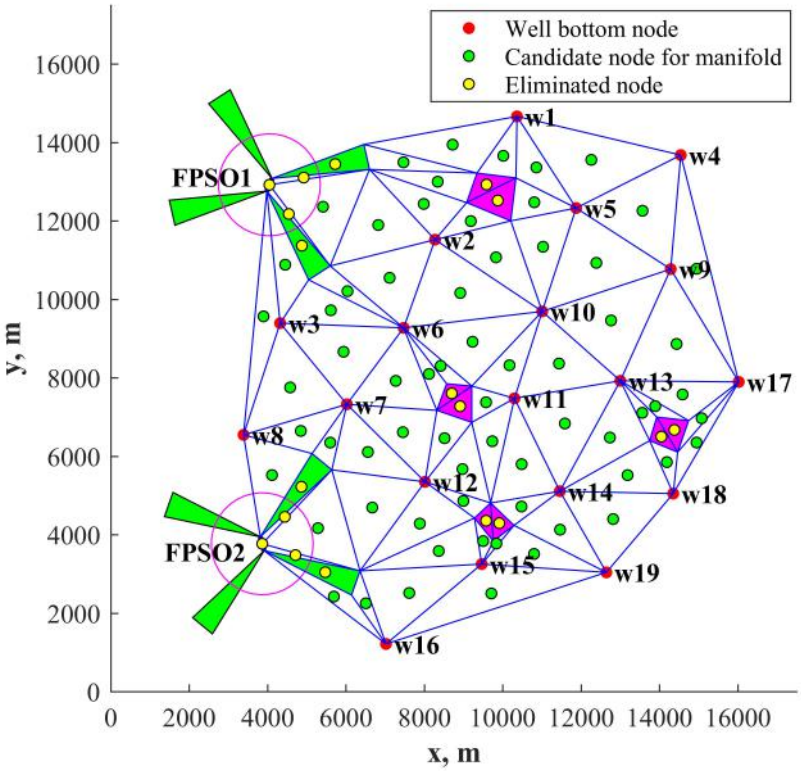

Figure 5.6: Delaunay triangulation of the case in chapter 4

A lot of algorithms have been developed to generate the Delaunay triangulation, such as flip algorithms, BowyerWatson algorithm [93], divide and conquer algorithm [94] and so on. In this thesis, our purpose is to apply this into the optimization process, so that we do not go too deep into the generating algorithm, instead, the developed Delaunay triangulation module in MATLAB is used.

5.3.3 Models for initial solution

The proposed **MODEL 1** and **MODEL 2** are for the designed number of manifold, as for searching the initial solution, the candidate manifold positions replace the designed manifold nodes in the models, changing the problems through "finding the positions of manifolds on the continuous plane" to "finding the manifolds from the discrete candidate nodes". Therefore, both **MODEL 1** and **MODEL 2** need to be modified for the application in initial solution searching.

Suppose the candidate manifold node set is $\mathcal{I}_{\mathcal{C}}$, and the number of candidate node is N_C, the original manifold node set $\mathcal{I}_{\mathcal{M}}$ should be replaced by $\mathcal{I}_{\mathcal{C}}$, so that the over all node set shown by eq.(5.1) for **MODEL 1** and eq.(5.45) for **MODEL 2** need to be mofified.

Any calculations toward the node set $\mathcal{I}_{\mathcal{M}}$ should be replaced by the calculations toward the node set $\mathcal{I}_{\mathcal{C}}$, including the ajacent matrix $\boldsymbol{V}$, distance matrix $\boldsymbol{d}$ in both **MODEL 1** and **MODEL 2**, the segment intersection matrix $\boldsymbol{C_X}$ in **MODEL 1** and the well production rate matrix $\boldsymbol{Q^w}$ in **MODEL 2**.

A set of extra binary variables, $\boldsymbol{u}$ is introduced, to indicating the selection of the candidate manifold nodes, $\boldsymbol{u} = [u_1, u_2, ..., u_{N_C}]$. $u_i = 1$ means the ith candidate node is selected as one of the manifold position, otherwise, $u_i = 0$.

The constraints about the manifold node in both **MODEL 1** and **MODEL 2** should be modified through including the binary variable u_i. In some cases, we use subscript "k_m" to present the elements in set $\boldsymbol{u}$, and in other cases, we use subscript "i", depending on the need of distinguishing from the subscripts of the other variables.

The number of selected candidate nodes should be equal to the designed manifold number, therefore

$$\sum_{i=1}^{N_C} u_i = N_W \tag{5.73}$$

Eq.(5.73) should be added into both **MODEL 1** and **MODEL 2**.

The contraints of **MODEL 1** and **MODEL 2** that related to the treatment of manifold node set $\mathcal{I}_{\mathcal{M}}$ should be modified considering the candidate selection variable $\boldsymbol{u}$.

Let's take **MODEL 1** as example to explain the basic criteria of modifying the constraints. Eq.(5.34), eq.(5.35), eq.(5.36), eq.(5.39),and eq.(5.40) are the constraints for the manifold nodes. For the candidate manifold node k_m, if it is selected as the manifold position, $u_{k_m} = 1$, these original constriants are effective, while if it is not selected, $u_{k_m} = 0$, candidate node u_{k_m} will not belong to the system and all those constraints should be set to be zero in order to eliminate the effect of this unselected candidate node on the optimization model. For instance, eq.(5.74) represents the requirements for the manifold nodes about the connection variable $\boldsymbol{x}$. If $u_{k_m} = 1$, the terms in the first column are effective, and eq.(5.74) degenerates back to the original constriant shown by eq.(5.34), while if $u_{k_m} = 0$, the terms in the second column are effective, which lead to $x_{ij} = 0$, and $x_{ji} = 0$, $j \in \mathcal{I}, i \in \mathcal{I}_\mathcal{C}$, indicating that the candidate node k_m is isolated.

Based on this criteria, for **MODEL 1**, original constraints eq.(5.34), eq.(5.35), eq.(5.36), eq.(5.39),and eq.(5.40) should be replaced by eq.(5.74), eq.(5.75), eq.(5.76), eq.(5.77) and eq.(5.78), respectively.

$$\begin{cases} 1 + \Psi(u_{k_m} - 1) \leq \sum\limits_{j \in \mathcal{I}} x_{ij} \leq 1 + \Psi(1 - u_{k_m}), & \sum\limits_{j \in \mathcal{I}} x_{ij} \leq \Psi u_{k_m} \quad \forall i \in \mathcal{I}_\mathcal{C} \\ \sum\limits_{j \in \mathcal{I}} x_{ji} \leq \sum\limits_{tm=1}^{Tm} p_{k_m,tm} S_{tm} + \Psi(1 - u_{k_m}), & \sum\limits_{j \in \mathcal{I}} x_{ji} \leq \Psi u_{k_m} \quad \forall i \in \mathcal{I}_\mathcal{C} \end{cases} \tag{5.74}$$

$$\begin{cases} 2 + \Psi(u_{k_m} - 1) \leq \sum\limits_{j \in \mathcal{I}} q_{mj,i} \leq \sum\limits_{tm=1}^{Tm} p_{k,tm} S_{tm} + \Psi(1 - u_{k_m}) & \forall i \in \mathcal{I}_\mathcal{C} \\ \sum\limits_{j \in \mathcal{I}} q_{mij} = 0, \quad \sum\limits_{j \in \mathcal{I}} q_{mji} \leq \Psi u_{k_m} & \forall i \in \mathcal{I}_\mathcal{C} \end{cases} \tag{5.75}$$

$$\begin{cases} 1 + \Psi(u_{k_m} - 1) \leq \sum\limits_{j \in \mathcal{I}} q_{fij} \leq 1 + \Psi(1 - u_{k_m}), & \forall i \in \mathcal{I}_\mathcal{C} \\ \sum\limits_{j \in \mathcal{I}} q_{fji} = 0, \quad \sum\limits_{j \in \mathcal{I}} q_{fij} \leq \Psi z u_{k_m}, & \forall i \in \mathcal{I}_\mathcal{C} \end{cases} \tag{5.76}$$

$$1 + \Psi(u_{k_m} - 1) \leq \sum_{tm=1}^{Tm} p_{k_m,tm} \leq 1 + \Psi(1 - u_{k_m}), \quad \sum_{tm=1}^{Tm} p_{k_m,tm} \leq \Psi u_{k_m} \tag{5.77}$$

$$k_m = i - N_F - N_B - N_W \quad \forall k_m \in 1, 2, ..., N_C, \quad \forall i \in \mathcal{I}_C \tag{5.78}$$

For the same reason, original constraints eq.(5.56), eq.(5.57), eq.(5.62) and eq.(5.63) in **MODEL 2** are replaced by eq.(5.79), eq.(5.80), eq.(5.81) and eq.(5.82), respectively.

$$\begin{cases} 2+\Psi(u_i-1) \le \sum\limits_{j\in\mathcal{I}_\mathcal{W}} y_{ij} \le \sum\limits_{tm=1}^{Tm} p_{i,tm}S_{tm} + \Psi(1-u_i), & \forall i \in \mathcal{I}_\mathcal{C} \\ \sum\limits_{j\in\mathcal{I}_\mathcal{W}} y_{ij} \le \Psi u_i, & \forall i \in \mathcal{I}_\mathcal{C} \end{cases} \tag{5.79}$$

$$\begin{cases} 1+\Psi(u_i-1) \le \sum\limits_{tm=1}^{Tm} p_{k_m,tm} \le 1+\Psi(1-u_i), & \forall i \in \mathcal{I}_\mathcal{C} \\ \sum\limits_{tm=1}^{Tm} p_{i,tm} \le \Psi u_i, & \forall i \in \mathcal{I}_\mathcal{C} \end{cases} \tag{5.80}$$

$$\begin{cases} 1+\Psi(u_{k_m}-1) \le \sum\limits_{j\in\mathcal{I}} x_{ij} \le 1+\Psi(1-u_{k_m}) & \forall i \in \mathcal{I}_\mathcal{C} \\ x_{ij} \le \Psi u_{k_m} & \forall i \in \mathcal{I}_\mathcal{C} \\ \sum\limits_{j\in\mathcal{I}} x_{ji} = 0, & \forall i \in \mathcal{I}_\mathcal{C} \\ k_m = i - N_F - N_B \end{cases} \tag{5.81}$$

$$\begin{cases} 1+\Psi(u_{k_m}-1) \le \sum\limits_{j\in\mathcal{I}} q_{f\,ij} \le 1+\Psi(1-u_{k_m}) & \forall i \in \mathcal{I}_\mathcal{C} \\ q_{f\,ij} \le \Psi u_{k_m} & \forall i \in \mathcal{I}_\mathcal{C} \\ \sum\limits_{j\in\mathcal{I}} q_{f\,ji} = 0, & \forall i \in \mathcal{I}_\mathcal{C} \\ k_m = i - N_F - N_B \end{cases} \tag{5.82}$$

After the above treatments, the models of determining initial solution for **MODEL 1** and **MODEL 2** are obtained, which are named **MODEL 1-I** and **MODEL 2-I**. As the candidate manifold node set $\mathcal{I}_\mathcal{C}$ is the input information, the related parameters such as adjacent matrix $\boldsymbol{V}$, distance matrix $\boldsymbol{d}$, segment intersection matrix $\boldsymbol{C_X}$, and production rate matrix $\boldsymbol{Q^w}$ could all be obtained as input for the **MODEL 1-I** and **MODEL 2-I**, the rest of the constriants and objective functions are all linear, as a result, **MODEL 1-I** and **MODEL 2-I** are MILP models, which could be solved by GUROBI solver. The obtained results are then set as the initial solutions for **MODEL 1** and **MODEL 2**, for the iteration process shown by Figure 4.5.

The overall solution process of **MODEL 1** and **MODEL 2** for the layout optimization of satellite well-manifold system and the cluster manifold system is shown by Figure 5.7.

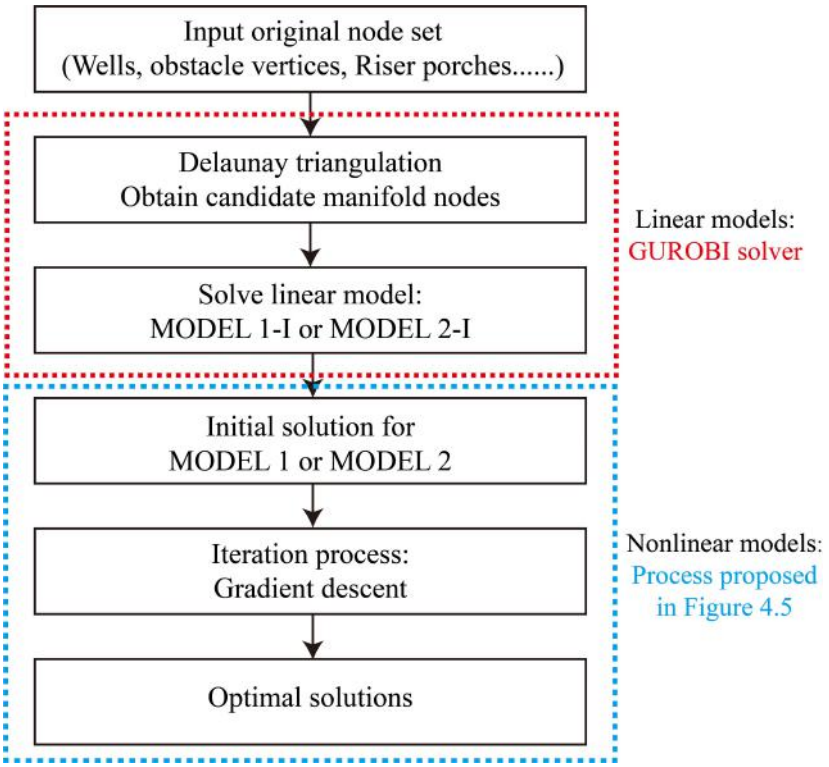

Figure 5.7: Overall solution process of the optimization models for manifold system

5.4 Case studies

5.4.1 Basic information

The offshore field taken for case studies in Chapter 4 for satellite well system as shown in Figure 4.6 is used again here, for the layout optimization of manifold system. Using the same basic case is convenient for comparing the differences between different subsea system concepts.

The basic input information includes the following categories:

(1) The distribution of related equipment or facilities, including the well bottoms, subsea obstacle areas, FPSO locations and orientations, and the mooring line cluster distributions. This information has been presented in Chapter 4, in Table 4.1, Table 4.3 and Table 4.4.

(2) The available types of equipment, including the FPSOs and manifolds. There are four different sizes of FPSO for selection, each with different processing capacities and the maximum number of riser connections, as well as the price, as shown in Table 4.2 in Chapter 4. Four manifold sizes are available, with different slots and price, as shown in Table 5.1.

(3) For the cluster manifold system (scenario 2), 8in short flexible jumper is applied to connect wellhead and manifold. For the satellite well-manifold

Table 5.1: Available manifold sizes and the prices

	Slots number	Price, $\times 10^6$\$
Type 1	4	10
Type 2	6	12
Type 3	8	16
Type 4	10	20

system, the short jumper is also required to connect the facilities and flowline, which is also 8in, presenting the "facility-jumper-PLET-flowline-PLET-jumper-facility" structure [95]. In this thesis, we include the cost of PLET into the cost of flowline and assuming that the same size of flowline and jumper are with the same price. Therefore, in scenario 1, the cost of the jumper has been included in the flowline, without being separately presented.

From the manifold to the riser base, the size of the flowline should be larger due to the comingling of the produced fluid from several wells. On one hand, 8in flexible flowline is currently the largest size for deepwater oil field [4], steel pipe should be the choice for both the flowlines between the manifolds and the riser bases and the risers. On the other hand, the flowline size should be no larger than the size of the riser. Steel catenary riser (SCR) is selected for the riser system, and 10in seems to be the proper size for deepwater Brazil [96], though there might be even larger sizes, in this thesis, we select 10in steel catenary riser for case studies, in order to provide the synthetically understanding of the cost of the production system. Therefore, the 10in steel pipe is selected for the flowline between manifolds and riser base.

Drilling cost stays the same as chapter 4. Riser length is assumed to be constant, which is 3000m, and the riser projection length is 1300m. The corresponding prices are listed in Table 5.2.

Table 5.2: Cost of flowline, riser, and drilling operation

Item	Price, $\$/m$
8in flowline and jumper	2300
10in flowline	3500
10in Steel Catenary Riser	4500
Vertical drilling	7500
Horizontal drilling	21000

Based on this provided basic information, the subsea arrangement of the satellite well-manifold system, and the cluster manifold system, could be obtained using the proposed optimization models.

5.4.2 Results and Discussions

Scenario 1: Satellite well-manifold system

A. Initial solutions As discussed above, two objective functions are studied, the first is the total cost, as shown by eq.(5.41), the second is the hybrid objective function combining both total cost and pressure loss, as shown by eq.(5.42). The first objective function is mainly studied and discussed, and the second one will be taken as one of the comparisons, to show the effect of different objective functions on the subsea arrangement.

The designed manifold number is 4, and the oil price is \$60/*bbl*. The Delaunay triangulation of the provided node sets is shown in Figure 5.8. The green round dots and yellow round dots are the geometric centers of the Delaunay triangles. Green ones are candidate positions for the manifolds, while the yellow ones are eliminated since they are inside the obstacle areas. Four of the candidates are selected as the initial solution based on the proposed MODEL 1-I and the solution method.

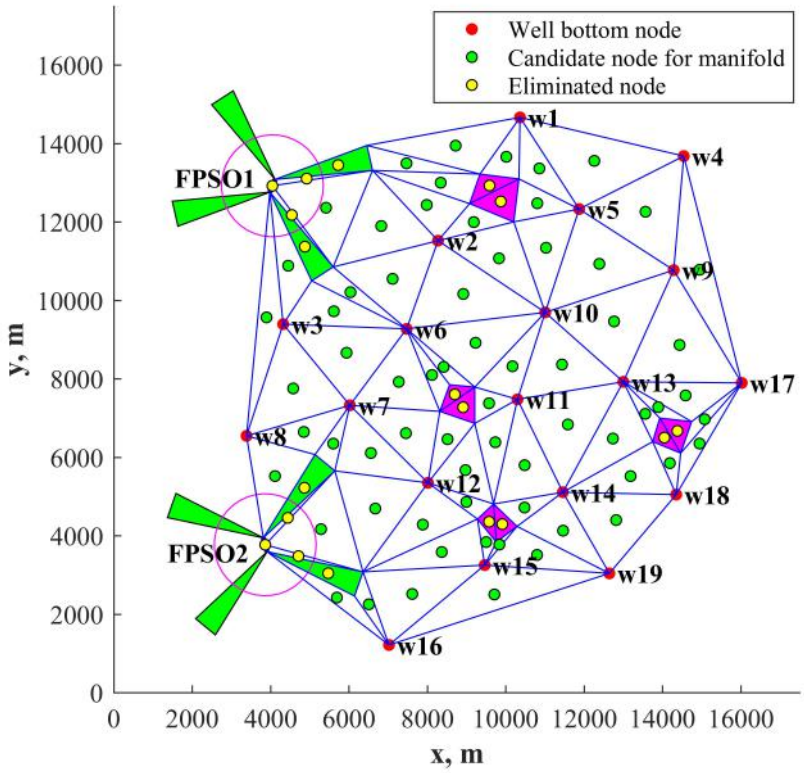

Figure 5.8: Delaunay triangulation of the case in chapter 4

In order to present the effectiveness of the proposed Delaunay triangulation, we randomly select four positions on the $X-Y$ plane as the comparison. The initial manifold positions through Delaunay triangulation and the randomly selected initial manifold positions are presented in Table 5.3

Table 5.3: Initial manifold postions through Delaunay triangulation and the random selection

Manifold No.	Initial manifold positions	
	Delaunay triangulation	Random selection
M1	(8368.05,3584.05)	(10888.37,12463.4)
M2	(5287.37,4166.29)	(12872.25,6411.96)
M3	(5415.52,12361.79)	(7999.19,4234.7)
M4	(9829.73,11071.76)	(6047.14,8648.82)

Applying **MODEL 1-I** proposed in section 5.3, the initial layout based on Delaunay triangulation could be obtained, as shown in Figure 5.9(a). As for the randomly selected manifold positions, these positions could be substituted into the **MODEL-I** proposed in section 5.2, resulting in a MILP model. The obtained subsea layout is shown in Figure 5.9(b).

B. Optimized results and comparisons Starting from these initial solutions respectively, the final optimized layouts are achieved through the proposed iteration strategy. The final optimized layouts based on different initial solutions are shown in Figure 5.11 (a) and Figure 5.11 (b), respectively. The detailed optimization results are presented in Table 5.4. The evolution process of the objective function value as well as the step length factor, α, is shown in Figure 5.10.

Table 5.4 and Figure 5.10 indicate that for both methods of selecting initial solutions, the objective values generally evolve to better ones. The final optimal solutions are achieved when the step length factor α equals to 0, which means the convergence criteria shown in eq.(4.40) has been satisfied. For the initial solution from Delaunay triangulation, the optimized total cost is 5.163 million dollars less than the initial value. For the initial solution from random selection, the optimized total cost is 25.147 million dollars less than the initial value. The decrement of total cost indicates that the proposed solution method using the gradient descent algorithm is effective.

When comparing the optimized results from these two different initial solutions, the first one that based on Delaunay triangulation is better, with the total cost 4.802 million dollars less than the other one. This difference results from the selection of initial solutions. According to the analysis from L.Cooper et al.[43, 91] about

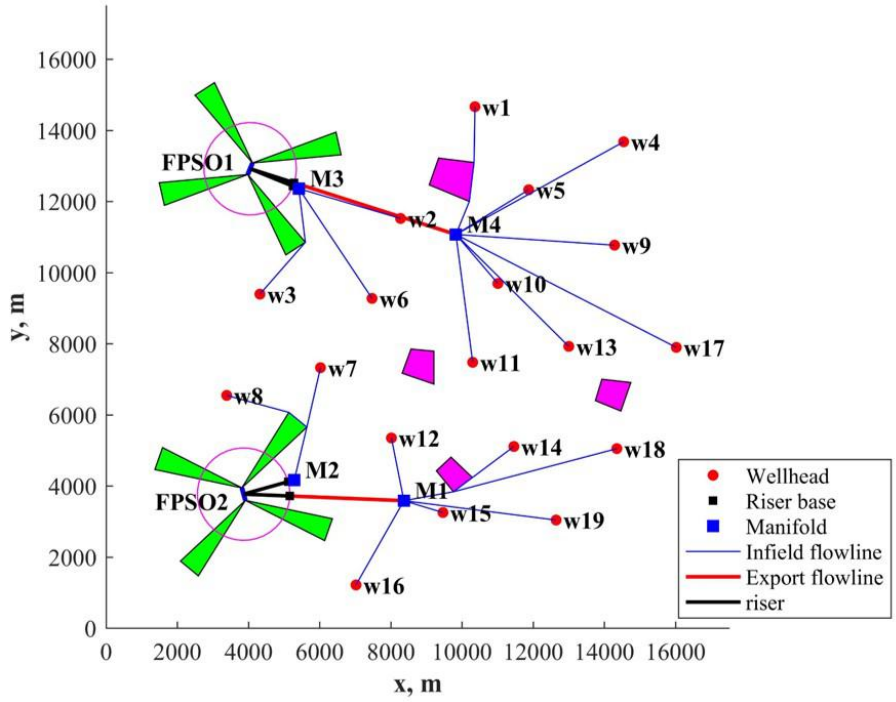

(a) Initial Layout based on Delaunay triangulation

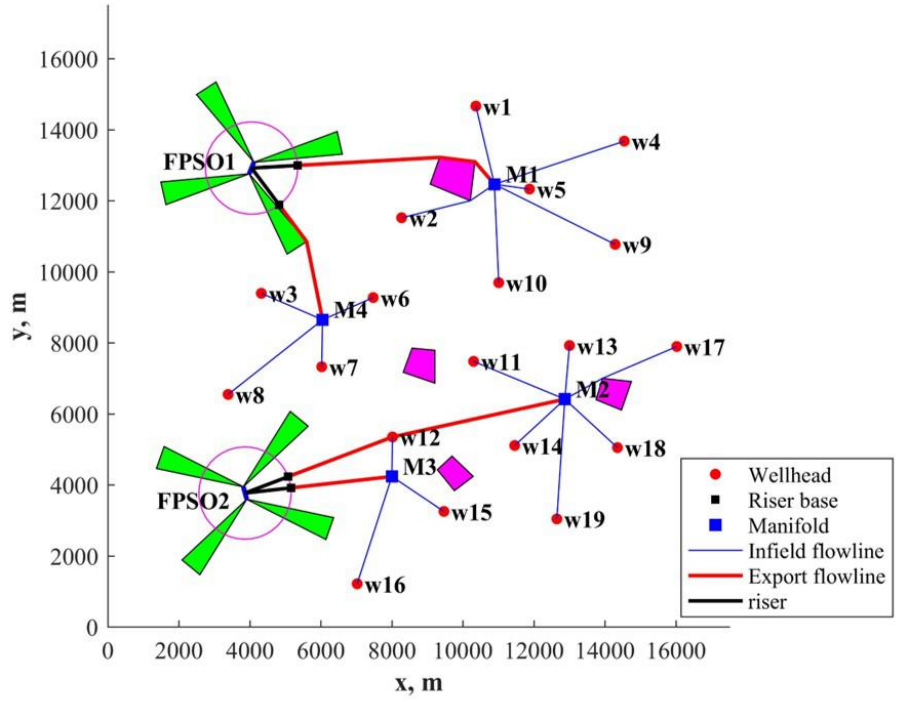

(b) Initial Layout based on random selection

Figure 5.9: Initial subsea layout based on Delaunay triangulation and random selection

"Location-Allocation" problems, there are a series of local optimum for the "service facilities", in our case, which is the manifold positions. Therefore, for the random selected manifold positions, we do not know how far it is from the global optimum,

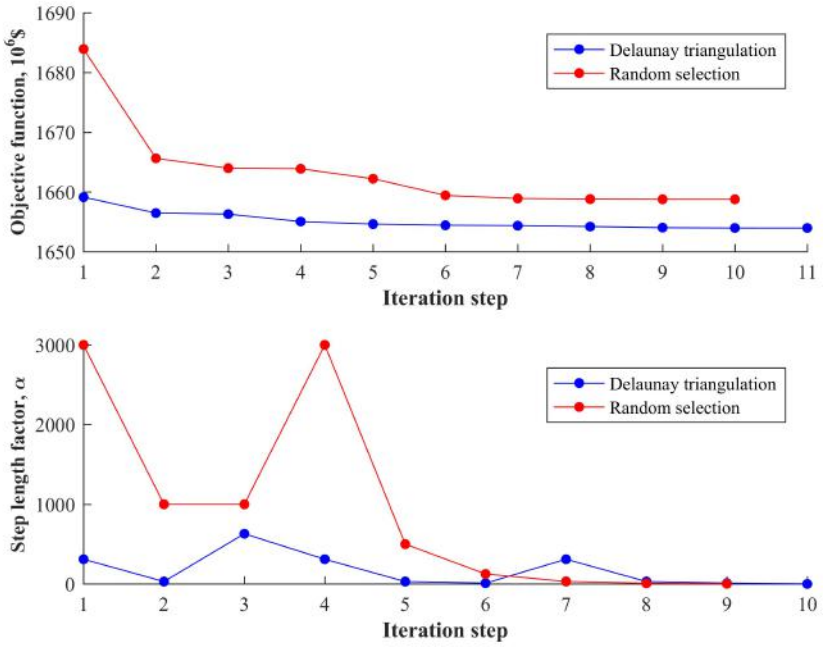

Figure 5.10: Evolution process of the objective function value and the corresponding step length factor, α

and it is easy to converge to one of the local optimums. Of course, if we are lucky enough, it is also possible that we selected one set of initial positions close to the global optimum, and obtained the best solution. But the random process is full of uncertainties, it is hard to keep the quality of the initial solution every time. In order to find the relative better solution, we have to select the initial solutions for several times, repeat the calculation, and choose the best one, which will be very time consuming and we still can't determine whether the results are close to the global optimum.

But the proposed initial solution selection process based on Delaunay triangulation brings some differences. On one hand, the geometric centers of all Delaunay triangles located inside the convex hull of the discrete nodes defined for the related facilities of obstacle vertices, and they distribute throughout the convex hull area, as shown in Figure 5.8, which means that when we are trying to find out the manifold positions from these candidate nodes (using **MODEL 1-I**), it is actually a rough global search process, helping us obtain the initial solution that close to the global optimum, so that it is more likely to converge to the global optimum. We use "likely" here because we are still not sure whether the final result is exactly the global optimum due to the complexity of this kind of problem and the convergence criteria we set for the iteration, as well as the approximation of the gradient calculation, but what is certain is that the optimization result will be close to the global optimum, which is the "suboptimal". The accuracy is enough for engineering

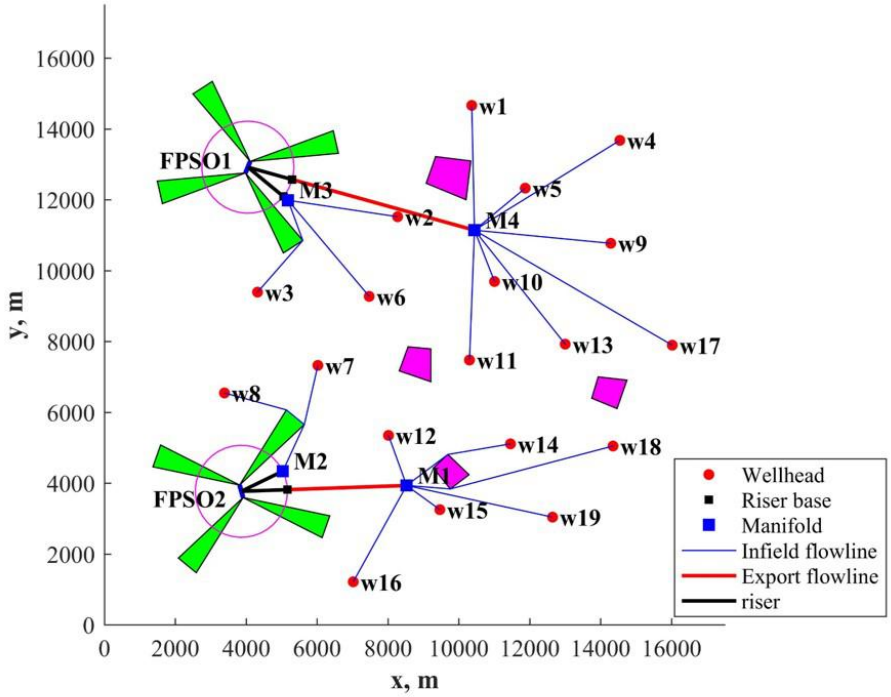

(a) Optimized Layout based on Delaunay triangulation

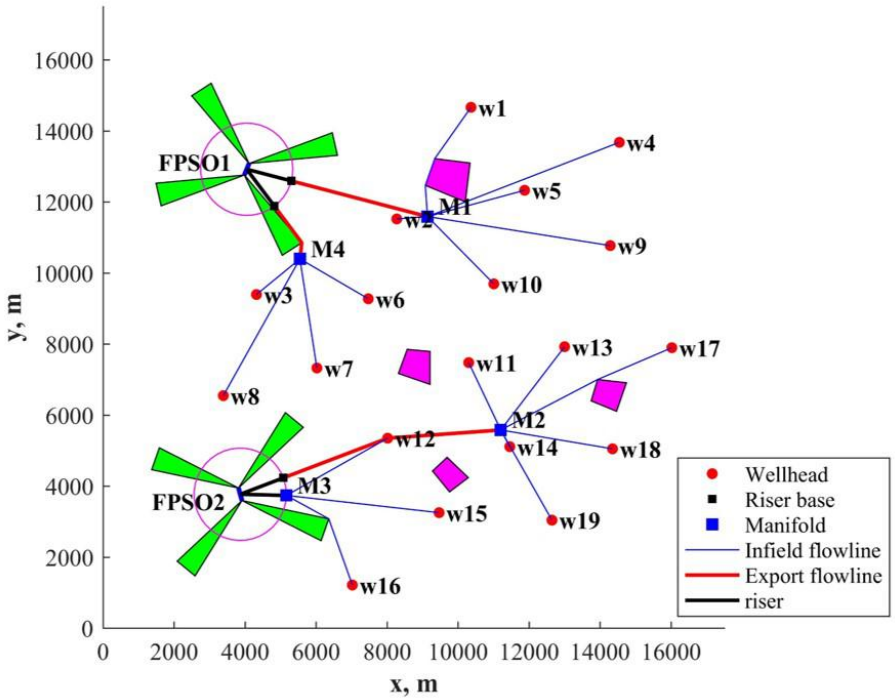

(b) Optimized Layout based on random selection

Figure 5.11: Optimized subsea layout based on Delaunay triangulation and random selection

applications.

On the other hand, the Delaunay triangulation is unique for the provided node set

Table 5.4: Detailed results of initial solutions and optimized solutions

	Delaunay triangulation		Random selection	
	Initial	Optimized	Initial	Optimized
Total Cost $\times 10^6$\$	1659.14	1653.98	1683.92	1658.78
FPSO Cost $\times 10^6$\$	800	800	800	800
Flowline Cost $\times 10^6$\$	219.06	213.90	247.85	222.70
Riser Cost $\times 10^6$\$	108	108	108	108
Drilling Cost $\times 10^6$\$	484.08	484.08	484.08	484.08
Manifold Cost $\times 10^6$\$	48	48	44	44
Total production rate $\times 10^3 bbl/d$	191.37	191.37	191.37	191.37
Payback period $days$	144.50	144.05	146.65	144.46
Flowline length (8in infield) m	69873.20	65988.66	45805.90	60163.10
Flowline length (10in infield) m	16672.69	17750.11	40712.81	24093.20
Manifold slots	(4,4,6,8)	(4,4,6,8)	(4,4,6,6)	(4,4,6,6)
FPSO capacities (FPSO1) bbl/d	120000	120000	120000	120000
FPSO capacities (FPSO2) bbl/d	120000	120000	120000	120000
Pressure loss $\times 10^{-12} d^{-1}$	0.109	0.1075	0.105	0.1033

[92], so that if the optimization is run repeatedly, we are finding the initial manifold positions from the same candidate nodes and will obtain the same initial solutions every time, thus obtaining the same final optimization results. Therefore, compared with the random selection, Delaunay triangulation could bring high-quality optimization results with excellent stability.

As can be seen in Table 5.4, though the optimized total cost based on the initial solution from Delaunay triangulation is lower than the other one, the pressure loss is higher, which means that it is possible that some subsea layouts are with relatively lower pressure loss. Therefore, the second objective function shown by eq.(5.42) is used, to study the effect of pressure loss on the subsea arrangement. We set $\beta_1 = 0.1, \beta_2 = 0.9$ in order to set the pressure loss as the dominant term while including enough information about the cost. The optimized subsea layout is shown in Figure 5.12, and the detailed results are presented in Table 5.5.

Different objective functions result in different subsea layout. For example, when using minimum total cost, well 11 is connected to manifold 4 (M4) and well 12 is connected to manifold 1 (M1), which are assigned to FPSO 1 and FPSO 2, respectively, as shown in Figure 5.9 (a), while when using the hybrid objective function, these two wells are connected to manifold 1 (M1), which is connected to FPSO 2, as shown in Figure 5.12.

Table 5.5 includes the comparison of the detailed optimization results between the two objective functions. The optimized total cost considering the minimum total cost is 6.90 million dollars lower than the total cost considering the hybrid objective, while the total pressure loss is higher. Through the detailed components of the production system, the main differences occur in the cost of the flowlines. We could find that the length of 8in flowline considering hybrid objective function is 11163m shorter compared with the value considering the minimum total cost. And the 10in flowline is 9308m longer, resulting in higher total cost since the 10in flowline is more expensive. The reason is due to the definition of pressure loss shown by eq.(3.12): $E = QL/D^4$. The increment of flowline internal diameter leads to a more significant change of the value E compared with the increment the flowline length L. Since the weight of the pressure loss in the hybrid objective function is set to be 0.9, presenting the dominant of pressure loss, the flowline length between manifolds and FPSOs which are with larger diameter tend to be longer while the flowline length between wellheads and manifolds which are with smaller diameter tend to be shorter, in order to reduce the value of the hybrid objective function, while increasing the total cost due to the pressure difference.

Therefore, different objective functions provide different variation tendencies for the related parameters. For the hybrid objective function, the optimization results are a kind of trade-off between the total cost and the pressure loss. For the proposed

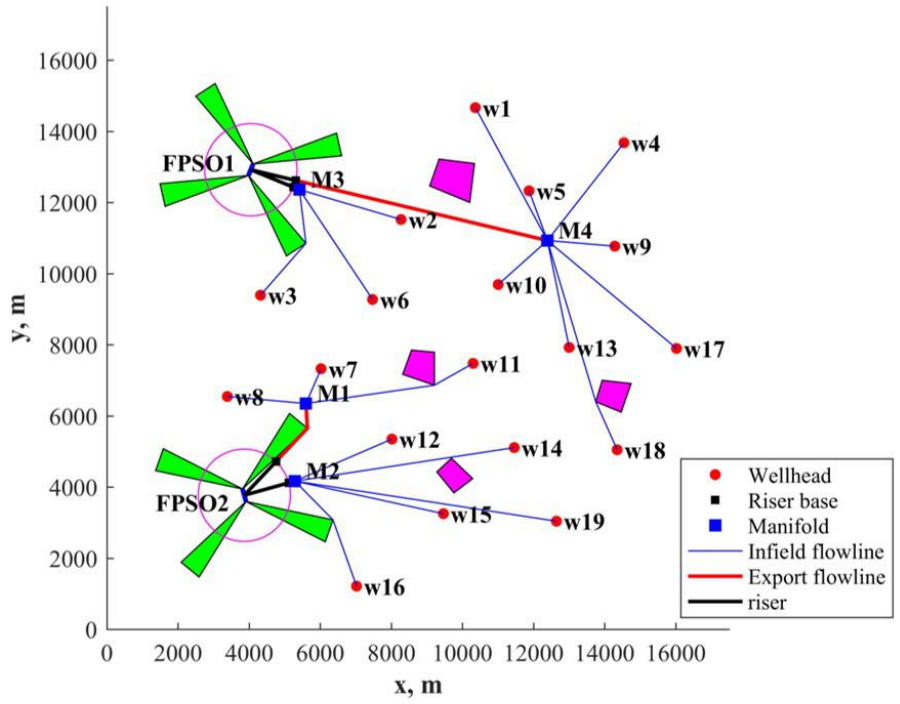

(a) The initial layout

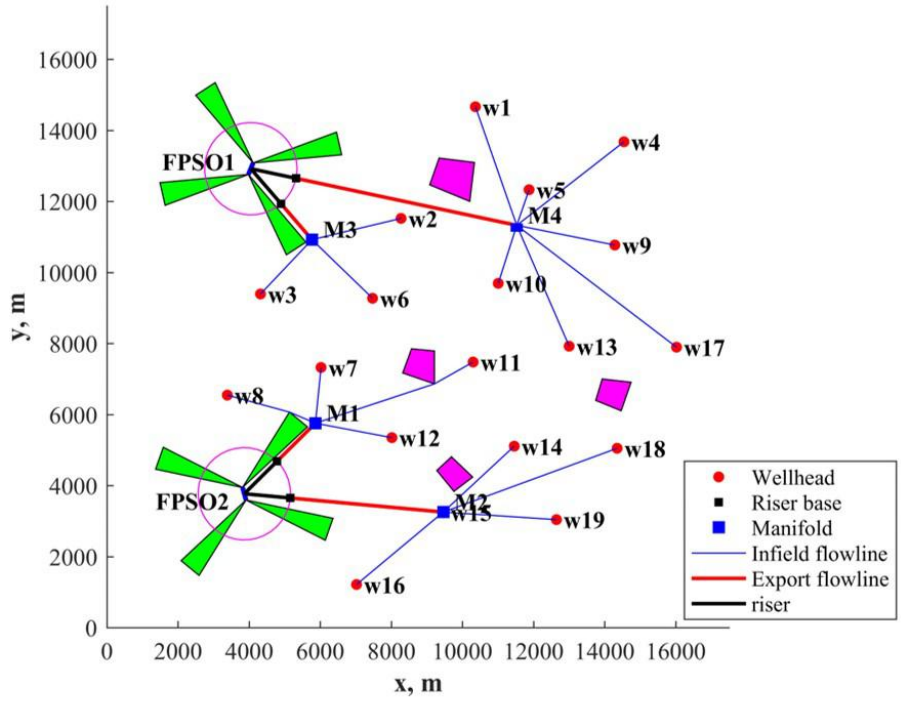

(b) The optimized layout

Figure 5.12: Initial subsea layout and the optimized subsea layout based on the hybrid objective function

models, the most important part is the constraints that including the description of the relationship between all kinds of parameters to correctly define the whole production system. It is flexible to use customized objective functions for the optimization

depending on the needs or requirements of the projects in practical applications.

Table 5.5: Detailed results of the optimization results based on different objective functions

	Objective 1: Total cost	Objective 2: Hybrid total cost and pressure loss
Total Cost, $\times 10^6$\$	1653.98	1660.88
FPSO Cost, $\times 10^6$\$	800	800
Flowline Cost, $\times 10^6$\$	213.90	220.80
Riser Cost, $\times 10^6$\$	108	108
Drilling Cost, $\times 10^6$\$	484.08	484.08
Manifold Cost, $\times 10^6$\$	48	48
Total production rate, $\times 10^3 bbl/d$	191.37	191.37
Payback period, $days$	144.05	144.65
Flowline length (8in infield),m	65988.66	54825.42
Flowline length (10in infield), m	17750.11	27058.41
Manifold slots	(4,4,6,8)	(4,4,6,8)
FPSO capacities, (FPSO1) bbl/d	120000	120000
FPSO capacities, (FPSO2) bbl/d	120000	120000
Pressure loss, $\times 10^{-12} d^{-1}$	0.1075	0.1022

Scenario 2: Cluster manifold system

In scenario 1, the detailed discussions about the proposed solution method and different objective functions have been presented. For the cluster manifold system, we focus on the minimum total cost as the case study, to show how does the proposed model work. In this scenario, short jumper is used to connect the wellhead and manifold, and the jumper length is 50m, which is standardized for the whole field. Similarly, the first step is to use Delaunay triangulation for the initial manifold positions, the Delaunay triangulation is the same with Figure 5.8. Using the proposed **MODEL 2-I**, the initial solution could be obtained through solving the MILP model, and the results are shown in Figure 5.13(a). Starting from the initial solution, the optimized layout could be achieved through the proposed iteration process, and the results are shown in Figure 5.13(b).

In Figure 5.13, since the jumper length is much shorter than the flowline length and the well trajectory projection length, the wellheads and jumpers are not visible,

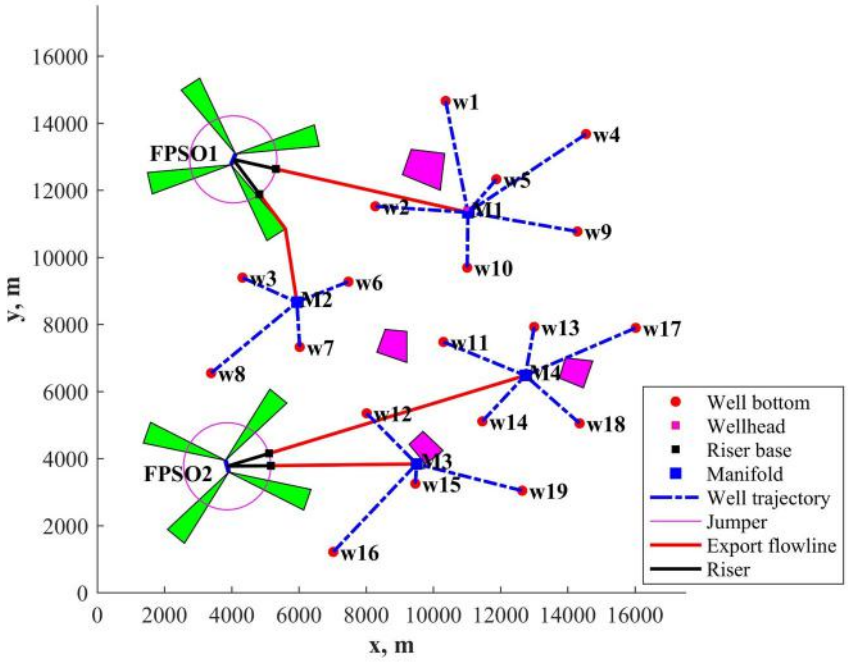

(a) The initial subsea layout for cluster manifold system

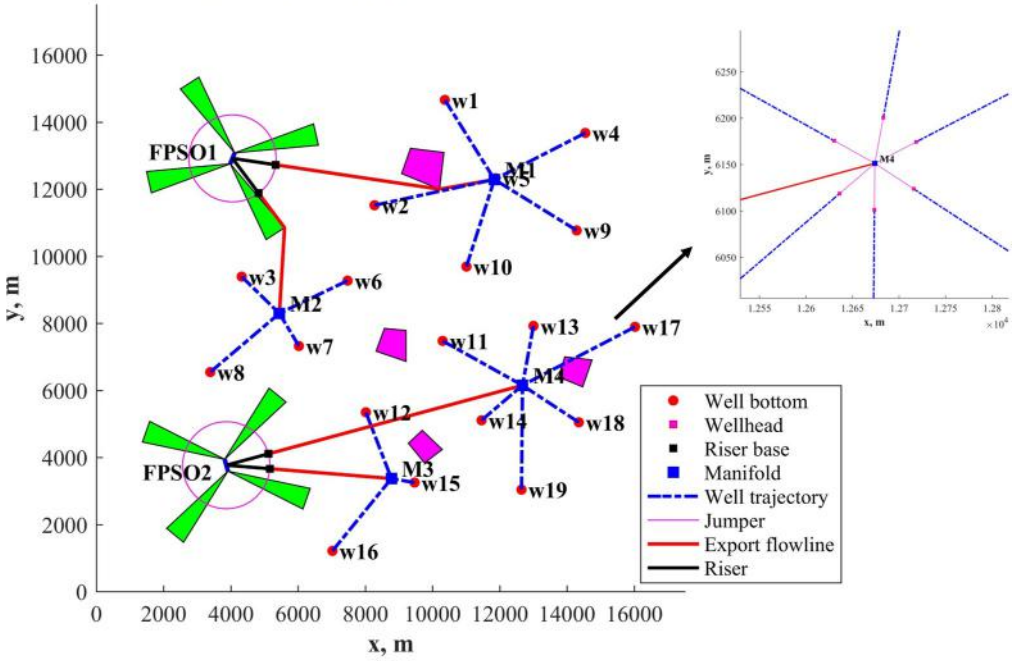

(b) The optimized subsea layout for cluster manifold system

Figure 5.13: The initial and optimized subsea layout for the 4 cluster manifold system

so that beside Figure 5.13(b), a partially enlarged figure shows the area around manifold 4, presenting the positions of the connected wellheads and the jumpers, in order to illustrate an example showing the whole layout.

As can be seen from the figure, the well trajectories are not limited by the subsea obstacle areas because these trajectories are underground. This characteristic makes the manifolds be like "big satellite wellheads" as discussed before. Due to the

Table 5.6: Detailed optimization results comparison between satellite well-manifold system and cluster manifold system

	Satellite well-manifold system	Cluster manifold system
Total Cost, $\times 10^6$\$	1653.98	2661.95
FPSO Cost, $\times 10^6$\$	800	1000
Flowline+ Jumper Cost, $\times 10^6$\$	213.90	153.22
Riser Cost, $\times 10^6$\$	108	108
Drilling Cost, $\times 10^6$\$	484.08	1354.55
Manifold Cost, $\times 10^6$\$	48	44
Total production rate bbl/day	191371.66	297996.20
Payback period, $days$	144.05	148.88
Flowline and jumper length (8in), m	65988.66	950
Flowline length (10in export), m	17750.11	43776.78
Manifold slots	(4,4,6,8)	(4,4,6,6)
FPSO capacities (FPSO1), bbl/d	120000	160000
FPSO capacities (FPSO2), bbl/d	120000	160000
Pressure loss, $\times 10^{-12} d^{-1}$	0.1075	0.1012

commingling of the produced fluid, the number of the flowlines needed towards the FPSO is much fewer than the real satellite well system, as well as the risers.

Table 5.6 presents the detailed optimization results. The results of satellite well-manifold system and the cluster manifold system show significant differences. The total cost of scenario 2 is significantly higher than scenario 1, which is almost 1.01 billion dollars more. For cluster manifold system, compared with the flowline price, the horizontal drilling cost per meter is almost 5 times higher, which makes the manifolds tend to be located at the positions that reduce the horizontal drilling length as possible. Therefore, the well assignment of the cluster manifold system looks "more tight" compared with the satellite well-manifold system. Therefore,

though the in-field flowlines are replaced by jumpers, the reduced cost could not cover the cost increment brought by more expensive horizontal drilling and the longer export flowlines. Besides, the increase in the total production rate due to horizontal drilling requires larger processing capacities of FPSOs, which is also an aspect of higher cost. These factors finally result in a higher total cost.

But the total production rate increases by about 106624.53 bbl/d for the cluster manifold system. Therefore, the investment payback period is about 148.88 days, which is 4 days more than the satellite well-manifold system. This difference is relatively small compared with the difference in total cost. Therefore, for the cluster manifold system, we might invest much more, but could still get back the money not too late compared with satellite well-manifold system.

The effect of manifold number

In the previous case studies, we set the manifold number to be fixed to 4. It is prone to find that different manifold numbers should lead to different subsea arrangements. According to the provided information about the offshore field, there are 19 wells, and in the available manifold sizes, the maximum slots are 10, while the minimum slots are 4 so that at least we need 2 manifolds to cover the 19 wells, and at most, we need 5 manifolds. As a result, we set the manifold number to be equal to 2, 3, 4, 5, respectively, and the corresponding subsea layouts of both satellite well-manifold system and cluster manifold system are optimized through the proposed models. Figure 5.14 and Figure 5.15 presents the optimized results of these two scenarios, respectively.

As can be seen from both figures, different manifold numbers bring different optimized subsea layout. Figure 5.16 and Figure5.17 presents a detailed cost comparison of the results from the different manifold number, for the two scenarios, respectively.

For the satellite well-manifold system, vertical drilling is applied, so that the production rate of each well keep the same under different manifold number, as well as the FPSO cost because the processing capacity stays the same due to the constant production rate. Drilling cost also keeps stable, because vertical drilling cost is only related to the vertical depths of the well bottoms, which are the input fixed values. Due to the increase of manifold number, more risers and manifolds are required, so that the riser cost and manifold cost both will be higher. The flowline cost includes the cost of 8in in-field flowline and the 10in export flowline. When the manifold number increases, the length of 8in in-field flowline decrease while the length of 10in export flowline increase. And their combination reaches the lowest under 4 manifolds, while 5 manifolds correspond to the highest flowline cost. Due to the contribution of the variations about these cost components, the total cost will be higher under larger manifold numbers.

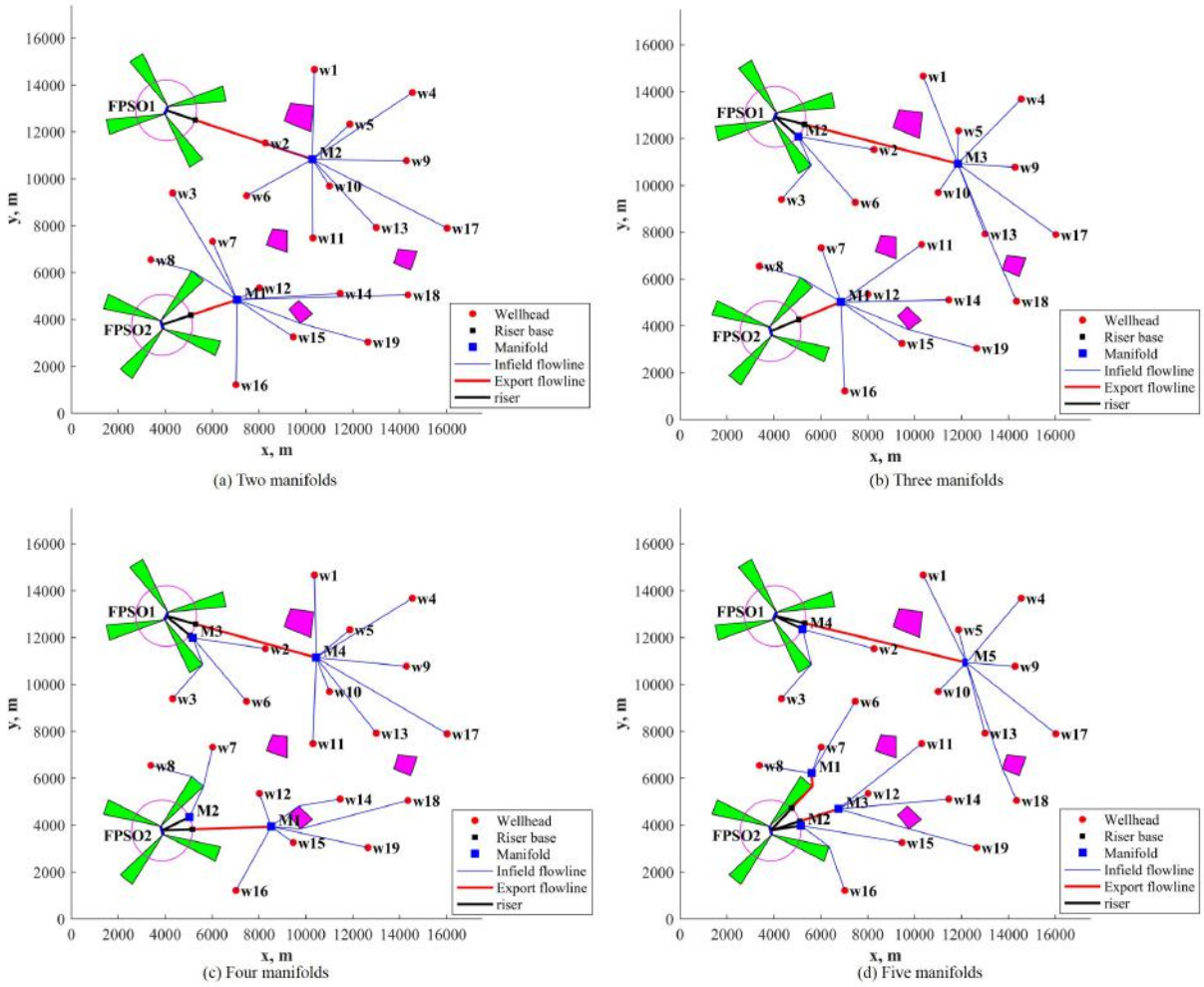

Figure 5.14: The optimized subsea layout under different manifold numbers: satellite well-manifold system

For the cluster manifold system, when the manifold number changes from 2 to 5, the FPSO processing capacities stay the same under different manifold numbers but compared with the above scenario, the processing capacity is higher due to higher production rate bought by horizontal drilling. The 10in export flowlines will increase when there are more manifolds, thus the flowline cost keeps ascending. More manifolds require more risers, therefore the cost of both increase. Drilling cost is related to the horizontal drilling length, which equals to the difference between the well bottom-manifold horizontal distance and the jumper length, as defined in the process of mathematical modelling. Therefore, fewer manifolds make the drilling extend too far, resulting in long horizontal drilling length, thus increasing the cost when there are more manifolds, the horizontal drilling length will be reduced, which could also be found in Figure 5.15. Besides, the variation of drilling cost is very significant, which compensates the cost increment of other components, and finally making the total cost follow its trend, which is more manifolds bring lower total cost.

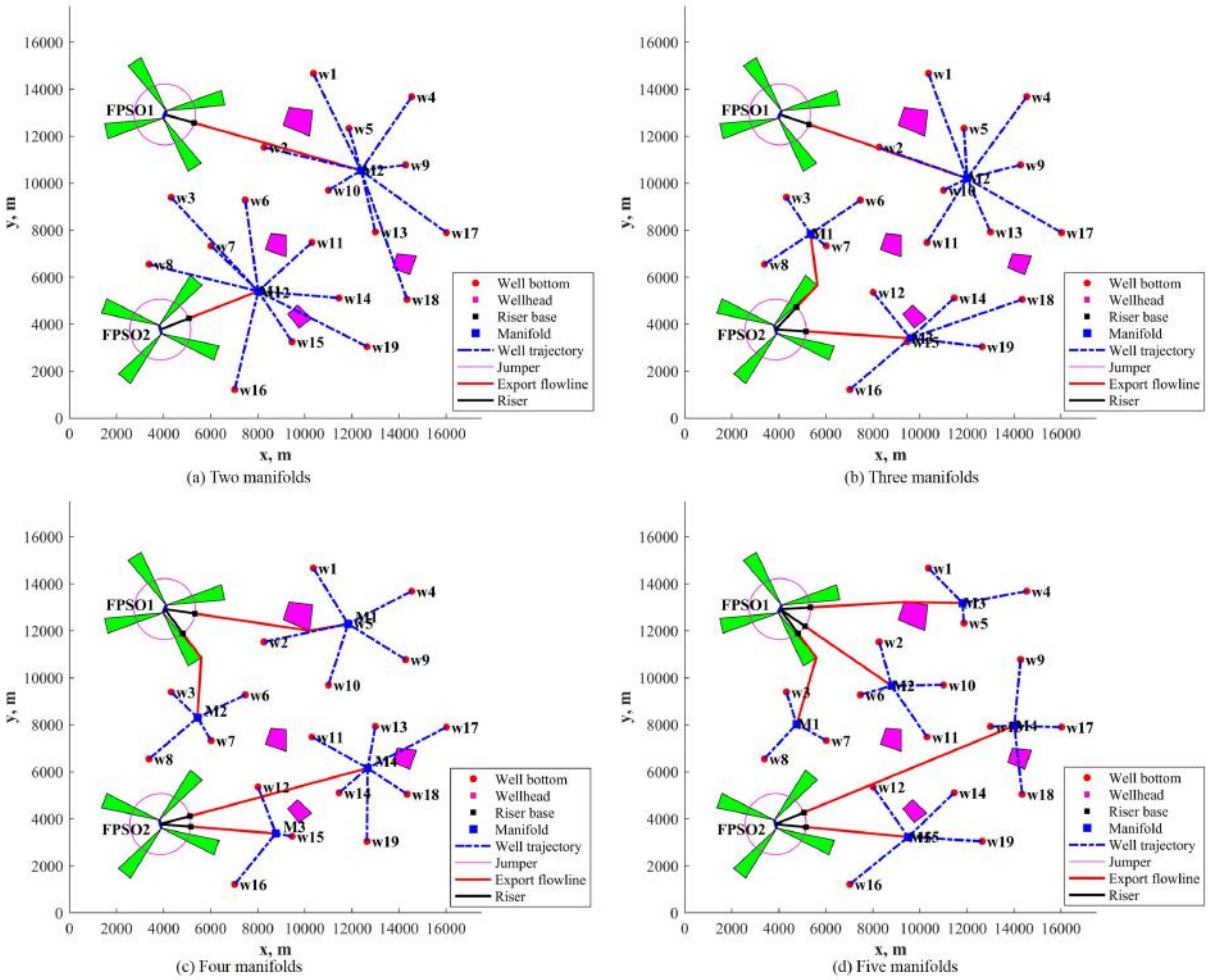

Figure 5.15: The optimized subsea layout under different manifold numbers: cluster manifold system

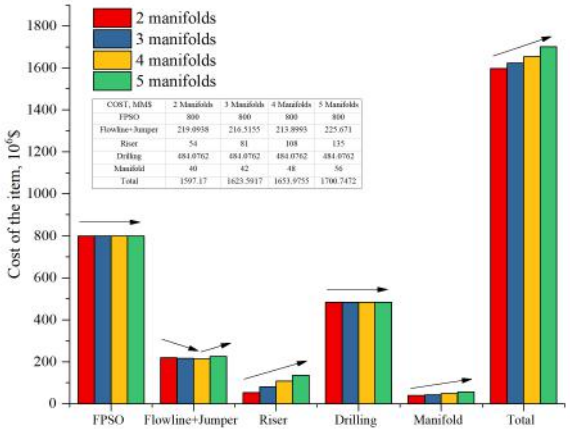

COST, MM$	2 Manifolds	3 Manifolds	4 Manifolds	5 Manifolds
FPSO	800	800	800	800
Flowline+Jumper	219.0938	216.5155	213.8995	225.671
Riser	54	81	108	135
Drilling	484.0762	484.0762	484.0762	484.0762
Manifold	40	42	48	56
Total	1597.17	1623.5917	1653.9755	1700.7472

Figure 5.16: Detail cost comparison of the cases with different manifold number (Satellite well-manifold system)

Figure 5.18 presents the total production rates, payback periods and the pressure loss levels of different manifold number. The vertical wells are selected for the

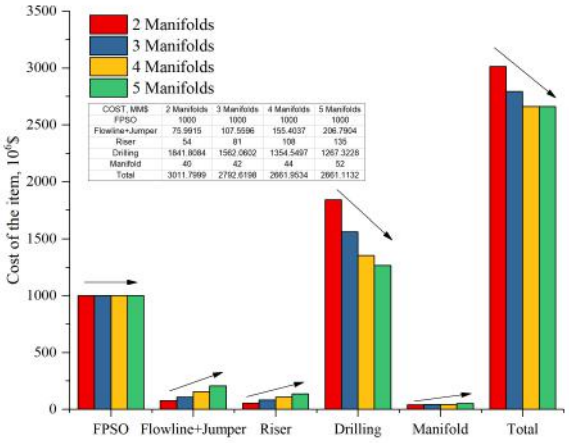

Figure 5.17: Detail cost comparison of the cases with different manifold number (Cluster manifold system)

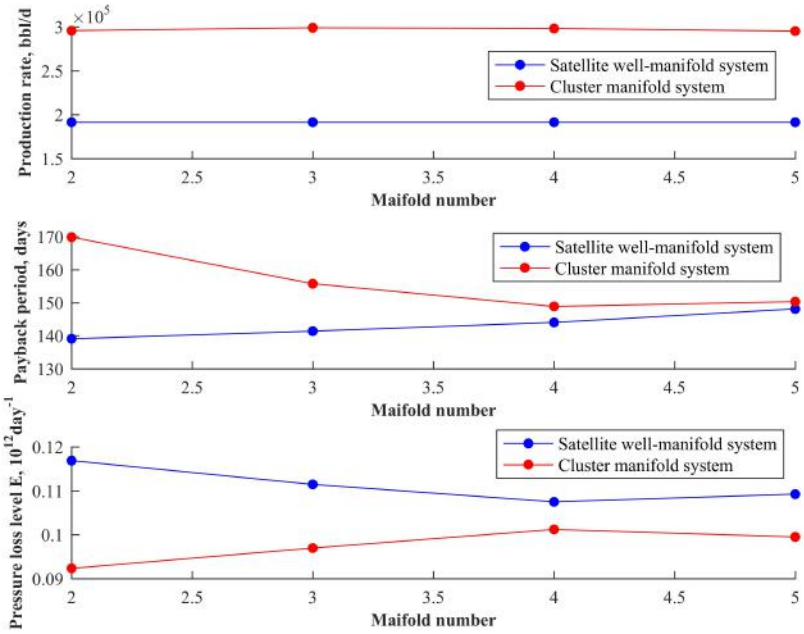

Figure 5.18: The total production rate, payback period, and pressure loss level of different manifold number

satelite well-manifold system, so that the total production rate stays the same when the manifold number increases. For cluster manifold system, since the horizontal displacements of the wells are all relatively long and reach the upper limit of the production interval length as indicated by Figure 4.4, the total production rate stays almost at the same level under different manifold number, but is always higher than the satelite well-manifold system.

Due to relatively stable production rate under different manifold nunmber, the payback period presents the same trend as the total cost. And the payback period

of cluster manifold system is always longer than the other one.

As discussed above, more manifolds result in shorter 8in in-field flowline length and longer 10in export flowline length, and the effect of diameter changing on the pressure loss is more significant than the length changing, therefore, the pressure loss level of satellite well-manifold system decreases when there are more manifolds due to shorter length of 8in flowline. For the cluster manifold system, only 10in export flowline is required, and more manifolds lead to the longer length, resulting in higher pressure loss level. Since the satellite well-manifold system has longer flowline length and smaller size of flowline (8in) than the cluster manifold system, under the same number of the manifold, the pressure loss level of the former one is always higher than the latter one.

The trend of the total cost, total production rate, payback period and pressure loss level under different manifolds discussed above indicates the effect of manifold numbers, but we can not say that the layout with the minimum cost is the best or the layout with the shortest payback period or lowest pressure loss level is the best. Because there are several other technical issues that are not included in the optimization models. For example, the flowline between manifolds and wellheads in scenario 1 could not be too long in order to prevent too large temperature drop that might cause flow assurance problems. Further analysis about the fluid flow inside the flowline is required to identify the risk of flow assurance problems. Besides, longer horizontal displacement means more difficult operation and higher risk, which should also be carefully discussed. we need to keep in mind that an optimal solution to the model does not imply that the analyst has an optimal solution ready to be implemented for the real world problem. Rather, the result from the model should be thought of as an aid to, but not as a replacement for the analyst intuition.

In this thesis, we proposed the subsea arrangement optimization models mainly aims at provide the decision makers several feasible options of the subsea production system arrangement with a better understanding of how the total cost depends upon the various parameters.

5.5 Chapter summary

(1) In this chapter, we focused on the concept of the manifold system and proposed optimization models for the subsea layout design. Two scenarios are considered, scenario 1 considers satellite well-manifold system with vertical wells, and scenario 2 considers the cluster manifold system with horizontal wells. The proposed models for both scenarios are Mix-integer nonlinear programming problems (MINLP).

(2) The same solution method as the optimization models for satellite well system considering horizontal wells is applied, which is based on gradient descent algorithm.

In order to find better initial solutions, the Delaunay triangulation method is applied to generate a series of candidate positions.

(3) GUROBI solver is applied for the solution process. The same offshore field as chapter 4 is taken for the case study. The layouts of both scenarios are optimized, and the effects of the initial solution and manifold number on the subsea production system layout are discussed, as well as how the variation of subsea layout affects the objective function. The case studies indicate the feasibility and flexibility of the proposed models and the good performance of the solution method.

(4) The optimization results of the two scenarios are compared. The cluster manifold system is with higher total cost and higher total production rate than the satellite well-manifold system. And the payback period is slightly higher. The proposed models provide a better understanding of how the total cost depends upon the various parameters.

Chapter 6

Conclusions and Future work

6.1 Conclusions

This thesis focuses on the optimization of the subsea production system arrangement. Two basic concepts are selected, which are satellite well system with Floating Production Storage Offloading unit (FPSO), and the manifold system with FPSO, respectively. The optimization models are established under four different scenarios: satellite well system considering vertical wells, satellite well system considering horizontal wells, the manifold system with satellite distributed vertical wells and manifold system with clustered directional wells. Three major objectives are considered: lowest total cost, shortest payback period, and minimum total pressure loss. The models are developed through mixed-integer programming (MIP). Through the proposed optimization models, the subsea flowline network, flowline route, FPSO processing capacities, manifold sizes, and locations (for the manifold system), wellhead locations and well trajectories, and well production rates could be figured out.

In the proposed mathematical models, drilling cost is integrated, through adding into the effect of wellhead location on the well trajectory and the subsea flowline. Flowline crossing avoidance is set as one of the constraints to ensure that the flowlines between facilities will not affect with each other. FPSO is selected as the floating facility in this work. The processing capacity of FPSO is considered to limit the connections of the flowlines and risers. Besides, seabed obstacles are considered as one of the limitations for the subsea flowline route. All these considerations are decribed mathematically make the optimization model more practical.

The proposed MIP models are with nonlinearities. Based on the gradient descent algorithm, the MIP models are decomposed to a series of linear models, which are solved by optimizer GUROBI. The final optimal solutions are obtained through the iteration process. The Delaunay Triangulation method is applied to discrete the solution space for a rough global search in order to obtain good initial solutions.

An offshore with 19 wells, 2 FPSOs and a series of subsea obstacle areas are taken as the case studies for all the proposed scenarios. The results of different scenarios are compared, as well as the results of different objective functions. The case studies indicate good performance of the proposed models and solution method, providing a convenient and reliable tool for the real world applications.

The case study presents the optimized subsea production system arrangement of different scenarios, and the total cost, payback period and pressure loss of different scenarios present significant differences. But we need to keep in mind that these optimal solutions to the models do not imply that the analyst has optimal solutions ready to be implemented for the real-world problem. Besides, it is not enough to determine which kind of scenario is better based on these optimization results. Because there are still a lot of technical issues related to the engineering operations or production which is required to be synthetically evaluated. Through the work of the thesis, the decision-makers will be provided with several feasible options of the subsea production system arrangement with a better understanding of how the total cost depends upon the various parameters, which contributes to the subsequent further evaluations.

6.2 Future works

In the thesis, for the cluster manifold system, the payback period is with serious nonlinearity and discontinuities, bringing difficulties in solving the model if it was taken as the objective function. Intelligent algorithms such as Genetic Algorithm and Simulated Annealing, are possibly good choices to help solve these complicated problems. In future work, we will try to develop the solution method applying intelligent algorithms, in order to provide a way for more complicated models.

This thesis focused on two typical concepts: satellite well system and manifold system. Another typical concept, daisy chain system will be studied in the future. The "travelling sales man" model will be introduced to help build up the optimization model.

In practical application, one offshore field might be developed through several different concepts simultanously, for example, some wells are satellite distributed and tied back to the FPSO while others are clustered through manifold. Therefore, the subsea arrangement optimization under the hybrid subsea concepts could include more general situations. The models will be more complicated, requiring more decision variables and constraints.

In this thesis, the well production rate is calculated based on theoretical equations. As a future work, the reservoir simulation technology could be introduced to predict the well production. Besides, the scheduling of well drilling activities could

be linked to both reservoir simulation and subsea layout optimization, in order to obtain both the subsea production system arrangment, but also the scheduling of the operation and production activities throughout the life cycle.

Bibliography

[1] MOROOKA, C. K., GALEANO, Y. D., OTHERS. "Systematic design for offshore oilfield development". In: *The Ninth International Offshore and Polar Engineering Conference*, Brest, France, 1999.

[2] CASTRO, G., MOROOKA, C., BORDALO, S., et al. "Decision-making process for a deepwater production system considering environmental, technological and financial risks". In: *Proceedings-SPE Annual Technical Conference and Exhibition*, San Antonio, Texas, U.S.A, 2002.

[3] BEER, P., RIBBECK, L. R., JEFFERIES, A. "Gemini Subsea System Design". In: *Offshore Technology Conference*, Houston, Texas, U.S.A, 2000.

[4] BUCKLEY, K., UEHARA, R. "Subsea Concept Alternatives for Brazilian Pre-Salt Fields". In: *Offshore Technology Conference Brasil*, Rio de Janeiro, Brazil, 2017.

[5] BARNES, K., MCCASLIN JR, L. "Gulf of Mexico Discovery", *Oil & Gas J*, v. 47, pp. 96, 1948.

[6] HOPKINS, J., DIXON, B., WEISS, F. "A Subsea System for Deep Water Completion and Production". In: *Offshore Technology Conference*, Dallas, Texas, U.S.A, 1969.

[7] DEJONG, J., ADAMSON, S. "Garoupa Subsea Production System". In: *Offshore Europe*, Aberdeen, Scotland, UK, 1979.

[8] BAI, Y., BAI, Q. *Subsea engineering handbook*. Gulf Professional Publishing, 2018.

[9] NAVEIRO, J. T., HAIMSON, D., OTHERS. "Sapinhoá Field, Santos Basin Pre-Salt: From Conceptual Design to Project Execution and Results". In: *Offshore Technology Conference*, Rio de Janeiro, Brazil, 2015.

[10] PALAGI, C. L., OTHERS. "Campos Basin Deepwater Production Development an Overview". In: *17th World Petroleum Congress*, Rio de Janeiro, Brazil, 2002.

[11] LONGO, C. E. C. V., NETO, S. J. A., DE PAULA, M. T. R., et al. "Albacora Leste Field-Subsea Production System Development". In: *Offshore Technology Conference*, Houston, Texas, U.S.A, 2006.

[12] CRUZ, R. O. D. M., ROSA, M. B., BRANCO, C. C. M., et al. "Lula NE pilot project - An ultra-deep success in the Brazilian Pre-salt". In: *Offshore Technology Conference*, Houston, Texas, U.S.A, 2016.

[13] DE ABREU CAMPOS, N., DA SILVA FARIA, M. J., DE MORAES CRUZ, R. O., et al. "Lula Alto-Strategy and Execution of a Megaproject in Deep Water Santos Basin Pre-Salt". In: *Offshore Technology Conference Brasil*, Rio de Janeiro, Brazil, 2017.

[14] DE MELO, R. T., DOS SANTOS, T. M., VALENÇA, C. J. G. M., et al. "Libra Subsea Achievements and Future Challenges". In: *Offshore Technology Conference*, Houston, Texas, U.S.A, 2019.

[15] HEY, C., RASMUSSEN, J., TATTERSALL, S., et al. "SS: Tahiti Project Subsea System Design/Qualification". In: *Offshore Technology Conference*, Houston, Texas, U.S.A, 2009.

[16] ROBERT, D. "Reliability and interchangeability for a cost effective subsea system: SKUID". In: *12th World Petroleum Congress*, Houston, Texas, USA, 1987.

[17] KNUDSEN, T., LINDLAND, H. "Value of Subsea Standardised Systems". In: *European Production Operations Conference and Exhibition*, Aberdeen, Scotland, UK, 1994.

[18] HUNDSEID, J., FLATEN, G., FOSSUM, K. T. "Subsea System Design for the HPHT Kristin Field Development, Thermal and Pressure Loads". In: *Offshore Technology Conference*, Houston, Texas, U.S.A, 2004.

[19] LINDSETH, S., RØSBY, E., VIST, B., et al. "Aasta Hansteen Subsea Production System for Deep Water and Harsh Environment". In: *Offshore Technology Conference*, Houston, Texas, U.S.A, 2019.

[20] PEREIRA DE OLIVEIRA, C. A., GUIMARAES DIAS, M. A. "Albacora, a Deepwater Giant Field Development". In: *SPE Latin America Petroleum Engineering Conference*, Rio de Janeiro, Brazil, 1990.

[21] MCLNTURFF T.L. "Troika Subsea Production Template and Manifold System". In: *Offshore Technology Conference*, Houston, Texas, U.S.A, 1998.

[22] BEDNAR, J. "Troika Subsea Production System - An Overview". In: *Offshore Technology Conference*, Houston, Texas, U.S.A, 1998.

[23] DAVISON, C., DYBERG, P., MENIER, P. "Fast-Track Development of Deepwater Kuito Field, Offshore Angola". In: *Offshore Technology Conference*, Houston, Texas, U.S.A, 2000.

[24] TRIGGS, S., MORGAN, J. "Fast Track Subsea System Solution for the Ceiba Field Development". In: *Offshore Technology Conference*, Houston, Texas, U.S.A, 2002.

[25] CAHUZAC, C., BOURCIER, F. "Moho Bilondo-The First Deep Water Development Offshore the Republic of Congo". In: *Offshore Technology Conference*, Houston, Texas, U.S.A, 2009.

[26] CARRIER, P. "Moho Bilondo-Compact Development:Layout and Planning Management". In: *Offshore Technology Conference*, Houston, Texas, U.S.A, 2009.

[27] CARRE, D., O'SULLIVAN, J. "Moho Bilondo: Subsea Production System Experience". In: *Offshore Technology Conference*, Houston, Texas, U.S.A, 2009.

[28] JU, G. T., LITTELL, H. S., COOK, T. B., et al. "Perdido Development: Subsea and Flowline Systems". In: *Offshore Technology Conference*, Houston, Texas, U.S.A, 2010.

[29] BUK JR, L., COSTA, O. C., DE SIQUEIRA, A. G., et al. "Albacora Subsea Raw Water Injection Systems". In: *Offshore Technology Conference*, Houston, Texas, U.S.A, 2013.

[30] ARIAS, B. J., CHITALE, A., BISHOP, S. R., et al. "Role of Integrated Asset Modeling in Optimizing Na Kika Production". In: *International Petroleum Technology Conference*, Dubai, U.A.E, 2007.

[31] OGUCHI, A., REMI-JOHN, B., OKONKWO, G. "Usan Field: Maximizing Production from New Drillwells in a Hydraulically Constrained Deepwater Subsea System Using IPM suite". In: *SPE Nigeria Annual International Conference and Exhibition*, Lagos, Nigeria, 2016.

[32] BARNAY, G. "Girassol: The Subsea Production System Presentation and Challenges". In: *Offshore Technology Conference*, Houston, Texas, U.S.A, 2002.

[33] LAFITTE, J., PERROT, M., LESGENT, J., et al. "Dalia Subsea Production System, Presentation and Challenges". In: *Offshore Technology Conference*, Houston, Texas, U.S.A, 2007.

[34] NELSON, S. G. "AKPO: The Subsea Production System". In: *Offshore Technology Conference*, Houston, Texas, U.S.A, 2010.

[35] BREWER, R., AJAYI, O., ILESANMI, O., et al. "Delivery of Nigeria's First Brownfield Deepwater Triple Daisy Chained Subsea System". In: *Offshore Technology Conference*, Houston, Texas, U.S.A, 2015.

[36] SLEIGHT, N. C., OLIVEIRA, N. "BC-10-Optimizing Subsea Production". In: *Offshore Technology Conference Brasil*, Rio de Janeiro, Brazil, 2015.

[37] DELESCEN, K., NICHOLSON, M., OLIJNIK, L., et al. "BC-10 Subsea Production System Integrated Approach". In: *Offshore Technology Conference Brasil*, Rio de Janeiro, Brazil, 2015.

[38] BEDNAR, J. M. "The Zinc Subsea Production System : An Overview". In: *Offshore Technology Conference*, Houston, Texas, U.S.A, 1993.

[39] HOMER, S. T., SEAFLO, R., CHITWOOD, J. E., et al. "Deepwater Templates and Cluster Well Manifolds : Is There a Single Correct Approach ?" In: *Offshore Technology Conference*, Houston, Texas, U.S.A, 1993.

[40] JONES, J. "Subsea Production Systems - Trends in the Nineties". In: *Offshore Technology Conference*, Houston, Texas, U.S.A, 1995.

[41] RITTER, P., LANGNER, C., SGOUROS, G., et al. "Popeye Project: Subsea System", *SPE Drilling & Completion*, v. 12, n. 04, pp. 256–265, 1997.

[42] DEVINE, M. D., LESSO, W. G. "Models for the Minimum Cost Development of Offshore Oil Fields", *Management Science*, v. 18, n. 8, pp. 378–387, 1972.

[43] COOPER, L. "Location-allocation problems", *Operations research*, v. 11, n. 3, pp. 331–343, 1963.

[44] SHARIFF, S. R., MOIN, N. H., OMAR, M. "Location allocation modeling for healthcare facility planning in Malaysia", *Computers & Industrial Engineering*, v. 62, n. 4, pp. 1000–1010, 2012.

[45] IYER, R., GROSSMANN, I., VASANTHARAJAN, S., et al. "Optimal planning and scheduling of offshore oil field infrastructure investment and

operations", *Industrial & Engineering Chemistry Research*, v. 37, n. 4, pp. 1380–1397, 1998.

[46] CARVALHO, M., PINTO, J. "An MILP model and solution technique for the planning of infrastructure in offshore oilfields", *Journal of Petroleum Science and Engineering*, v. 51, n. 1-2, pp. 97–110, 2006.

[47] GUPTA, V., GROSSMANN, I. E. "An efficient multiperiod MINLP model for optimal planning of offshore oil and gas field infrastructure", *Industrial & Engineering Chemistry Research*, v. 51, n. 19, pp. 6823–6840, 2012.

[48] VAN DEN HEEVER, S. A., GROSSMANN, I. E. "An iterative aggregation/disaggregation approach for the solution of a mixed-integer nonlinear oilfield infrastructure planning model", *Industrial & engineering chemistry research*, v. 39, n. 6, pp. 1955–1971, 2000.

[49] ORTIZ-GÓMEZ, A., RICO-RAMIREZ, V., HERNANDEZ-CASTRO, S. "Mixed-integer multiperiod model for the planning of oilfield production", *Computers & Chemical Engineering*, v. 26, n. 4-5, pp. 703–714, 2002.

[50] WANG, Y., ESTEFEN, S. F., LOURENÇO, M. I., et al. "Optimal design and scheduling for offshore oil-field development", *Computers & Chemical Engineering*, v. 123, pp. 300–316, 2019.

[51] DOBERSEK, D., GORICANEC, D. "Optimisation of tree path pipe network with nonlinear optimisation method", *Applied thermal engineering*, v. 29, n. 8-9, pp. 1584–1591, 2009.

[52] EL-MAHDY, O. F. M., AHMED, M. E. H., METWALLI, S. "Computer aided optimization of natural gas pipe networks using genetic algorithm", *Applied Soft Computing*, v. 10, n. 4, pp. 1141–1150, 2010.

[53] SANAYE, S., MAHMOUDIMEHR, J. "Optimal design of a natural gas transmission network layout", *Chemical Engineering Research and Design*, v. 91, n. 12, pp. 2465–2476, 2013.

[54] KABIRIAN, A., HEMMATI, M. R. "A strategic planning model for natural gas transmission networks", *Energy policy*, v. 35, n. 11, pp. 5656–5670, 2007.

[55] ÜSTER, H., DILAVEROĞLU, Ş. "Optimization for design and operation of natural gas transmission networks", *Applied Energy*, v. 133, pp. 56–69, 2014.

[56] MIKOLAJKOVÁ, M., HAIKARAINEN, C., SAXÉN, H., et al. "Optimization of a natural gas distribution network with potential future extensions", *Energy*, v. 125, pp. 848–859, 2017.

[57] MIKOLAJKOVÁ, M., SAXÉN, H., PETTERSSON, F. "Linearization of an MINLP model and its application to gas distribution optimization", *Energy*, v. 146, pp. 156–168, 2018.

[58] WANG, Y., DUAN, M., XU, M., et al. "A mathematical model for subsea wells partition in the layout of cluster manifolds", *Applied Ocean Research*, v. 36, pp. 26–35, 2012.

[59] WANG, Y., DUAN, M., FENG, J., et al. "Modeling for the optimization of layout scenarios of cluster manifolds with pipeline end manifolds", *Applied Ocean Research*, v. 46, pp. 94–103, 2014.

[60] WANG, Y., ZHAO, H., WANG, D., et al. "Modeling for the optimization evaluation of layout scenarios of subsea cluster manifolds considering three connection types", *Marine Technology Society Journal*, v. 48, n. 6, pp. 98–111, 2014.

[61] RODRIGUES, H., PRATA, B., BONATES, T. "Integrated optimization model for location and sizing of offshore platforms and location of oil wells", *Journal of Petroleum Science and Engineering*, v. 145, pp. 734–741, 2016.

[62] VIEIRA, I. N., ALBRECHT, C. H., DE LIMA, B. S. L. P., et al. "Towards a computational tool for the synthesis and optimization of submarine pipeline routes". In: *The Twentieth International Offshore and Polar Engineering Conference*, Beijing, China, 2010.

[63] KANG, J. Y., LEE, B. S. "Optimisation of pipeline route in the presence of obstacles based on a least cost path algorithm and laplacian smoothing", *International Journal of Naval Architecture and Ocean Engineering*, v. 9, n. 5, pp. 492–498, 2017.

[64] XIAO, J. J., A.-M. A. J. Q. A. M. "Automated route finding for production flowlines to minimize liquid inventory and pressure loss". In: *SPE Annual Technical Conference and Exhibition*, San Antonio, Texas, U.S.A, 2006.

[65] DE LUCENA, R. R., BAIOCO, J. S., DE LIMA, B. S. L. P., et al. "Optimal design of submarine pipeline routes by genetic algorithm with different constraint handling techniques", *Advances in Engineering Software*, v. 76, pp. 110–124, 2014.

[66] ROCHA, D. M., CARDOSO, C. D. O., BORGES, R. G., et al. "Optimization of submarine pipeline routes considering slope stability". In: *Offshore Technology Conference*, Houston, Texas, U.S.A, 2015.

[67] BAIOCO, J. S., ALBRECH, C. H., JACOB, B. P., et al. "Multi-Objective Optimization of Submarine Pipeline Routes Considering On-Bottom Stability, VIV-Induced Fatigueand Multiphase Flow". In: *The Twenty-fifth International Ocean and Polar Engineering Conference*, Hawaii, U.S.A, 2015.

[68] FONSECA DOS SANTOS, T. D., ROCHA, D. M., PEREIRA, L. I., et al. "OTIMROTA-Multiline: Computational Tool for the Conceptual Design of Subsea Production Systems". In: *Offshore Technology Conference*, Rio de Janeiro, Brazil, 2017.

[69] GONG, D., GEN, M., XU, W., et al. "Hybrid evolutionary method for obstacle location-allocation", *Computers & Industrial Engineering*, v. 29, n. 1-4, pp. 525–530, 1995.

[70] CHU, P. C., BEASLEY, J. E. "A genetic algorithm for the generalised assignment problem", *Computers & Operations Research*, v. 24, n. 1, pp. 17–23, 1997.

[71] POURVAZIRI, H., NADERI, B. "A hybrid multi-population genetic algorithm for the dynamic facility layout problem", *Applied Soft Computing*, v. 24, pp. 457–469, 2014.

[72] HRSTKA, O., KUČEROVÁ, A. "Improvements of real coded genetic algorithms based on differential operators preventing premature convergence", *Advances in Engineering Software*, v. 35, n. 3-4, pp. 237–246, 2004.

[73] ZHANG, H., LIANG, Y., MA, J., et al. "An MILP method for optimal offshore oilfield gathering system", *Ocean Engineering*, v. 141, pp. 25–34, 2017.

[74] ZHANG, H., LIANG, Y., ZHANG, W., et al. "A unified MILP model for topological structure of production well gathering pipeline network", *Journal of Petroleum Science and Engineering*, v. 152, pp. 284–293, 2017.

[75] ROSA, V. R., CAMPONOGARA, E., FERREIRA FILHO, V. J. M. "Design optimization of oilfield subsea infrastructures with manifold placement and pipeline layout", *Computers & Chemical Engineering*, v. 108, pp. 163–178, 2018.

[76] REDUTSKIY, Y. "Integration of oilfield planning problems: infrastructure design, development planning and production scheduling", *Journal of Petroleum Science and Engineering*, v. 158, pp. 585–602, 2017.

[77] LAND, A.H., D. A. "An Automatic Method of Solving Discrete Programming Problems", *Econometrica*, v. 28, n. 3, pp. 497–520, 1960.

[78] SALHI, S., GAMAL, M. D. H. "A genetic algorithm based approach for the uncapacitated continuous location–allocation problem", *Annals of Operations Research*, v. 123, n. 1-4, pp. 203–222, 2003.

[79] SAINT-MARCOUX, J.-F., LEGRAS, J., OTHERS. "Impact on Risers and Flowlines Design of the FPSO Mooring in Deepwater and Ultra Deepwater". In: *Offshore Technology Conference*, Houston, Texas, U.S.A, 2014.

[80] NASH, I. "Arctic development of the Canadian Beaufort Sea,geohazards and export route options". In: *Offshore Technology Conference*, Copenhagen, Denmark, 2015.

[81] DNVGL-RP-F107. *Risk assessment of pipeline protection.* 2017.

[82] KAISER, M. J. "Modeling the time and cost to drill an offshore well", *Energy*, v. 34, n. 9, pp. 1097–1112, 2009.

[83] KENUPP, R., LOURENÇO, A., SOLTVEDT, S., et al. "The Longest Horizontal Section Ever Drilled in an Extended-Reach Well in Brazil". In: *Offshore Technology conference*, Rio de Janeiro, Brazil, 2017.

[84] BELTRAO, R., SOMBRA, C. L., LAGE, A. C. V. M., et al. "Challenges and new technologies for the development of the pre-salt cluster, Santos Basin, Brazil". In: *Offshore Technology Conference*, Houston, Texas, U.S.A, 2009.

[85] MOREIRA MATOSO RIBEIRO GOMES, F., DAL PONT, A., MAIA ARANTES, F., et al. "Subsea Projects Cost Reduction-Petrobras Approach, Results and Next Steps". In: *Offshore Technology Conference*, Houston, Texas, USA, 2017.

[86] JOSHI, S., OTHERS. "Augmentation of well productivity using slant and horizontal wells". In: *SPE Annual Technical Conference and Exhibition*, New Orleans, Louisiana, U.S.A, 1986.

[87] HOWELL, G. B., DUGGAL, A. S., HEYL, C., et al. "Spread moored or turret moored fpso's for deepwater field developments", *Offshore West Africa*, v. 10, 2006.

[88] BEGGS, D. H., BRILL, J. P., OTHERS. "A study of two-phase flow in inclined pipes", *Journal of Petroleum technology*, v. 25, n. 05, pp. 607–617, 1973.

[89] LINO, A., MASTRANGELO, C., PEREIRA, F., et al. "The Engineering of Pigging Equipment for Subsea Systems in Campos Basin". In: *Offshore Technology Conference*, Houston, Texas, U.S.A, 1997.

[90] GOOBIE, R. B., ALLEN, W. T., LASLEY, B. M., et al. "A Guide to Relief Well Trajectory Design using Multidisciplinary Collaborative Well Planning Technology". In: *SPE/IADC Drilling Conference and Exhibition*, London, England, U.K, 2015.

[91] COOPER, L. "Heuristic methods for location-allocation problems", *SIAM review*, v. 6, n. 1, pp. 37–53, 1964.

[92] DELAUNAY, B., VIDE, S., LAMÉMOIRE, A., et al. "Bulletin de lAcadémie des Sciences de lURSS", *Classe des sciences mathématiques et naturelles*, v. 6, pp. 793–800, 1934.

[93] BOWYER, A. "Computing dirichlet tessellations", *The computer journal*, v. 24, n. 2, pp. 162–166, 1981.

[94] PETERSON, S. "Computing constrained Delaunay triangulations in the plane", *URL http://www. geom. umn. edu/˜ samuelp/del_project. html. En del av Minnesota Center for Industrial Mathematics Undergraduate Industrial Mathematics Project*, 1998.

[95] SILVA, L., SOARES, C. G. "An integrated optimization of the floating and subsea layouts", *Ocean Engineering*, v. 191, pp. 106557, 2019.

[96] MOREU, M., TABOADA, M., TABOADA, A., et al. "Ultra-Deepwater Steel Riser Systems Hosted on FPSOs Offshore Brazil". In: *Offshore Technology Conference*, Houston, Texas, U.S.A, 2015.